A HYDRO-GEOPHYSICAL SURVEY FROM KAWAIHAE TO KAILUA-KONA, HAWAII

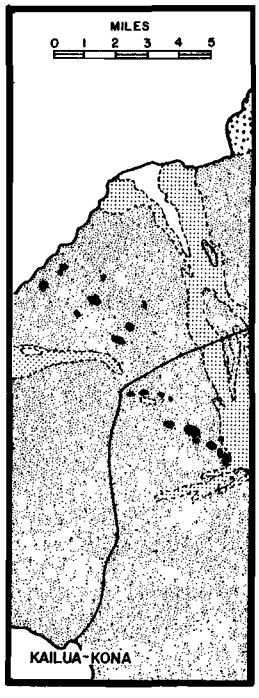

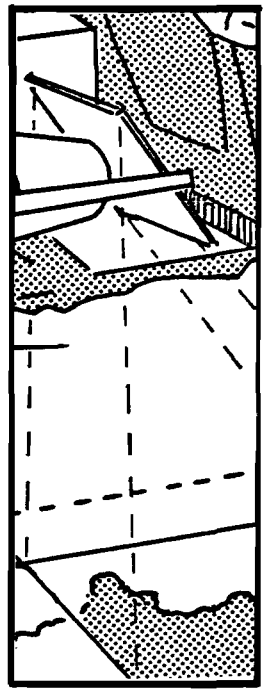

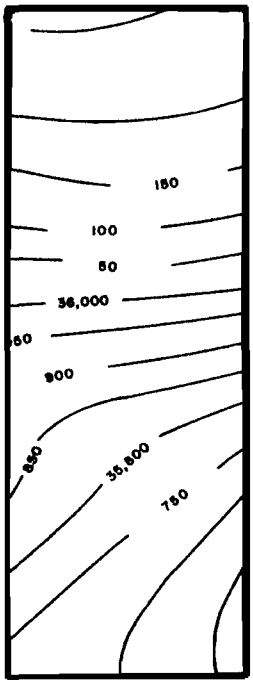

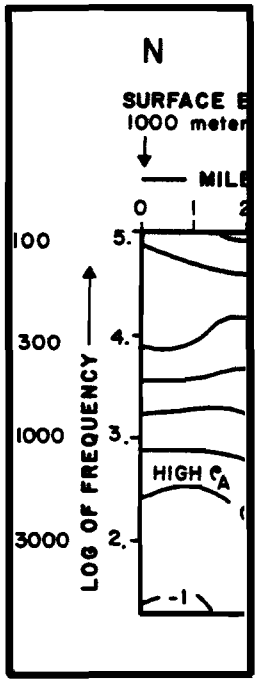

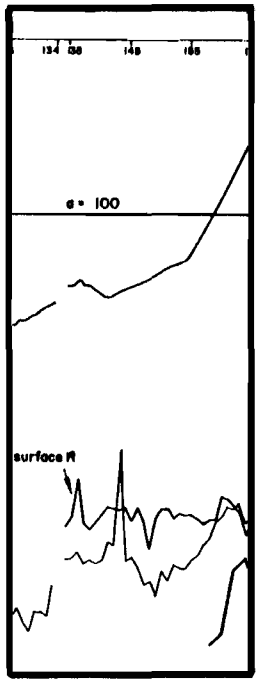

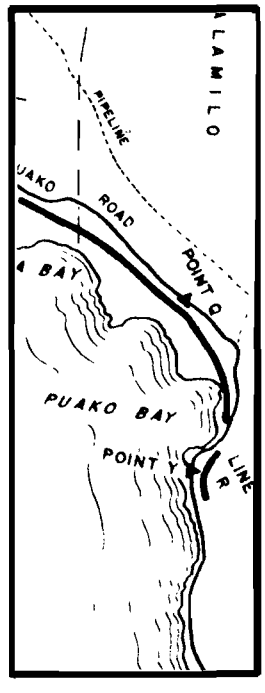

A Zuni Prayer

When our earth mother is replete with
living waters,
When spring comes,
The source of our flesh,
All the different kinds of corn,
We shall lay to rest in the ground.
With their earth mother's living waters,
They will be made into new beings.
Coming out standing into the daylight
Of their sun father,
Calling for rain,
To all sides they will stretch out their
hands.
Then from wherever the rain makers stay
quietly
They will send forth their misty breath;
Their massed clouds filled with water will
come out to sit down with us;
Far from their homes,
With outstretched hands of water they will
embrace the corn,
Stepping down to caress them with their
fresh waters,
With their fine rain caressing the earth,
With their heavy rain caressing the earth,
And yonder, wherever the roads of the rain
makers come forth,
Torrents will rush forth,
Silt will rush forth,
Mountains will be washed out,
Logs will be washed down,
Yonder all the mossy mountains
Will drip with water.
The clay-lined hollows of our earth mother
Will overflow with water,
From all the lakes
Will rise the cries of the children of the
rain makers,
In all the lakes
There will be joyous dancing --
Desiring that it should be thus,
I send forth my prayers.

As quoted by Ruth L. Bunzel in
Forty-Seventh Annual Report of
The Bureau of American Ethnology
to the Secretary of the Smith-
sonian Institution 1929-1930.

A HYDROGEOPHYSICAL SURVEY

FROM KAWAIHAE TO KAILUA-KONA, HAWAII

by

William M. Adams
Frank L. Peterson
Surendra P. Mathur
Larry K. Lepley
Clifton Warren
Richie D. Huber

Technical Report No. 32

HIG Series, HIG-WRRC - 4

This is a report of cooperative research published with the approval of the Director of Water Resources Research Center and the Director of the Hawaii Institute of Geophysics.

September 1969

Final Report

for

GEOPHYSICAL EXPLORATION FOR HAWAIIAN GROUND WATER - PHASE III

OWRR Project No. B-011-HI, Grant Agreement No. 14-01-0001-1893

Principal Investigators: Doak C. Cox & William M. Adams

Project Period: July 1, 1968 to June 30, 1969

The programs and activities described herein were supported in part by funds provided by the United States Department of the Interior as authorized under the Water Resources Act of 1964, Public Law 88-379, and the Hawaii State Department of Land and Natural Resources, Division of Water and Land Deveopment.

ABSTRACT

Several geophysical surveys have been conducted over the coastline area between Kawaihae and Kailua-Kona for the purpose of locating the optimum sites for possible development of ground water from the basal lens. A low-level aeromagnetic survey over the area and an infrared scanning effort along the coast with surface verification provided general reconnaissance information. Audiomagnetotelluric and D. C. electrical resistivity profiles defined more detailed, local structures.

The infrared scanning survey along the coastline did not reveal any thermal anomalies that are reasonably attributable to previously unknown outflows of brackish water of magnitudes adequate for currently anticipated commercial exploitation. However, the aeromagnetic and audiomagnetotelluric surveys locate four lines which are possible barriers to lateral movement of basal ground water. Due to recharge considerations, only two areas were identified for test drilling, and these lie at elevations of more than 1,200 feet. The D. C. electrical resistivity profiling was conducted at an elevation of about 100 feet or less. Based on the resistivity data, three possible sites for test drilling are selected -- two are in the north near Puako Bay and the other is above the present Kona Airport. The anomaly suggesting this latter site has probably been adequately tested by the test well already completed mauka of the site.

CONTENTS

FIGURES

TABLES

PREFACE

The studies reported here were supported jointly by the Hawaii State Department of Natural Resources and the Office of Water Resources Research, U. S. Department of the Interior. The work constitutes a part of the Water Resources Research Center's project supported in part by the federal agency, to develop geophysical methods of investigation of ground water in Hawaiian terrains. The particular phase covered in this report was a broad geophysical reconnaissance covering the coastal area between Kawaihae and Kailua-Kona, contributing to a part of the state agency's overall investigation of the water resources of the western part of the island of Hawaii.

Utilizing several geophysical methods to study subsurface geology indirectly from the surface, the reconnaissance had a two-fold objective: (1) to provide a fast, economical areal reconnaissance aid in the evaluation of ground-water resources and (2) to assist and provide supplemental data for the exploratory drilling phase of water-resources investigations in the area.

This report is the result of work by numerous scientists. To best identify the contribution of each, the authorship of the chapters in this report is specified. First, a geological review is presented. The geophysical surveys are then given, proceeding from the most general to the more specific. Additional contributions to the work are noted in the appropriate acknowledgements.

The reader is urged, at all times, to remember the opening sentence of Davis and DeWiest (1966)[1] in their chapter entitled, "Ground Water in Igneous and Metamorphic Rocks,"

> Few tasks in hydrogeology are more difficult than locating drilling sites for water wells in igneous and metamorphic rocks.

[1]From Davis, S.N. and R.J.M. DeWiest. 1966. *Hydrogeology*. J. Wiley and Sons, Inc. p. 318.

HYDRO-GEOLOGY

FRANK L. PETERSON

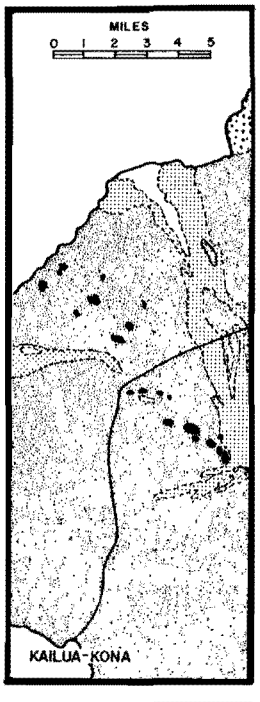

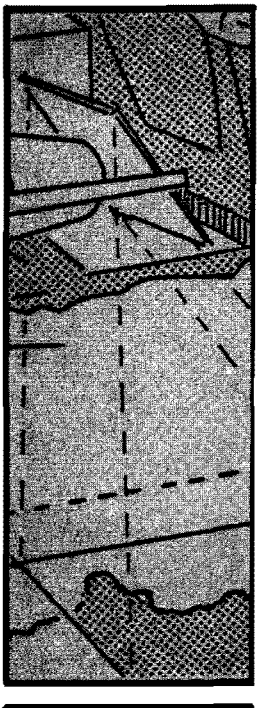

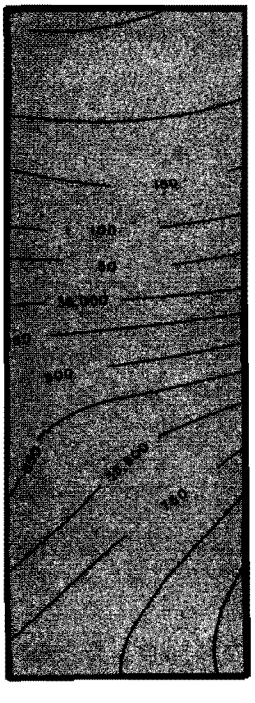

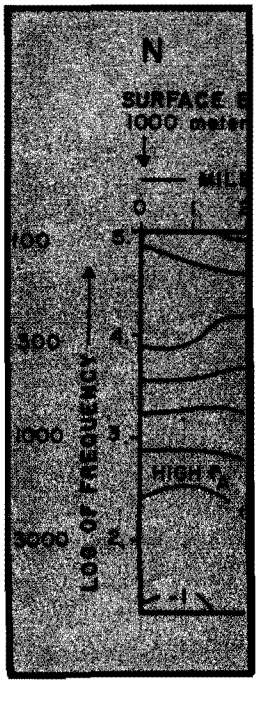

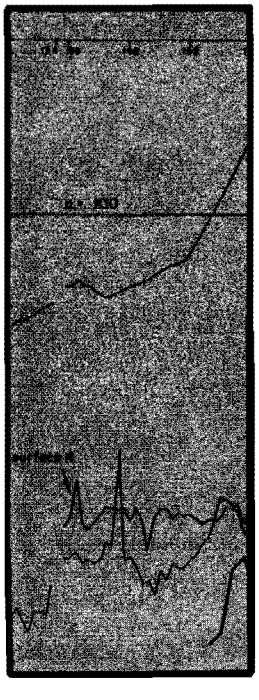

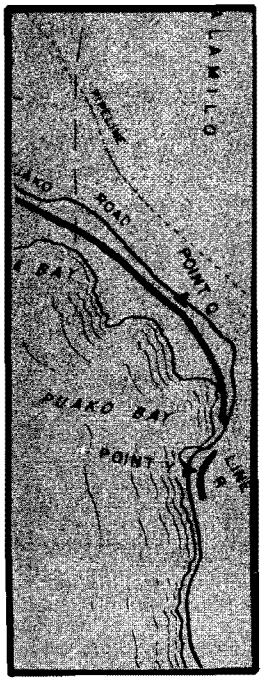

The area covered by these geophysical studies extends roughly from Kawaihae in the north to Kailua-Kona in the south and from the shoreline inland to the belt highway (FAP 19) on the west coast of the island of Hawaii (Fig. 1.1). These lands as well as adjacent portions of the western coast of Hawaii, because of their unique scenic, climatic, and recreational attractiveness, are being rapidly developed, by both the state of Hawaii and private agencies. Much of this area is very dry, and the lack of a readily available water supply has been the most serious deterrent to its development earlier.

SCOPE OF WORK

Four different geophysical surveys were made between Kawaihae and Kailua-Kona from June 1968 to June 1969. Infrared and aeromagnetic surveys were flown along the coastline, a surface resistivity survey was conducted a few hundred yards inland from the shore, and an audio-magnetotelluric (AMT) survey was run along the belt highway. A review of the literature on the geology and hydrology of the area and a study of the tidal-zone algae was made (Brilliande and Lepley, 1969).

GEOLOGY

The coastal area between Kawaihae and Kailua-Kona is underlain by lava flows from Mauna Kea, Mauna Loa and Hualalai volcanoes (Fig. 1.2). The lavas generally are basalt flows, partly pahoehoe, but primarily aa, although the Mauna Kea lavas of the Hamakua series in the northern part of the area are capped by Pahala ash. Sub-surface lava flows date back to perhaps the late Pliocene, however, all exposed rocks are Pleistocene in age (Doell and Cox, 1961). Both Mauna Loa and Hualalai historic flows are present in the area.

The northern part of the area is underlain by Mauna Kea lava flows of the Hamakua and Laupahoehoe series. The Hamakua volcanic series consists primarily of basalt and some andesite lava flows with minor amounts of inter-bedded ash. The Hamakua lavas are covered by Pahala ash, which is a few feet thick near the belt highway, and are found only in scattered patches along the coast. In general, the Hamakua lavas are moderately to highly porous and permeable and yield

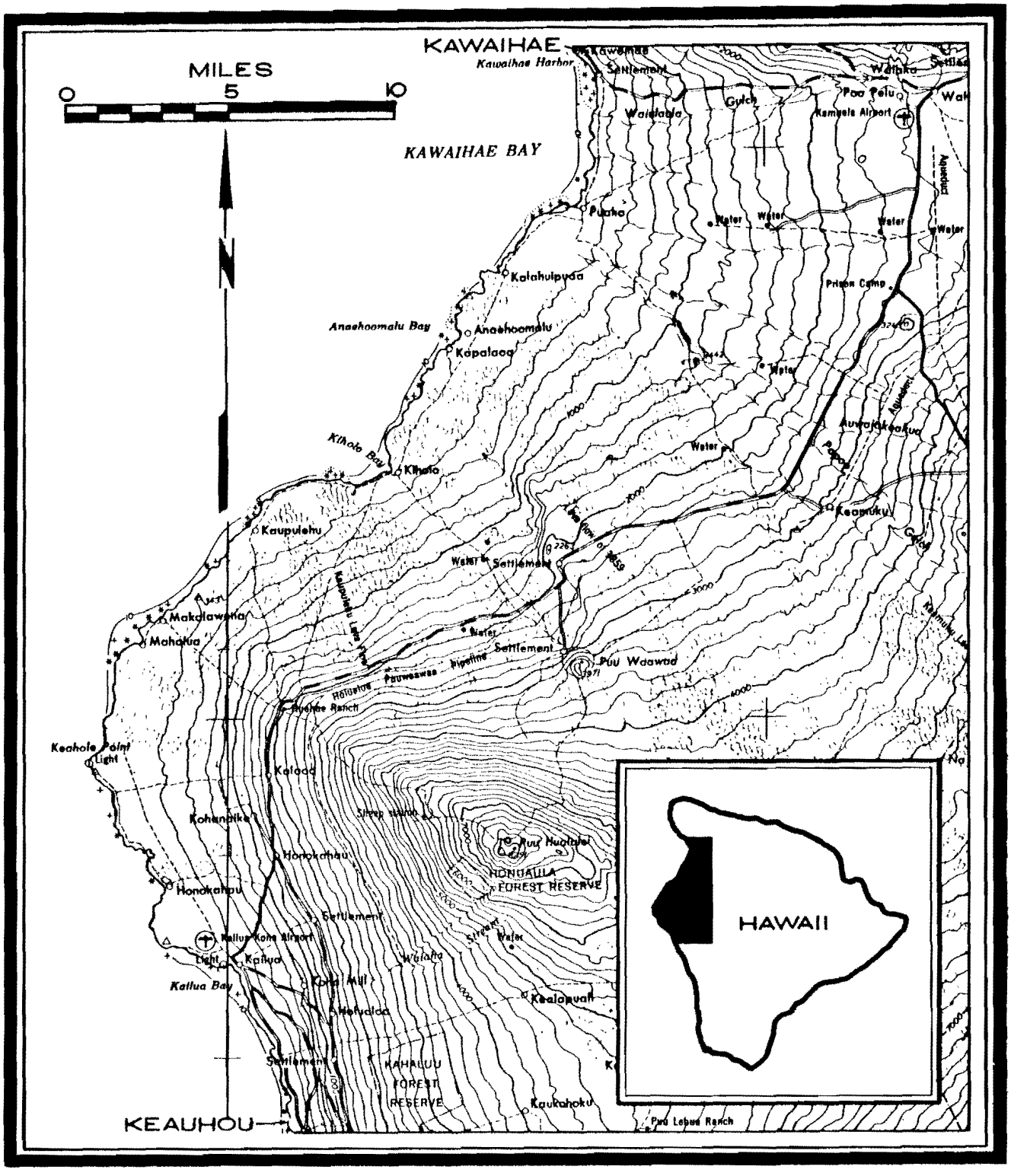

FIGURE 1.1. LOCATION MAP OF THE COASTAL AREA IN THE VICINITY OF KAWAIHAE TO KAILUA-KONA, HAWAII (AFTER USGS 1:250,000 SCALE TOPOGRAPHIC MAP).

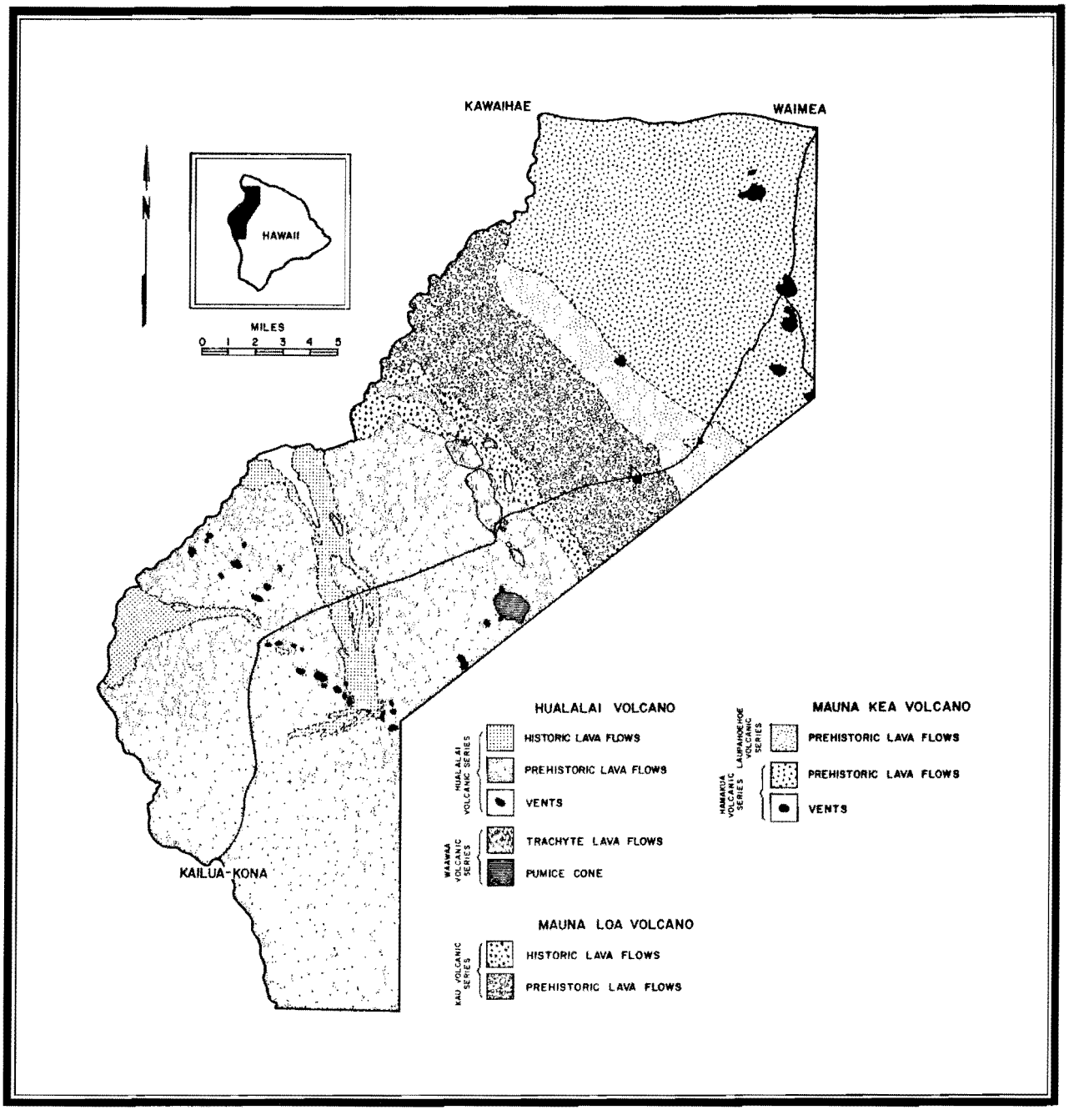

FIGURE 1.2. SURFACE GEOLOGY OF THE COASTAL AREA IN THE VICINITY OF KAWAIHAE TO KAILUA-KONA, HAWAII (AFTER STEARNS AND MACDONALD, 1946).

water freely to wells. Flows of the Laupahoehoe volcanic series outcrop along a two-mile-wide strip just south of the Hamakua lavas. These rocks consist primarily of andesite flows with numerous cinder cones at the sources of the short flows. The Laupahoehoe lavas generally are less porous and less permeable than the Hamakua lavas.

South of the Mauna Kea slopes, a strip of Mauna Loa lavas approximately 3½ to 7 miles wide flowed through the saddle between Mauna Kea and Hualalai and down into the ocean. These lavas, which are all members of the Kau volcanic series, are basalt flows similar in composition and structure to the Hamakua flows. One of the Kau flows in the area, the Kaniku flow,which erupted in 1859, is historic. The Kau lavas, like the Hamakua lavas, are highly porous and permeable and are saturated near sea level.

To the southwest of the 1859 flow is the slope of Hualalai. This slope is underlain generally by basalt lava flows of the Hualalai volcanic series, similar to the Kau flows from Mauna Loa and the Hamakua flows from Mauna Kea. At the north edge of the Hualalai lavas and approximately 5-miles inland from the sea, a thick trachyte flow, which erupted from Puu Waawaa, is exposed. The flow is partly covered with later Hualalai basalt flows and its base is not exposed. The Hualalai lavas generally are highly porous and permeable.

HYDROLOGY

This area, owing to its location within the rain shadow of Mauna Kea and Mauna Loa, receives little trade-wind rainfall. The rainfall on the area north of Hualalai is very slight and along the shoreline is only about 10 inches per year (Fig. 1.3). However, the rainfall near Kailua-Kona is considerably greater than on the northwestern coastal area. Along the shoreline the median annual rainfall is about 25 inches. The zone of greatest rainfall runs parallel to the 3,000-foot elevation contour on the southwest slopes of Hualalai and has about 75 inches of rain per year. Throughout the area more than half of the yearly rainfall occurs during the months of May through September (Taliaferro, 1958).

The infiltration capacity of the surface is very high and there are no perennial streams. Overland flow is negligible except very

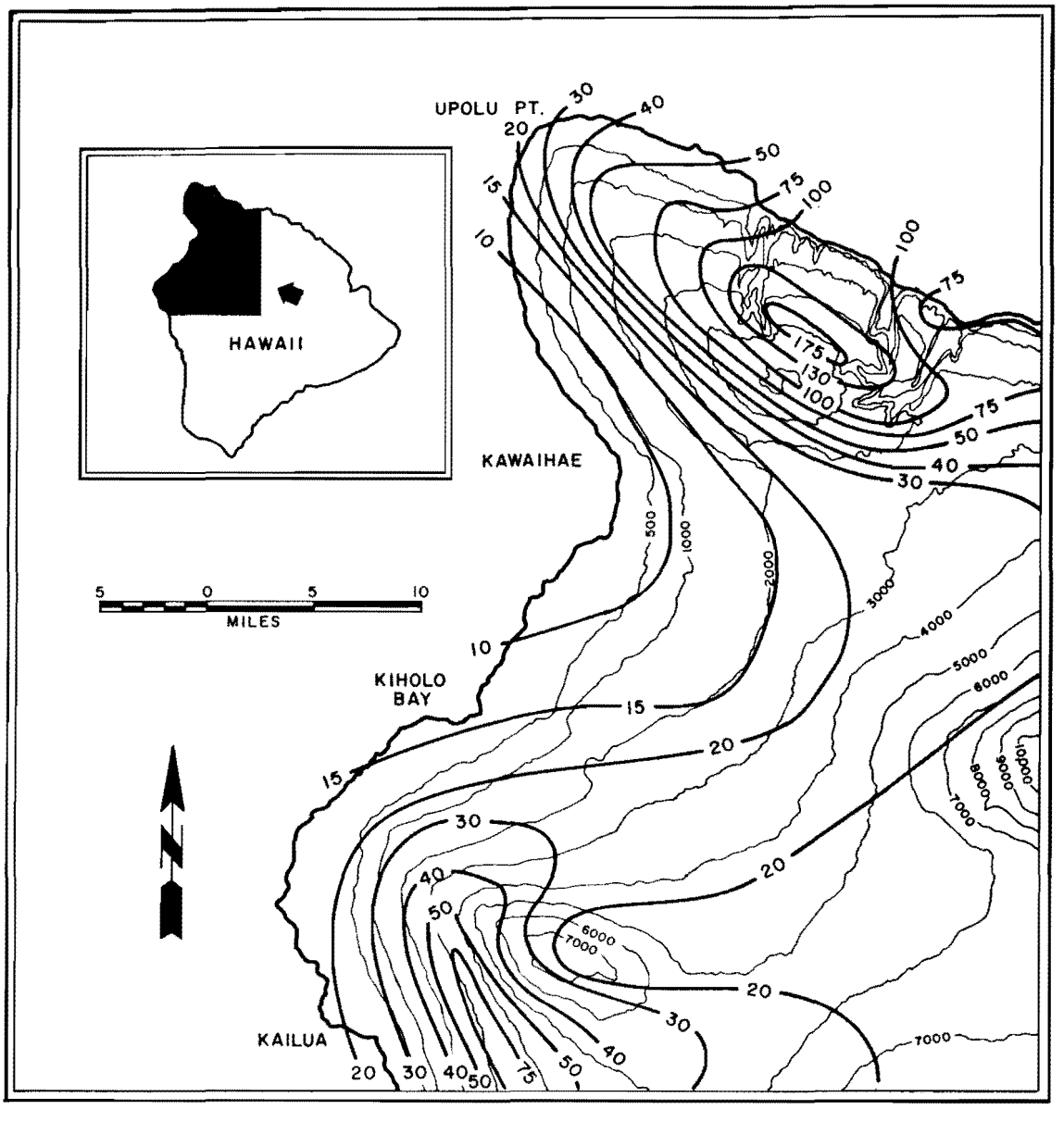

FIGURE 1.3. MEAN ANNUAL RAINFALL IN NORTHWEST HAWAII. CONTOURS ARE IN UNITS OF INCHES PER YEAR. (AFTER COX, ET AL., 1969)

locally during and immediately after severe storms when the gulches may have heavy discharges. The largest streams in the area are Waiaha Stream near Kailua-Kona and Waikoloa Stream near Kawaihae (Fig. 1.4). Streamflow records for these streams have been summarized by Davis and Yamanaga (1963 and 1968). No streams in the area offer promise of large dependable supplies of water.

Small amounts of ground water may be perched on ash beds or other tight layers under the slopes of Mauna Kea, Mauna Loa, and Hualalai, however, no perched ground water is definitely known in the area and there are no perched-water springs.

Dikes deep within the rift zones of Mauna Kea, Mauna Loa, and Hualalai possibly form compartments capable of impounding ground water at levels above the basal-water bodies. However, dikes probably do not control ground-water flow at or above sea level in the nearshore areas (Cox, *et al.*, 1969). The line of cinder cones northwest of the summit of Hualalai and the cinder cones north of the summit suggest the existence of dikes in these areas. The nature of their influence on ground-water movement is not known, but they appear to be so oriented and of such continuity as not to constitute a major barrier to ground-water flow (Cox, *et al.*, 1969). Cinder cones on the south flank of Manua Kea and on the north flank of Mauna Loa likewise suggest the existence of dike systems that may possibly intersect in the saddle area between the two mountains. Recent resistivity soundings by Zhody (1965) suggest that high-level dike-impounded water may be found in this area.

Probably the only significant ground-water body is a Ghyben-Herzberg lens, floating on and displacing sea water in the lava flows near sea-level throughout the coastal area between Kawaihae and Kailua-Kona. In general, recharge of fresh water to the basal lens is small throughout the area except on the western slopes of Hualalai where it is moderate to large. Consequently, the water-table gradient and the thickness of fresh water are both very small. Mixing of fresh ground water and sea water by ocean tides extends inland several thousand feet to a few miles and produces brackish ground water in the nearshore areas. Small amounts of brackish water from basal aquifers discharge freely along much of the shoreline.

Observations of the basal lens can be made only at and near the shore where numerous shallow wells, water holes, and coastal springs

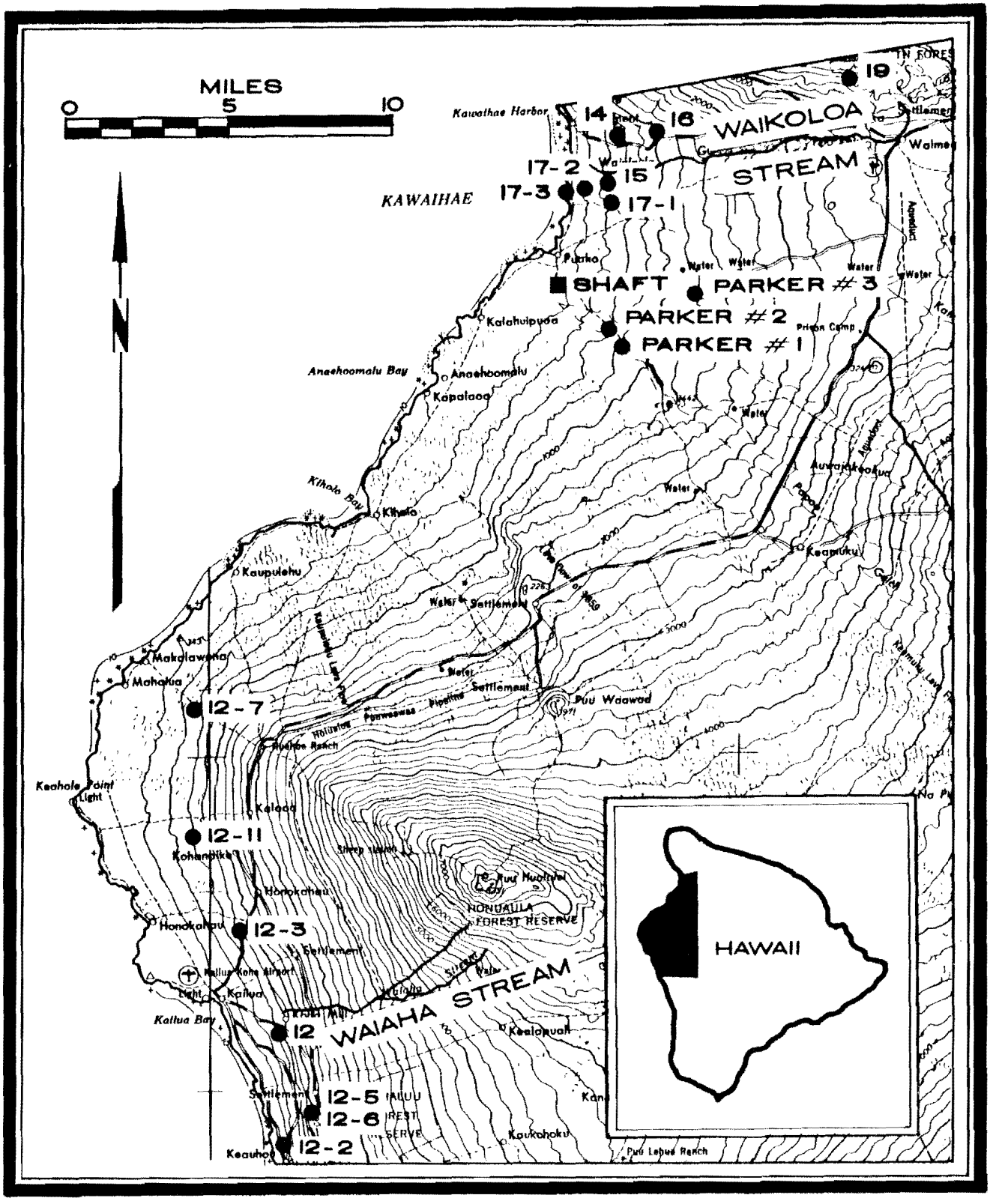

FIGURE 1.4. LOCATION MAP OF THE PRINCIPAL STREAMS AND DRILLED WELLS IN THE VICINITY OF KAWAIHAE TO KAILUA-KONA, HAWAII.

occur. However, there are a few sites inland where deep wells provide additional information pertinent to higher elevations. Stearns and Macdonald (1946) reported the chlorinity of more than 30 dug wells, springs and water holes between Hapuna Beach and Keauhou, approximately 5 miles south of Kailua-Kona. With the exception of the old Camp Drewes Marine well at Hapuna Beach, which produced water containing 560 ppm Cl^-, all of the chloride contents reported were greater than 1,000 ppm and most were greater than 2,000 ppm. A shoreline sampling program of coastal springs, ponds, and water holes between Kawaihae and Kailua-Kona was conducted to provide ground control for the infrared study, which appears as one of the sub-sections of this report. In general, the chlorinities measured ranged from 1,000 to over 15,000 ppm, and most of the values were greater than 2,500 ppm.

At least 17 known deep wells and one Maui shaft have been drilled in the near-coastal area between Kawaihae and Kailua-Kona (Fig. 1.4 and Table 1.1). Static water levels in these wells vary from less than 1-foot above sea level at Wells No. 17-3 and 17-4 only a few hundred feet from the shore to about 20 feet above sea level at Parker Ranch Well No. 3 approximately 5 miles from the shore. The chlorinity varies from 3,500 ppm Cl^- at Well No. 12-3 to only 8 ppm Cl^- at Well No. 12-5. In general, the water temperatures range from about 70 to 80°F. However, at Well No. 16 approximately 4 miles inland from Kawaihae, the water has a temperature of 96 to 98°F. The high temperature appears to be the result of residual volcanic heat, and presumably not only the fresh water but the underlying salt water may also be warmed. Furthermore, the underlying salt water may be warmer than normal even where no temperature anomaly is detected in the fresh water. If this is the case, the indicated head of 5 feet may be anomalously high, and in fact, the freshwater lens may be significantly thinner than is normally indicated by this head. This would occur because the warm salt water has a lower density than sea water of normal temperature, and consequently, the reference level for the Ghyben-Herzberg balance may be significantly higher than sea level (Cox, *et al.*, 1969).

The basalts comprising the basal aquifer generally are highly permeable and generally yield water readily to wells. The available results of pump tests are summarized in Table 1.1. At present, the principal pumpage from the basal aquifer is at Wells No. 12-5 and 12-6 near

TABLE 1.1. SUMMARY OF DRILLED WELLS BETWEEN KAWAIHAE AND KAILUA-KONA.

WELL NUMBER	OWNER AND (USE)	ALTITUDE (FEET ABOVE SEA LEVEL)	DEPTH (FEET)	STATIC WATER LEVEL (FEET ABOVE SEA LEVEL)	ANNUAL PUMPAGE (MILLION GALLONS)	CHLORIDES (PARTS PER MILLION)	TEMPERATURE (°F)	PUMP TEST RESULTS	
								PUMPING RATE (GALLONS PER MINUTE)	DRAWDOWN (FEET)
12	BWS (TEST WELL)	595	615	1.0	-	400-600	-	445	2.0
12-2	BISHOP ESTATE (TEST WELL)	100	194	-	-	1000	-	-	-
12-3	STATE OF HAWAII (TEST WELL)	801	853	1.5	-	3500	68	100	0.9
12-5	BWS (KONA WATER SYSTEM)	833	884	4.0	100	8	70	300	6.7
12-6	BWS (KONA WATER SYSTEM)	839	881	4.0	50	15-20	70	320	10.5
12-7	HUALALAI DEVELOP. CORP. (DOMESTIC AND IRRIGATION)	501	528	4.0	50	370	-	100	0.5
12-11	STATE OF HAWAII (TEST WELL)	680	702	3.2	-	740	70	300	2.0
14	STATE OF HAWAII (KAWAIHAE AND PUAKO WATER SUPPLY)	579	620	3.3	-	300	81	180	0.4
15	STATE OF HAWAII (TEST WELL)	392	430	3.3-5.1	-	500	79	180	0.0
16	STATE OF HAWAII (TEST WELL)	982	1040	5.2	-	265	96-98	200	8.5
17-1	DILROCK EASTERN (IRRIGATION)	350	376	4.5	-	600-700	-	-	-
17-2	DILROCK EASTERN (IRRIGATION)	188	218	2.0	--	600-700	-	550	1.0
17-3	DILROCK EASTERN (AIR CONDITIONING)	50	90	LESS THAN 1.0	730	2100-2800	-	-	-
19	STATE OF HAWAII (TEST WELL)	3613	924	NO WATER	-	-	-	-	-
PARKER #1	BOISE CASCADE (IRRIGATION)	813	850	6.1	-	500	82	400	1.8
PARKER #2	BOISE CASCADE (IRRIGATION)	621	-	5.1	-	370	81.5	-	-
PARKER #3 [1]	BOISE CASCADE (IRRIGATION)	1200	-	-	-	-	-	-	-
MAUI SHAFT	PARKER RANCH (STOCK WATER).	40	-	-	-	700	80	850	0.9

[1]Updated data for Parker #3: Depth - 1233 ft; Static Water Level - 20 ft; Chlorides - 25 ppm; Pumping Rate - 150 gpm; Drawdown - 2 ft.

Keauhou, which are sources in the Kona system of the Hawaii County Board of Water Supply, Well No. 12-7 near the Kona Village resort, a source for irrigation water and for domestic water which is subsequently treated, Well No. 14 near Kawaihae, which is a stand-by source in the Kawaihae-Puako system of the county water supply, and Wells No. 17-1, 17-2, and 17-3 at the Mauna Kea Beach Hotel near Kawaihae, which are sources of golf course irrigation water and air-conditioning cooling water. The Boise Cascade wells (Parker No. 1 and Parker No. 3) may soon be used as sources for irrigation water. In addition, small quantities of brackish water are pumped from the Parker Ranch Maui shaft and other shallow wells along the coast for watering livestock and for other uses.

The potential supply of fresh basal ground water in the area between Kawaihae and Kailua-Kona is not known with certainty. Cox, *et al.* (1969) estimated that the recharge to the basal ground-water body north of Hualalai and extending approximately to Kawaihae is probably less than 50 million gallons per day and that the shoreline discharge averages only a few million gallons per day per mile. Davis and Yamanaga (1968) estimated that the average daily recharge in the wet zone on the west slope of Hualalai probably amounts to several tens of millions of gallons.

BIBLIOGRAPHY

Cox, D. C., *et al.* 1969. *Coastal evidences of ground water conditions in the vicinity of Anaehoomalu and Lalamilo, South Kohala, Hawaii.* Technical Report No. 24. Water Resources Research Center, University of Hawaii. 53 p.

Davis, D. A. and G. Yamanaga. 1963. *Preliminary report on the water resources of Kohala Mountain and Mauna Kea, Hawaii.* Circular C14. Hawaii Division of Water and Land Development. 39 p.

Davis, D. A. and G. Yamanaga. 1968. *Preliminary report on the water resources of the Kona area, Hawaii.* Circular C46. Hawaii Division of Water and Land Development. 22 p.

Doell, R. R. and A. Cox. 1961. "Paleomagnetism of Hawaiian lava flows." *Nature.* Vol. 192. pp. 645-646.

Stearns, H. T. and G. A. Macdonald. 1946. *Geology and ground-water resources of the island of Hawaii.* Bulletin 9. Hawaii Division of Hydrography. 363 p.

Taliaferro, W. J. 1958. *Kona rainfall.* Hawaii Water Authority. 34 p.

Zohdy, A. A. R. 1965. *Preliminary report of the resistivity measurements on the islands of Oahu and Hawaii, Hawaii.* 41 p.

INFRARED SCANNING

WILLIAM M. ADAMS AND CLIFTON WARREN

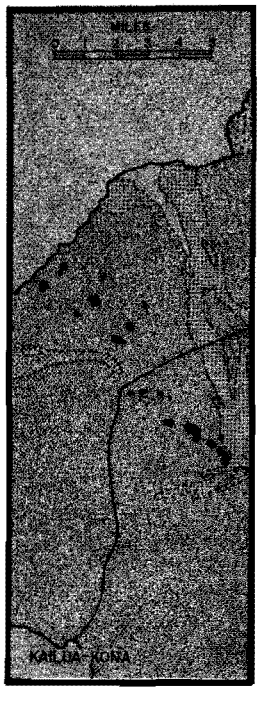

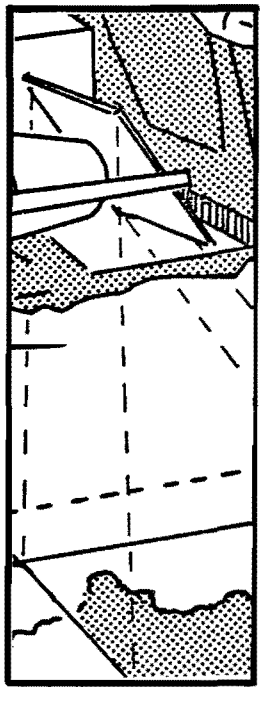

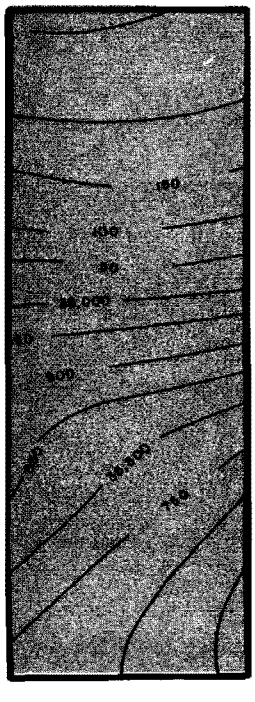

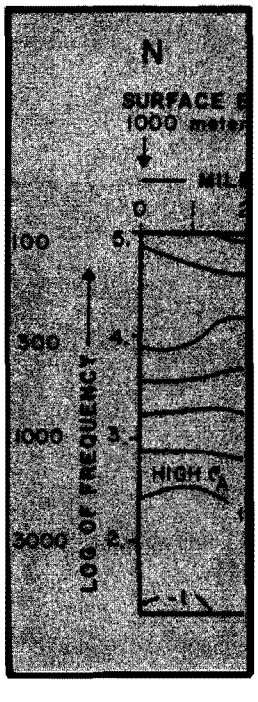

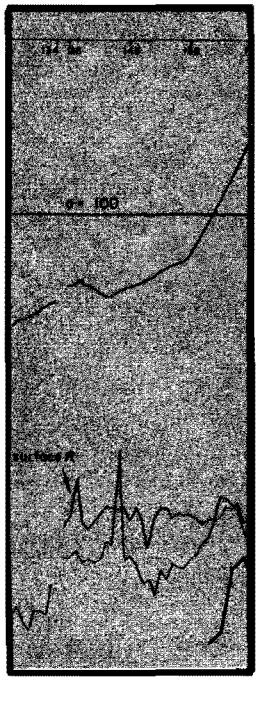

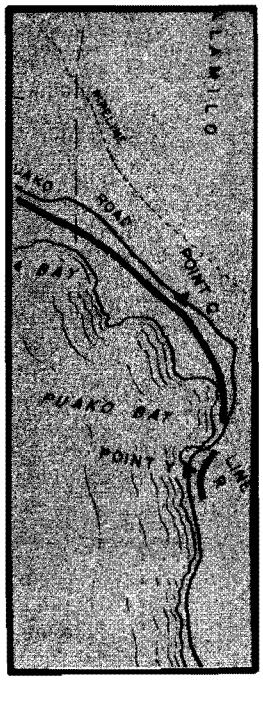

INTRODUCTION

This report covers the second and final phase of a project begun in June 1968 and previously reported by Adams and Lepley (1968). An infrared survey was made of the coastlines of the island of Hawaii under the sponsorship of the Hawaii State Department of Land and Natural Resources, Division of Water and Land Development and the Office of Water Resources Research. The first phase conducted in June 1968 surveyed the coastlines of the Kau and Puna Districts on the island of Hawaii and the second phase surveyed the coastlines from Cape Kumukahi clockwise to Upolu Point during June 1969.

As in the earlier effort, the infrared images were recorded in real-time imagery with AGA Thermovision instrumentation. However, based on past experience, the present effort attempted to establish a smoother operation and improve the reconnaissance technique and increase productivity. To accomplish this, a wider angle lens (11° x 11°) was employed with the AGA Thermovision, and an instrument port was installed in the same Apache aircraft used during the earlier survey conducted in 1968. In addition, the camera and auxillary equipment used to photograph the infrared images were also modified.

Index maps of all areas surveyed and a few sample mosaics of coastal areas having thermal anomalies have been compiled and are included in this report.

AREAS COVERED

The survey effort reported here was concentrated on the Kona to Kawaihae coastline although the southeast coast was also included. The area between Kailua-Kona and Kawaihae, located on the west coast of the island of Hawaii, span more than 20 miles of coastline (see Fig. 2.1). The climate of this leeward coastal area is generally dry except during periods of "Kona" weather.

TRAINING

Since the field chief had been directly involved with the previous phase, this previously gained experience eliminated much of the trial-and-error testing. The four members of the research team, besides the

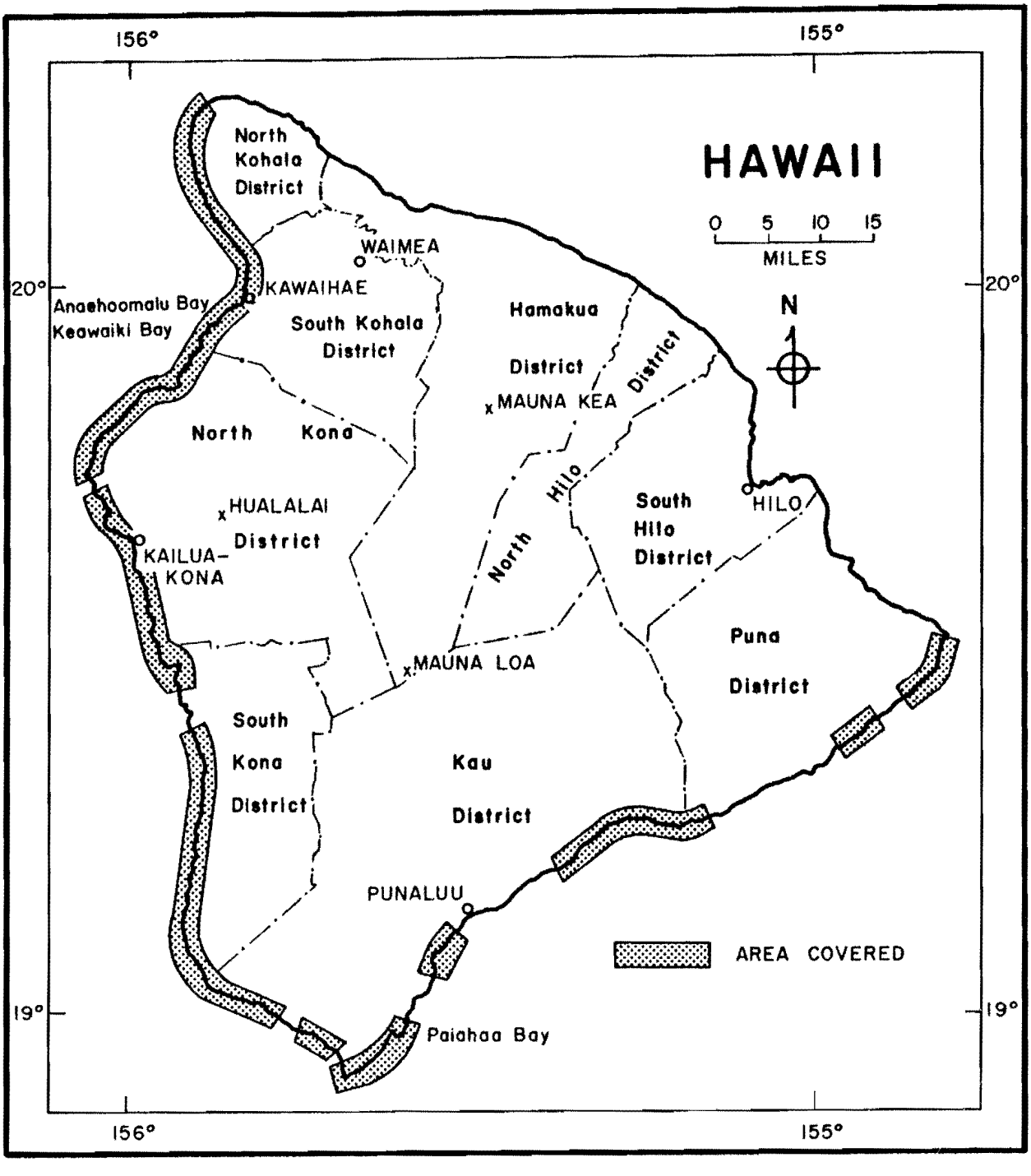

FIGURE 2.1. MAP OF HAWAII SHOWING AREAS COVERED ALONG THE WEST AND SOUTHEAST COASTS.

field chief, included the navigator, camera operator, and film processor. They were trained in all aspects of the operation, although each had a specialized job. Each member had previous experience in his specialization before the main research effort began.

Field pre-tests of the AGA Thermovision with a scanner having an 11° x 11° field of view was completed at Portland State University, Portland, Oregon. Dr. Leonard Palmer of the Department of Earth Sciences at Portland assisted in the pre-testing of the instruments. This operation was performed one week prior to the scheduled research effort in June. Pre-testing the equipment on the mainland proved to be particularly advantageous because equipment malfunction was discovered during the trial tests. The wider field of view of the scanner was deemed specially desirable, but acceptable images could not be obtained. Hence, the equipment was immediately returned to the manufacturer's service plant in New Jersey for electronic repairs.

INSTRUMENTATION

The AGA Thermovision instrumentation and basic operation has been described in a previous report (Adams and Lepley, 1968). Basically, the AGA Thermovision is a high-speed scanner which converts infrared energy in the 2 to 5.5 micron band from an electromagnetic wave to a visible image on the face of a cathode ray tube (CRT). Thus, it operates in a fashion very similar to a home television system.

There were several instrumentation changes during the past year which directly affected the scanning operation. Of these changes, the most important was the addition of a wide-angle lens to the infrared camera unit (Model 665). The wide-angle lens, which is attached to the forward end of the camera unit, has a field of view of 11° x 11° and, at the same altitude covers slightly more than four times the area covered by Model 661 which was used previously (Fig.2.2). The electro-optical operation is the same as described previously by Adams and Lepley (1968). However, when the wide-angle lens is removed, the range of focus is about 21 inches with a field of view of 5° x 5°. In other words, without the snap-away wide-angle lens, the user is left with a limited model. Therefore, the user should be absolutely certain that the wide-angle model of the Thermovision is suitable for the

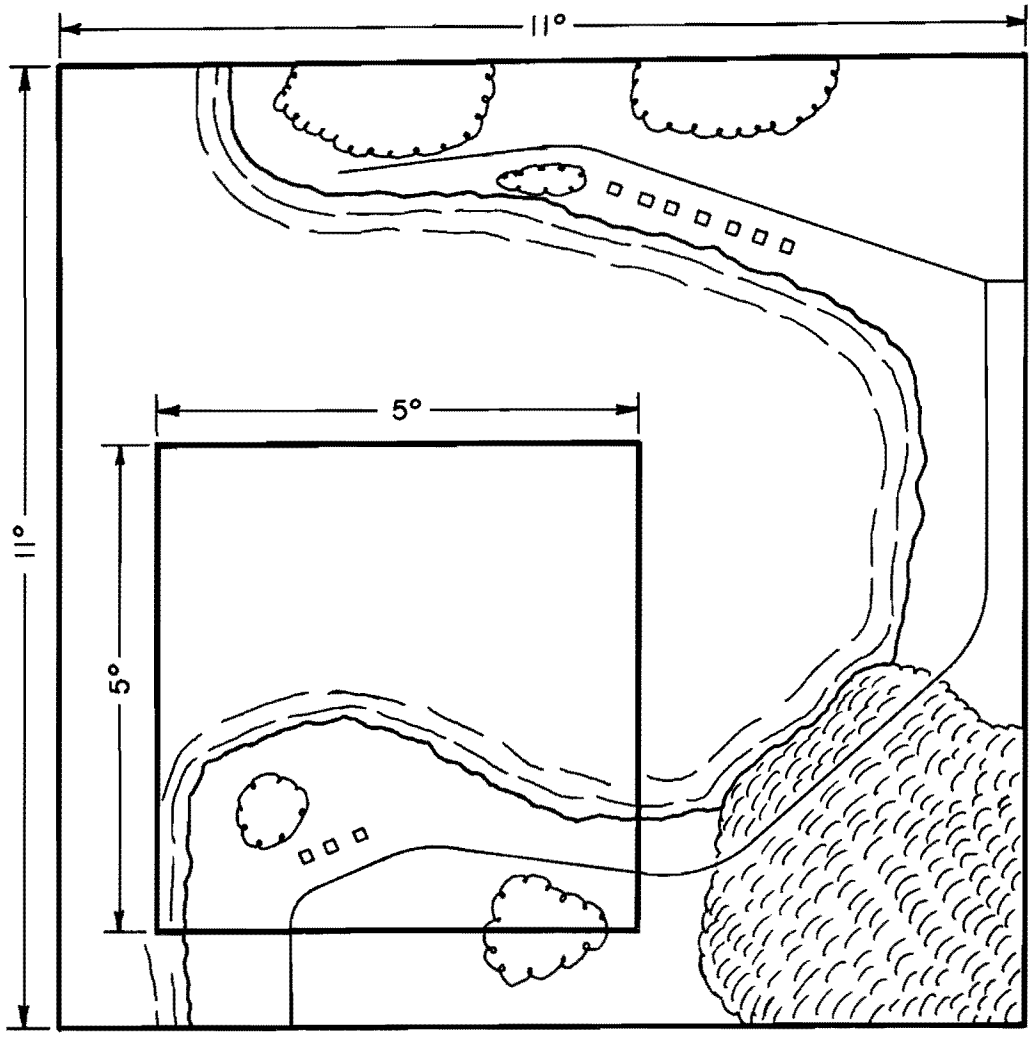

AGA THERMOVISION

IMAGE FIELD OF VIEW

MODEL 665 : 11° X 11°

MODEL 661 : 5° X 5°

FIGURE 2.2. COMPARISON OF FIELD OF VIEW - 5° X 5° VS 11° X 11°.

intended application. The benefits and disadvantages of this system are discussed in the RESULTS section.

A second change in instrumentation was the optional use of a 3.5 micron cut-on filter. This filter was designed to eliminate the sunglint which was a frequent problem during the June 1968 effort. When the filter is installed, the electromagnetic spectral band width is reduced to 2 microns (3.5 to 5.5). Thus, the filter effectively eliminates energy in the 2 to 3.5 micron band.

During pre-testing in Portland, the filter was found to be difficult to install during flight. It was necessary to remove the back plate of the camera and several components had to be disconnected before the filter could be mounted into place. Because of this difficulty, the filter was generally not used. Flights were completed before sunlight reflection became a problem. The Model 665 Thermovision was found to operate effectively at a sensitivity range of 10°C without being affected by sunglint and still be effective for detecting temperature anomalies (a fuller discussion is presented in the RESULTS section).

A third change was the use of an automatic or semi-automatic Nikon F Photographic Recorder. This system greatly facilitated the photographic process and was a far more efficient system than the 36-exposure manual-drive Minolta used in the previous research effort. Proportionately more time could be spent photographing instead of rewinding and threading film cassettes.

AIRCRAFT MOUNTING OF THE SYSTEM

The mounting of the system in the Piper Apache aircraft was greatly improved by the construction of an instrument port in the floor of the aircraft. The instrument port made it unnecessary to open the baggage door. To protect the camera unit and mirror, the 18-inch square instrument port, large enough to install other cameras to obtain a vertical downward view, was closed during takeoffs and landings. The layout of the system is shown in Figure 2.3. Since the AGA Thermovision should be forward looking and not angled more than 15° from a vertical axis, a front-surface mirror (provided by AGA) was attached to the camera to obtain the downward view. This mirror could be rotated about a horizontal axis in line with the fuselage of

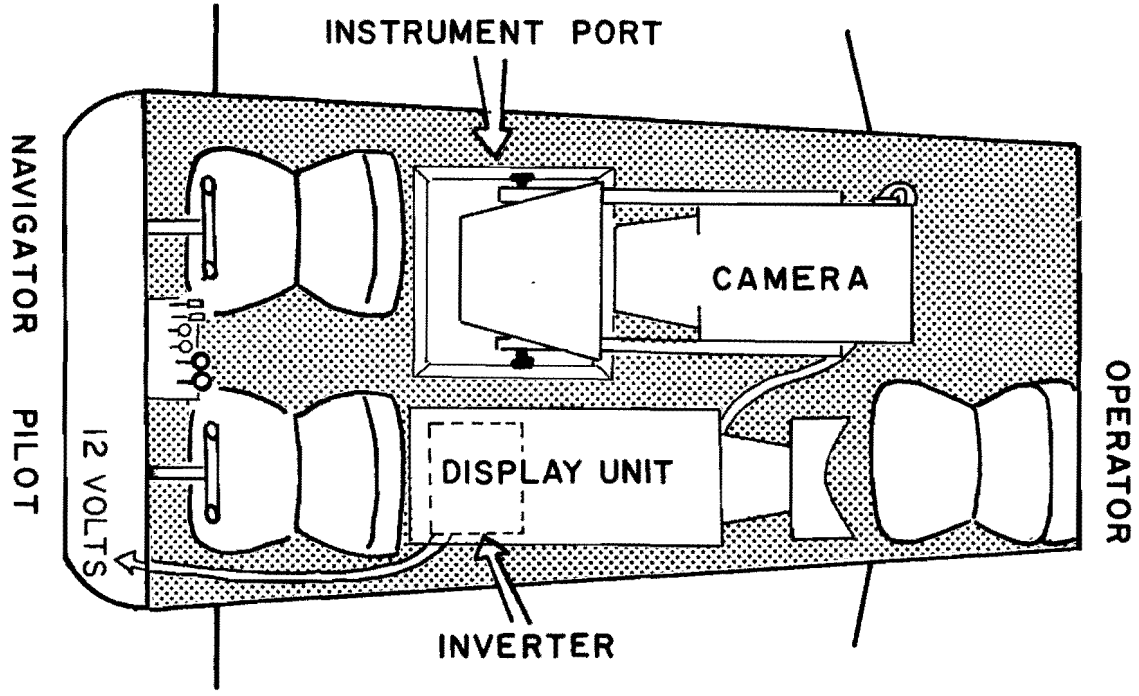

FIGURE 2.3. POSITION OF SYSTEM COMPONENTS IN CABIN OF APACHE AIRCRAFT.

the aircraft and allow the operator to track the coastline in a sweep perpendicular to the flight path (see Fig.2.4). Mounting the mirror completely within the aircraft cabin also eliminated some of the adverse effects which occurred when the unit was extended out of the baggage door in the earlier survey. The major improvement is the elimination of a flash which blotted out nearly one-fourth of many images.

As in the previous surveys, the power required to operate the system (300 watts at 110V AC) was provided by the electrical system of the aircraft via an inverter. A 20-amp circuit breaker was installed within reach of the pilot to enable him to control the 12V DC aircraft power line which was connected to a solid-state power inverter. Good grounding was essential to prevent noise from entering the system. This was particularly true when using the Nikon photographic recording system. Without proper grounding much noise was introduced into the system. The aircraft VHF transmitter also introduced noise into the system even with proper grounding, hence, the pilot refrained from transmitting during imaging.

The camera unit was mounted on the floor of the cabin with the display unit and inverter installed into a rack directly in front of the camera-operator. He remained in his seat while operating the camera rotation unit or the Nikon Recorder with his right hand and the display unit control with his left (Figs. 2.3 and 2.4).

FIELD PROCEDURE

An early morning flight was planned for each day. Adverse weather conditions (clouds, haze, etc.), personnel, and aircraft maintenance problems cancelled about 20 percent of the planned operations. A volcanic eruption on the island caused atmospheric contamination which adversely affected the images (see RESULTS section).

Nearly every morning during early summer, the Kona area has a cover of haze, which eventually "burns" off by late morning. This haze, has a detrimental effect on infrared images and results in varying degrees of attenuation of the incident infrared radiation at the detector. Most flights were completed during the daylight hours before 9 AM to avoid the adverse effects of the sun's radiation as well as to

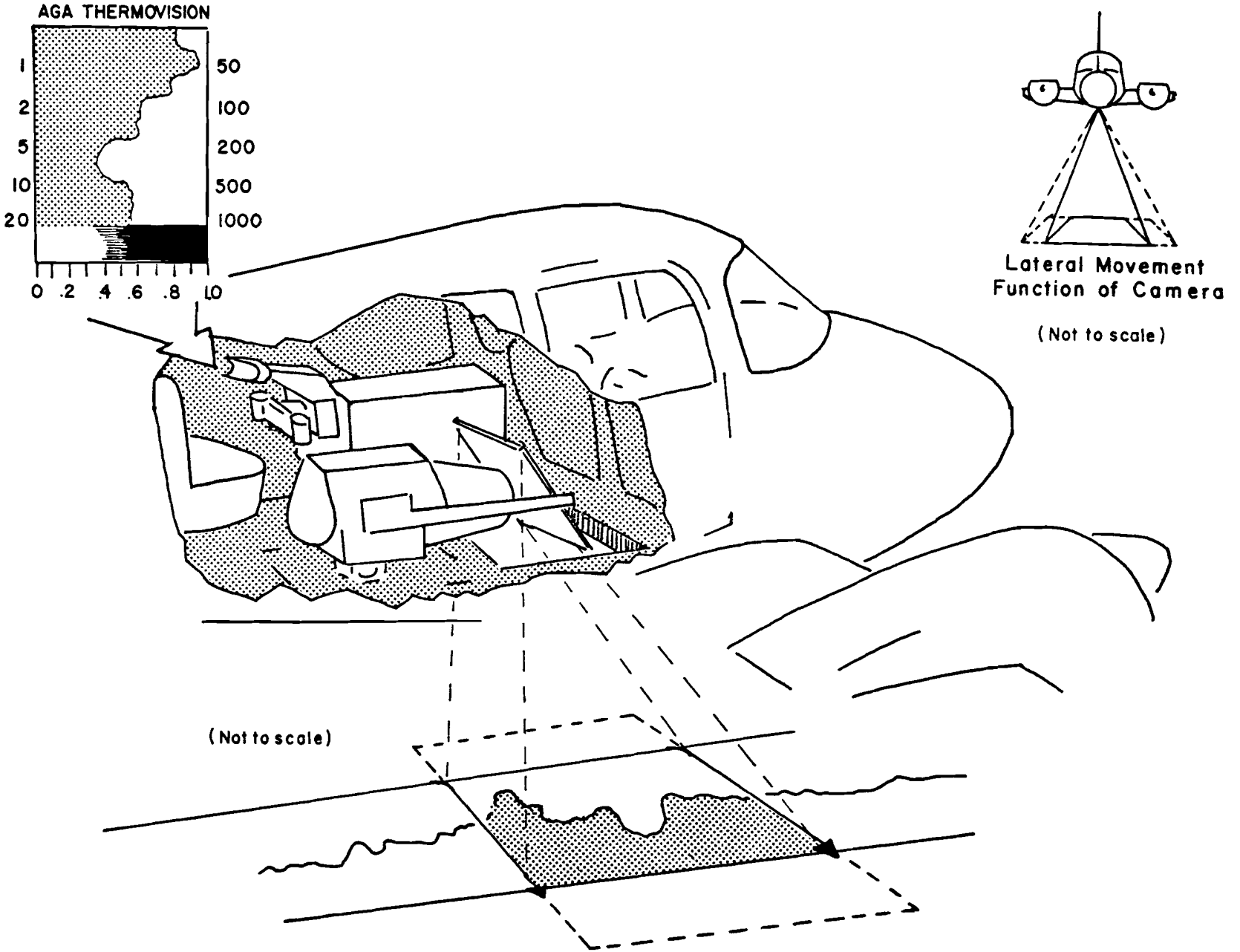

FIGURE 2.4. INSTALLATION OF CAMERA UNIT AND IMAGING PROCESS.

complete infrared scanning during low tide.

Each flight crew consisted of a pilot, navigator, and camera operator. The camera operator was responsible for filling the AGA Thermovision with liquid nitrogen, having enough film, and so forth. The navigator was responsible for planning flight paths and having proper maps and charts for each flight. The field chief coordinated all aspects of the survey.

Inflight operations were directed by the navigator with the operator indicating when acceptable images had been recorded. The navigator acted as the central communicator between the instrument operator and the pilot. In addition, it was the navigator's responsibility to map the areas scanned and to catalog film cassettes exposed in flight.

PHOTOGRAPHING THE IMAGE

A major improvement over the previous effort was the use of the Nikon F photographic recording system to photograph, and thus record permanently, the image appearing on the face of the cathode ray tube in the thermovision display unit. This system used 250-frame 35-mm film strips with continuous or semi-automatic advance and shutter operation. Since the continuous operation mode could not be adjusted to be slower than 2 frames per second, the system was used in the manual mode with automatic advance. This mode permitted the operator to photograph the image by pushing a button, located conveniently near the camera unit, which automatically advanced and cocked the film. Ground-area coverage was thus obtained without undue overlap of images and the time needed for loading and unloading film was reduced considerably. Forty percent overlap was preferred.

For comparison and identification purposes, color infrared and color ektachrome were used on certain flight paths in dual Minolta 35-mm cameras hand held and aimed orthographically through the instrument port.

RESULTS

The 11° x 11° field of view was a notable improvement over the 5° x 5° used in the previous research effort. Combined with good flight path planning, the wider field of view allowed for complete coverage of

all bays and peninsulas. Figure 2.5 shows a comparison of the coastline coverage of the Paiahaa Bay area on the southeast coast of Hawaii of the 5° x 5° lens with that of the 11° x 11° lens. There also seems to be an improvement in the tonal quality. The 11° x 11° model was used at a sensitivity of 10°C although the 5° x 5° model had best been utilized at 5°C.

The AGA's temperature sensitivity, or the temperature difference between black and white, of 10°C (Δt = 10°C) allowed for more gray tones with the consequent advantages of being able to identify both the thermal anomalies in the water and the features on land. Mounting the front-surface mirror inside the aircraft reduced sunglint. However, during certain positions of the aircraft, the angle of incident solar radiation did have an effect on the visual resolution of the image.

Since the AGA Thermovision operates with either emitted or reflected energy available in the 2 to 5.5 micron band, the lack of sunlight and its reflecting energy greatly assists the spatial identification of ambient or cooler temperatures. Thus, it was found that the best images for coastal water anomalies were obtained with minimum sunlight, between 5:30 and 9:30 AM before the more adverse effects of solar radiation had set in. Ground observations had indicated that by 9:30 black rocks around the cool fresh-water springs warmed up the sea water, and on-shore winds caused the warmer sea water to mask the cooler fresh water.[1]

During June 1969, the eruption of Kileaua volcano caused heavy pollution of the lower atmosphere and affected the quality of the infrared images by causing an effect similar to that caused by dense haze. Attentuation of the incident infrared radiation caused reduced thermal and spatial resolution in the images. This was presumably caused by the effective absorption and scattering of infrared radiation by the particles and gases, especially CO_2, spewed into the atmosphere by the erupting volcano. When weather conditions were clear, most of the images were of high quality.

Although many cool zones were discovered, as was pointed out in a previous report (Adams and Lepley, 1968), the image only reveals a thermal anomaly. Ground-based observations are required to ascertain

---

[1]Lepley, personal communication.

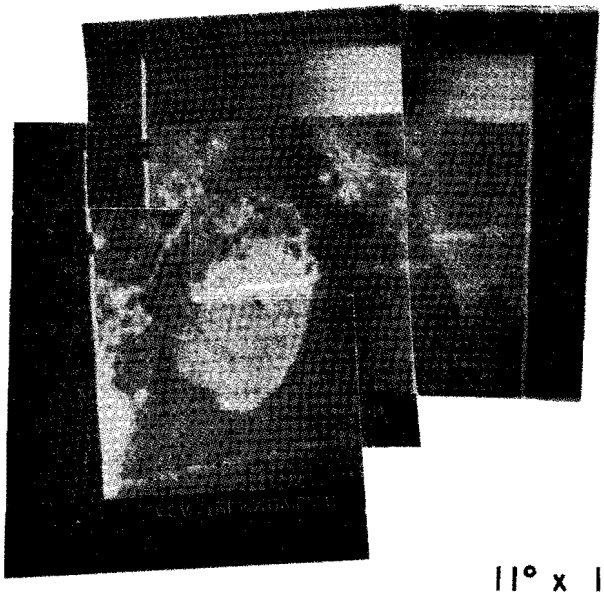

11° x 11°

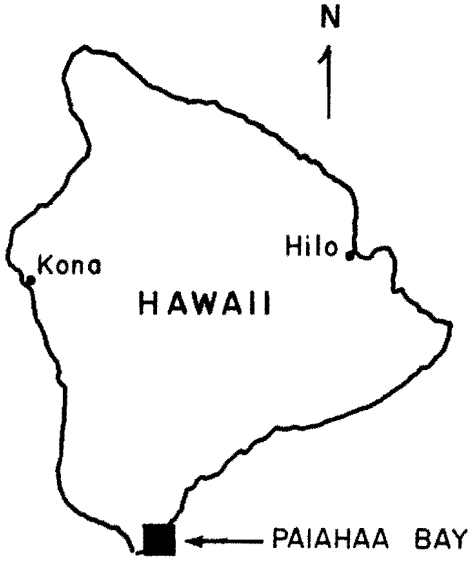

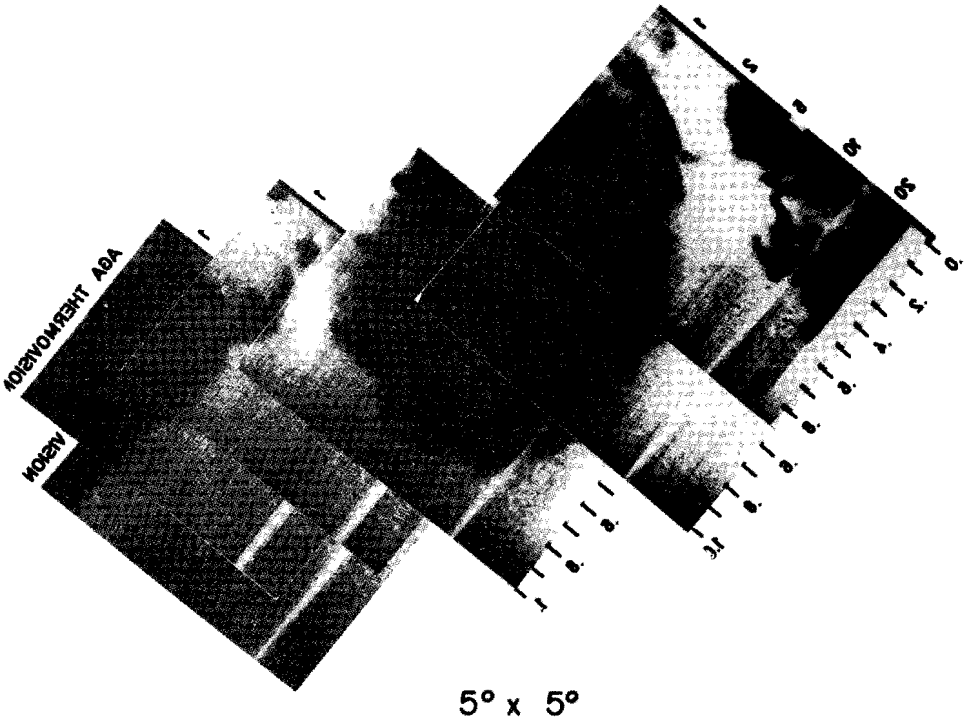

5° x 5°

FIGURE 2.5. COMPARATIVE MOSAICS OF PAIAHAA BAY AREA.

water quality. Designation of the locations of notable thermal anomalies does not necessarily imply association of fresher water. Other work has emphasized that not all thermal anomalies have associated fresher water, and not all fresher water has associated thermal anomalies. An infrared survey should only be considered a reconnaissance technique to obtain an instantaneous, synoptic sample. No meaningful quantitative or qualitative information can be obtained with current airborne procedures. Figures 2.6 and 2.7 are mosaics of the Kawaihae coastline which show thermal anomalies as darker areas along the coastline.

The compiling and cataloguing of this year's data has also greatly benefitted from the experience of the previous research efforts (see Appendix).

The measurements obtained during the June 1968 offshore survey are considered to be suitable for comparison with both the 1968 and 1969 infrared data. Offshore temperature and conductivity measurements were made at the surf zone from a 16-foot boat by alternately measuring temperature and conductivity at a cell suspended in two inches of water off the bow of the boat. Geographic distribution of the data is shown for the Kona coast in Figures 2.8, 2.9, and 2.10. Temperature above 70°F is shown by the bar to the left and resistivity is shown by the bar to the right. Comments on shore features visible from the boat, as taken from the log, are given in the enlargements of the areas covered. The northernmost resistivity high at Pauoa Bay is associated with a temperature *high* (not low) and Pauoa Bay did *not* display an infrared thermal anomaly. The resistivity anomaly at Waialua Bay had no corresponding thermal anomaly and hence no infrared anomaly was noted. The offshore ground survey indicated that the fresher water in Anaehoomalu Bay is not *cooler* than the ambient waters and, hence, no infrared anomalies were recorded. Based on these observations, it should be noted that not all coastal discharges have the associated cooler anomalies, and further, not all thermal anomalies are associated with coastal discharges, as emphasized by Adams and Lepley (1968).

Similar comparisons can be made for the remainder of the coast between the conductivity anomalies, temperature anomalies, and infrared anomalies shown in the Appendix.

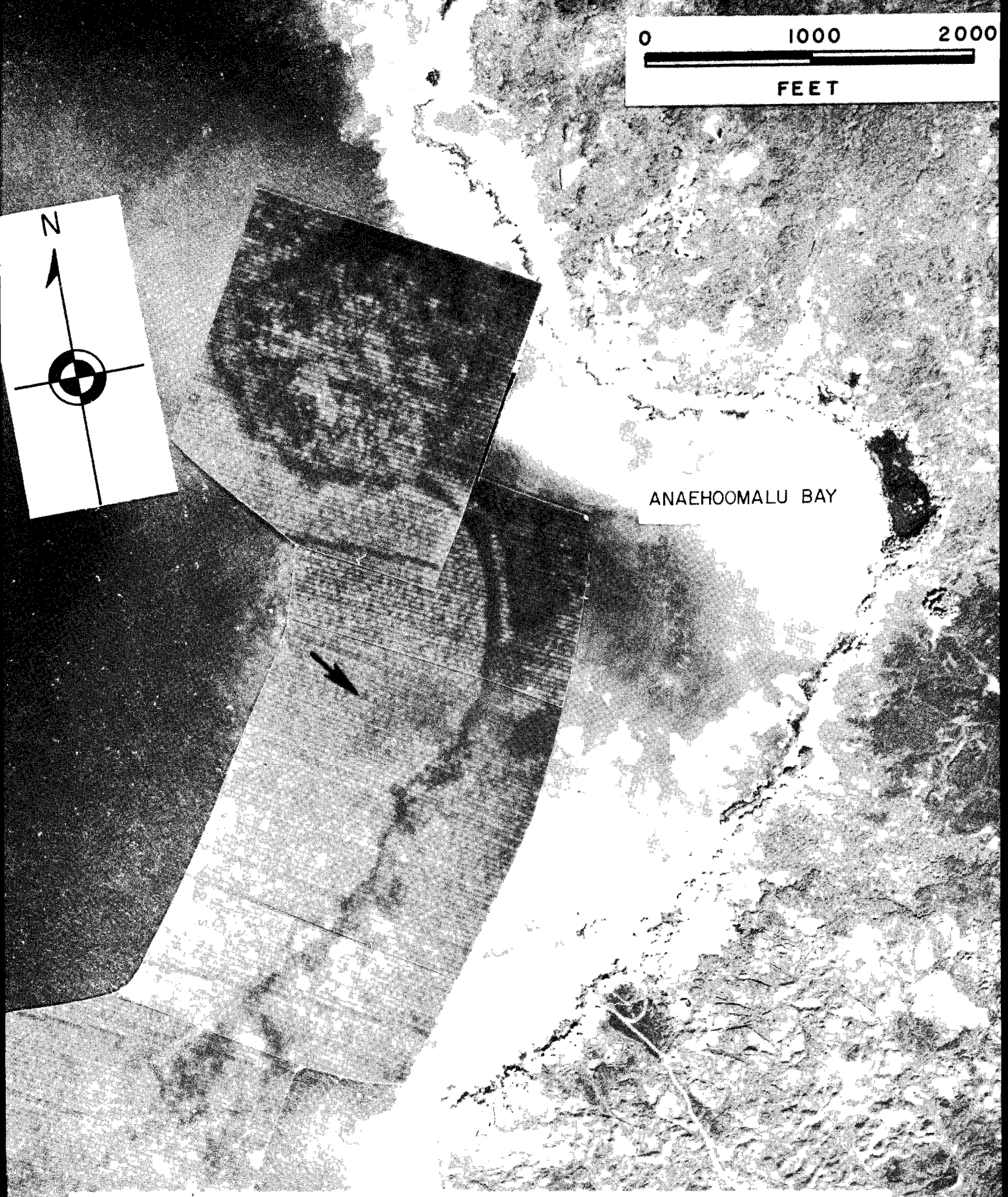

FIGURE 2.6. MOSAIC OF 11° X 11° INFRARED IMAGES MOUNTED ON AN AERIAL PHOTOGRAPH OF ANAEHOOMALU BAY (LOCATION SHOWN ON MAP 8 IN APPENDIX). THE THERMAL ANOMALY IS INDICATED BY BLACK ARROW.

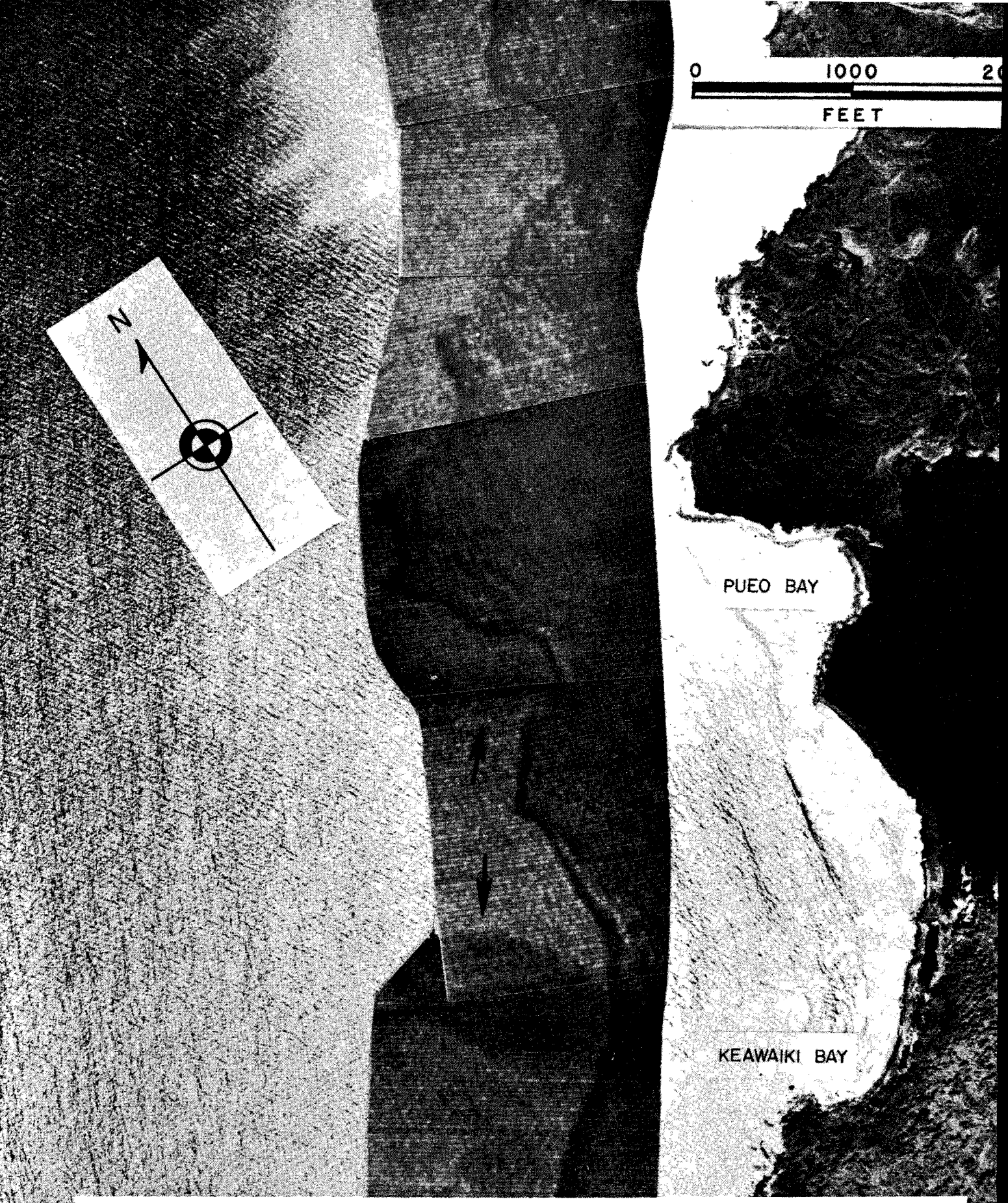

FIGURE 2.7. MOSAIC OF 11° X 11° INFRARED IMAGES OVERLAIN ON AERIAL PHOTOGRAPHY OF PUEO BAY TO KEAWAIKI BAY (LOCATION SHOWN ON MAP 9 IN APPENDIX). TWO THERMAL ANOMALIES ARE INDICATED BY BLACK ARROWS.

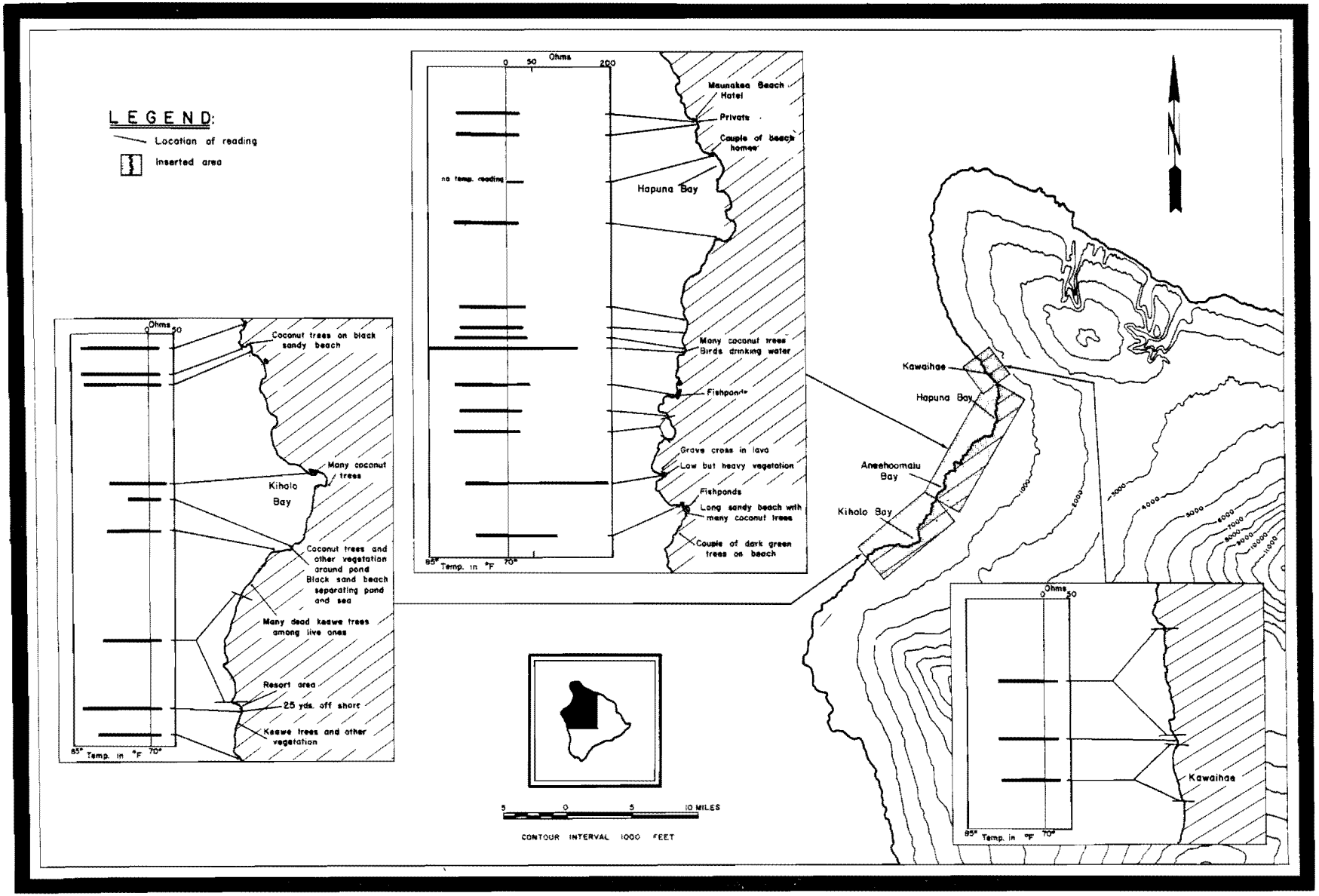

FIGURE 2.8. THE RESISTIVITY (EXPRESSED IN OHMS) AND TEMPERATURE (EXPRESSED IN DEGREES F) DATA OBTAINED BY AN OFFSHORE SURVEY ARE PLOTTED IN HORIZONTAL BAR GRAPHS IN THREE ENLARGED SEGMENTS FOR THE AREA BETWEEN WAIAKAILIO BAY TO KUMUKEHU POINT.

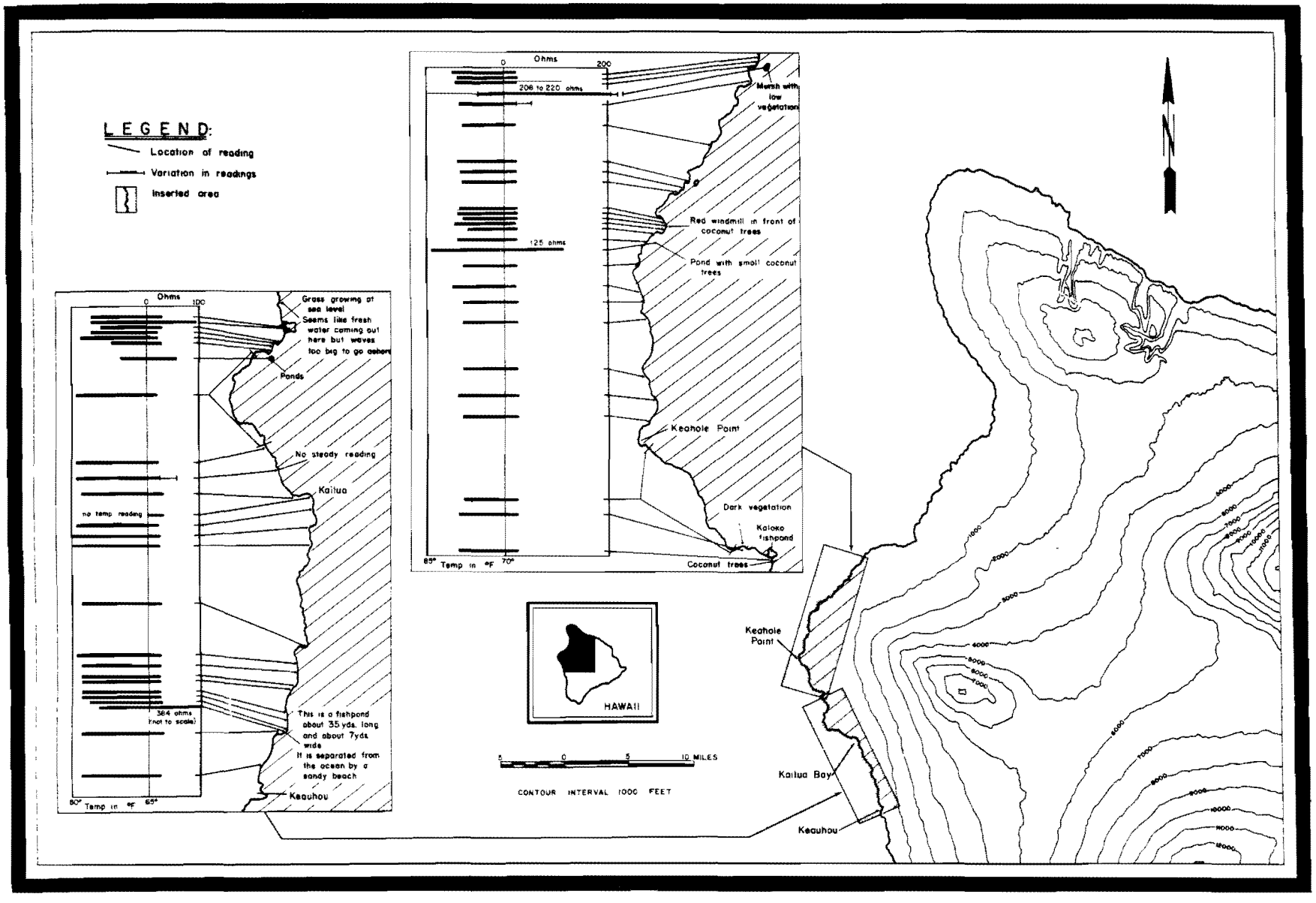

FIGURE 2.9. THE RESISTIVITY (EXPRESSED IN OHMS) AND TEMPERATURE (EXPRESSED IN DEGREES F) DATA OBTAINED BY AN OFFSHORE SURVEY ARE SHOWN IN TWO ENLARGED SEGMENTS FOR THE AREA BETWEEN KUMUKEHU POINT AND KEAUHOU BAY.

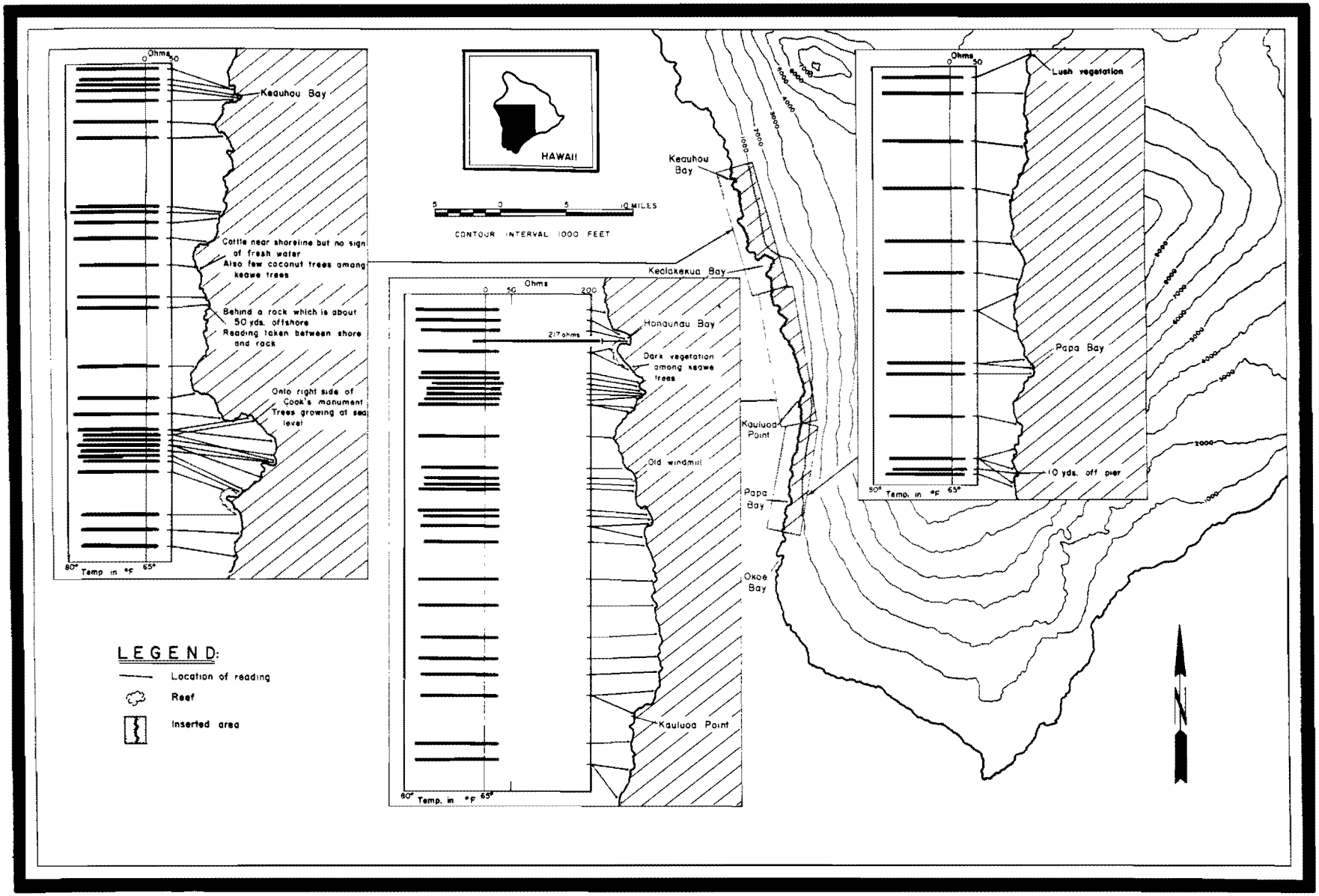

FIGURE 2.10. THE RESISTIVITY (EXPRESSED IN OHMS) AND TEMPERATURE (EXPRESSED IN DEGREES F) DATA OBTAINED BY AN OFFSHORE SURVEY ARE SHOWN IN THREE ENLARGED SEGMENTS FOR THE AREA BETWEEN KEAUHOU BAY AND HONOMALINO BAY.

ACKNOWLEDGEMENTS

In spite of much past experience, no research effort could be successful without the devotion and cooperation of each member of the research team. The accomplishments described in this report would not have been possible without these attributes. The success of this survey is primarily due to Roy Araki, Charles Dorigan, and Ken Peale, film processor, navigator, and camera operator, respectively. Their efforts, as well as that of the pilot, Jim Askern, are gratefully acknowledged.

The University's Piper Apache was made available through the efforts of Mr. Leonard Knowles who also provided much assistance when aircraft maintenance problems arose.

Funding of this project has been provided by the Hawaii Department of Land and Natural Resources, Division of Water and Land Development and the Federal Office of Water Resources Research of the Department of the Interior. Assistance and guidance essential to the success have been supplied by the AGA representative, Mr. Jack Patterson. The pre-test at the Portland State University was made possible by Dr. Leonard Palmer, who arranged for the pilot, aircraft, and darkroom facilities.

The facilities of the Hilo Campus have graciously been made available by Dr. H. F. Little, Chairman of the Department of Natural Sciences. The personnel of the Anthropology Department were especially hospitable. Ground transportation in the Hilo area was provided, in part, by Lance Thompson of C. Brewer and Co.

The observations on coastal waters conducted concommitantly with this scanning effort under the direction of Larry Lepley will be reported separately in a master's thesis being prepared by the junior author.

BIBLIOGRAPHY

Adams, William M. and Larry K. Lepley. 1968. *Infrared Images of the Kau and Puna Coastlines on Hawaii.* Technical Report No. 26. Water Resources Research Center, University of Hawaii. 51 p.

APPENDIX: CATALOG OF THE IMAGES

CATALOG OF THE IMAGES

The purposes of this report are to describe the instrumentation and procedures used, present representative examples of infrared imagery, and catalog the images for the western and southeastern coastline of the island of Hawaii.

In the course of the survey, more than one thousand usable Thermovision images of the coastline of Hawaii have been recorded. Due to overlap, approximately half of these suffice for complete coverage of the coastline.

The images are catalogued by geographic location. The image containing any particular point on the coastline is located by:

1) Finding the point of interest on the master index map,
2) Noting the number of the enclosing sub-index catalog map, (there are 44 such maps),
3) Turning to the appropriate sub-index catalog map,
4) Locating the point of interest on the sub-index catalog map,
5) Noting the number of the enclosing frame.
6) Finding the nearest triple-number code: an Arabic number, hyphen, Arabic number, hyphen, Roman numeral (see explanatory diagram).

The first Arabic number is the roll of film used that day, the second Arabic number is the day in June 1969 on which the imagery was taken, and the Roman numeral is the section of the film rolls (the film rolls were sectioned for ease in handling).

The original film are on file at the Water Resources Research Center on the Manoa Campus of the University of Hawaii. A montage of the entire coastline is also available for inspection there.

The end of a film section and the beginning of a new film section is indicated by a solid arrow with the pertinent code above or below the arrow. (See the sample explanatory diagram. The code designation above marks the end of section V of film roll 3 taken on June 8, 1969). When two sections overlap, the end of the lower-numbered section is indicated by a dashed-line film frame; the higher-numbered section by a solid-line film frame (see diagram).

Notable relative thermal anomalies are indicated by five-pointed stars. Any star not enclosed by a numbered film frame, for example,

bottom of sub-index map no. 5, can be located inside a numbered film frame on another sub-index catalog map (see map no. 6.).

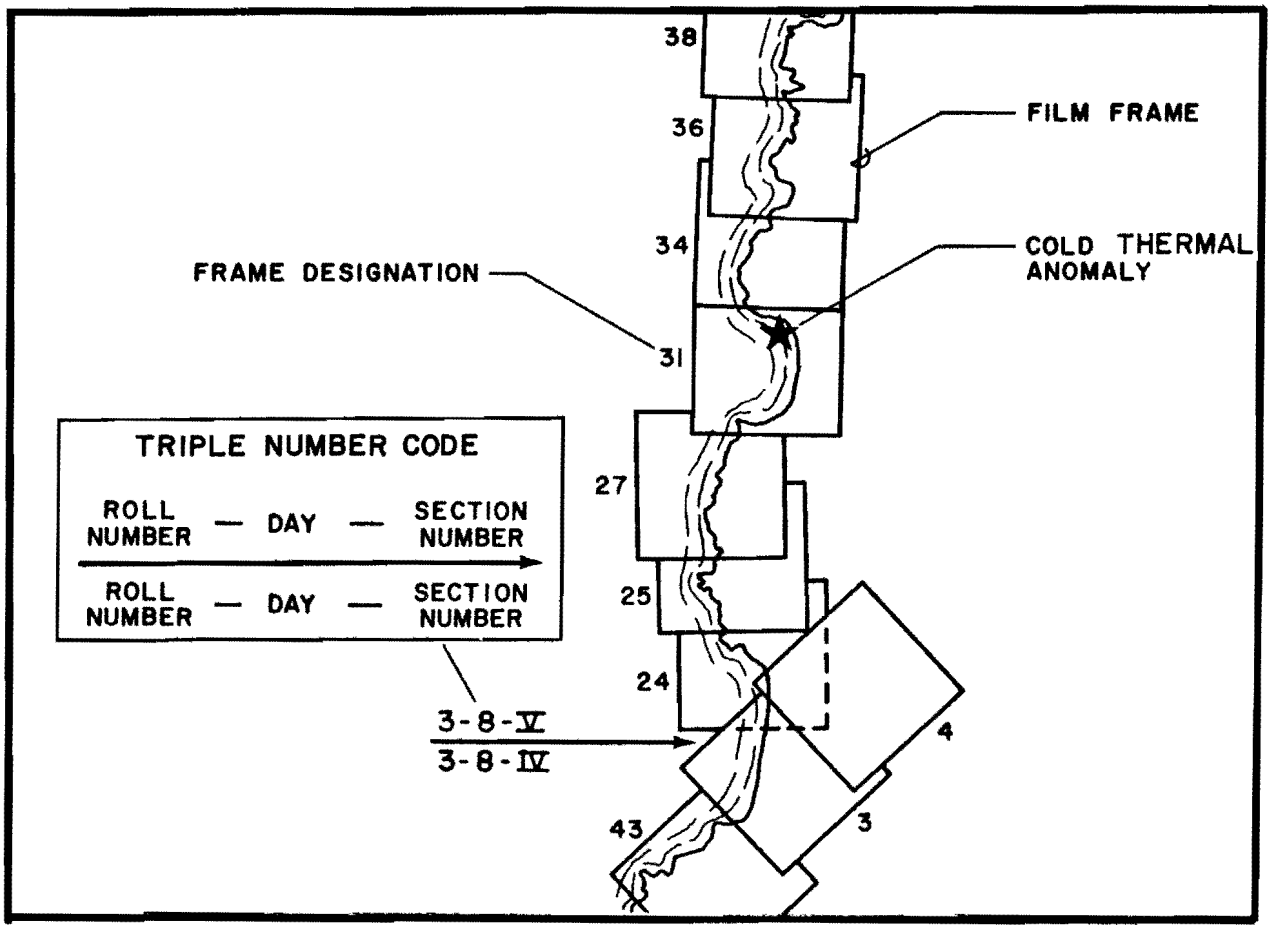

DIAGRAM OF CODE AND SYMBOLS USED IN THE CATALOG OF THE IMAGES.

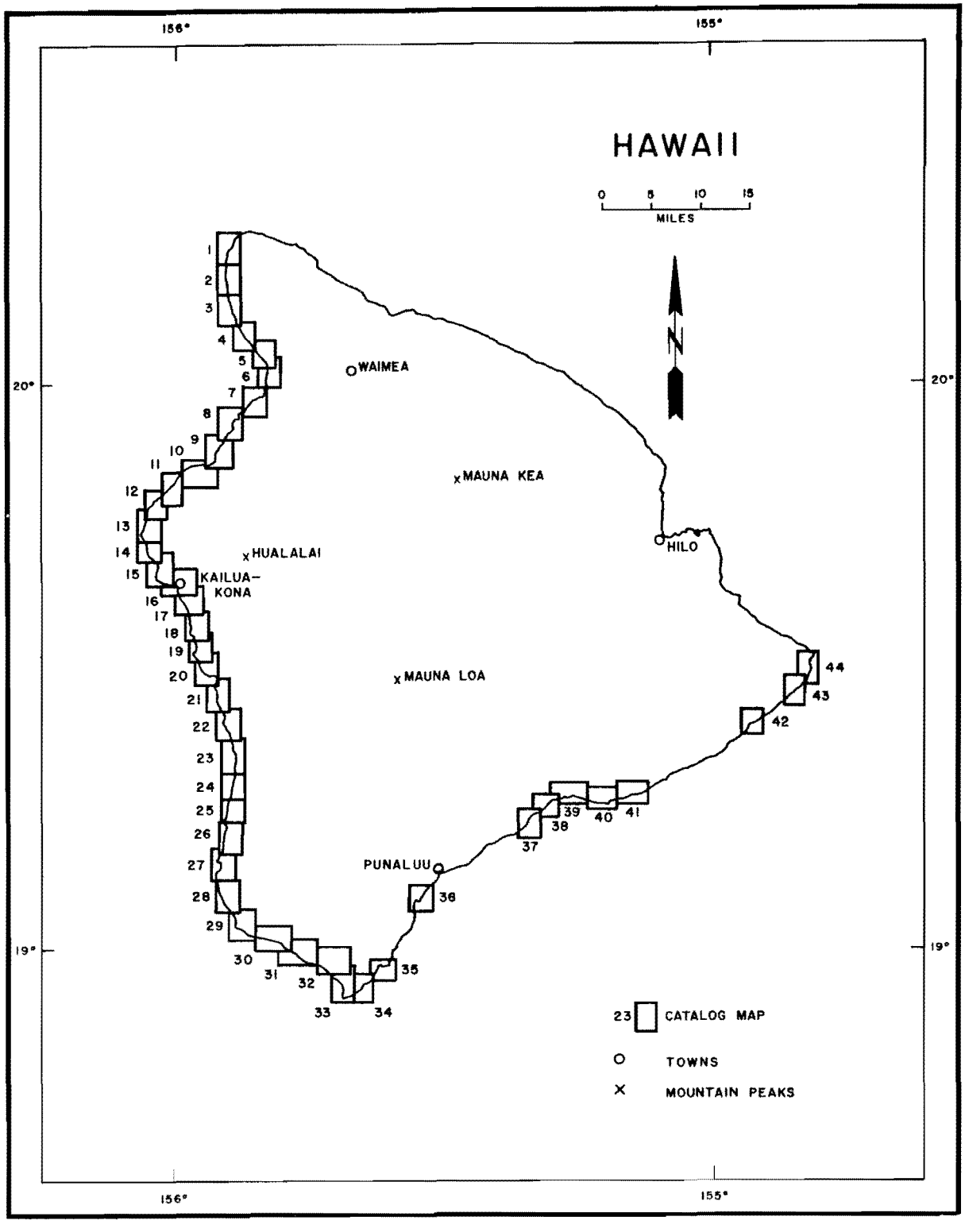

MASTER INDEX MAP

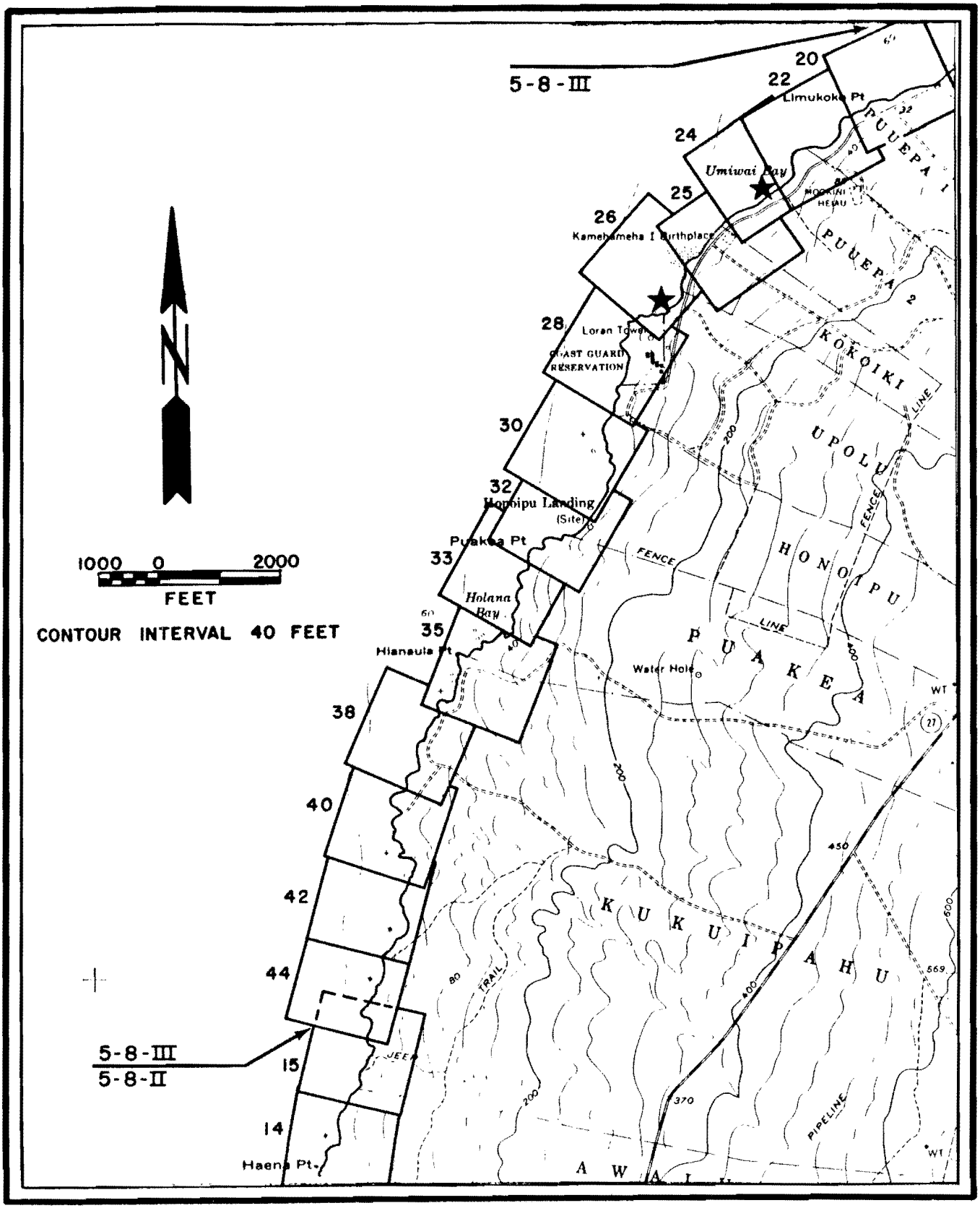

SUB-INDEX MAP NO. 1

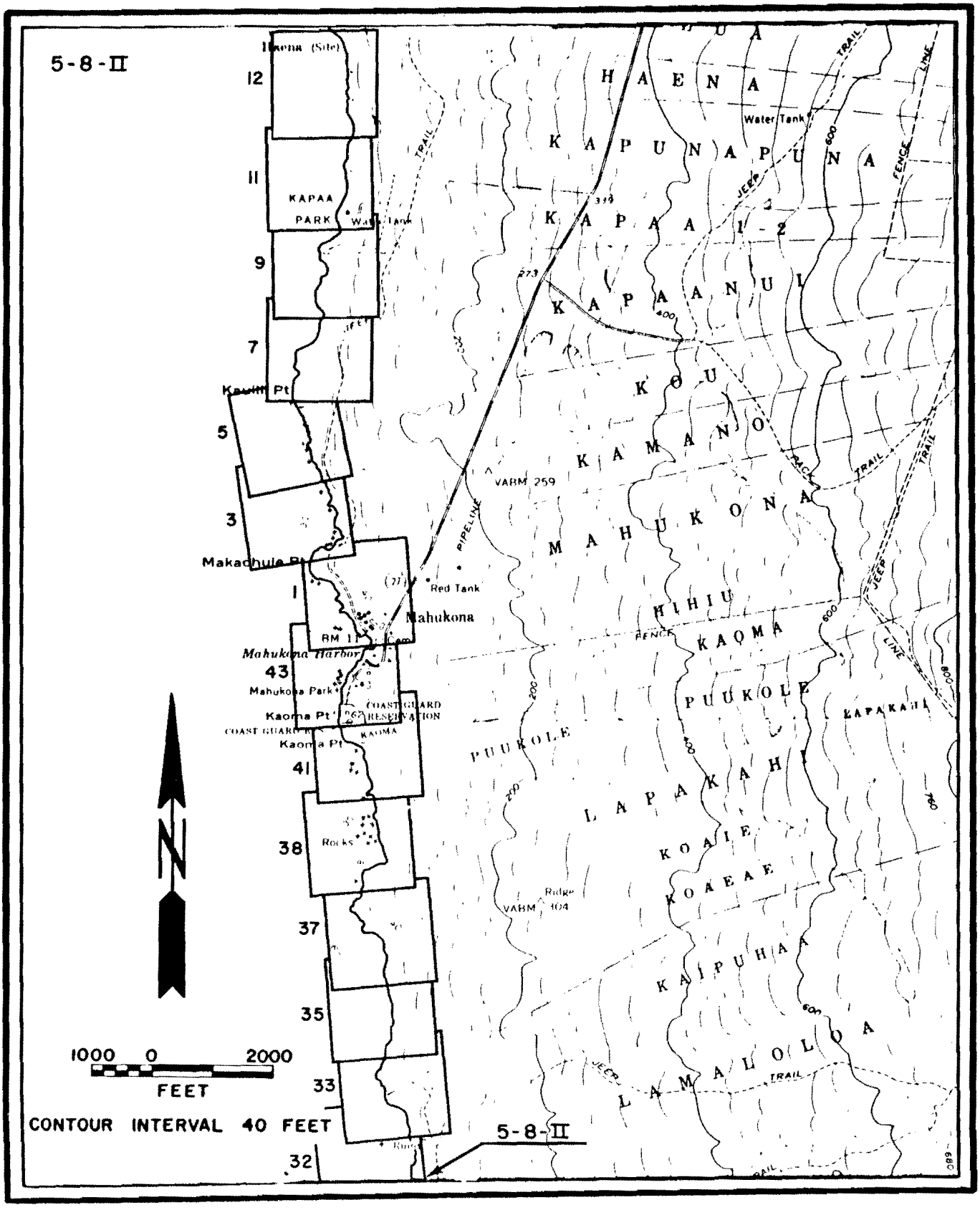

SUB-INDEX MAP NO. 2

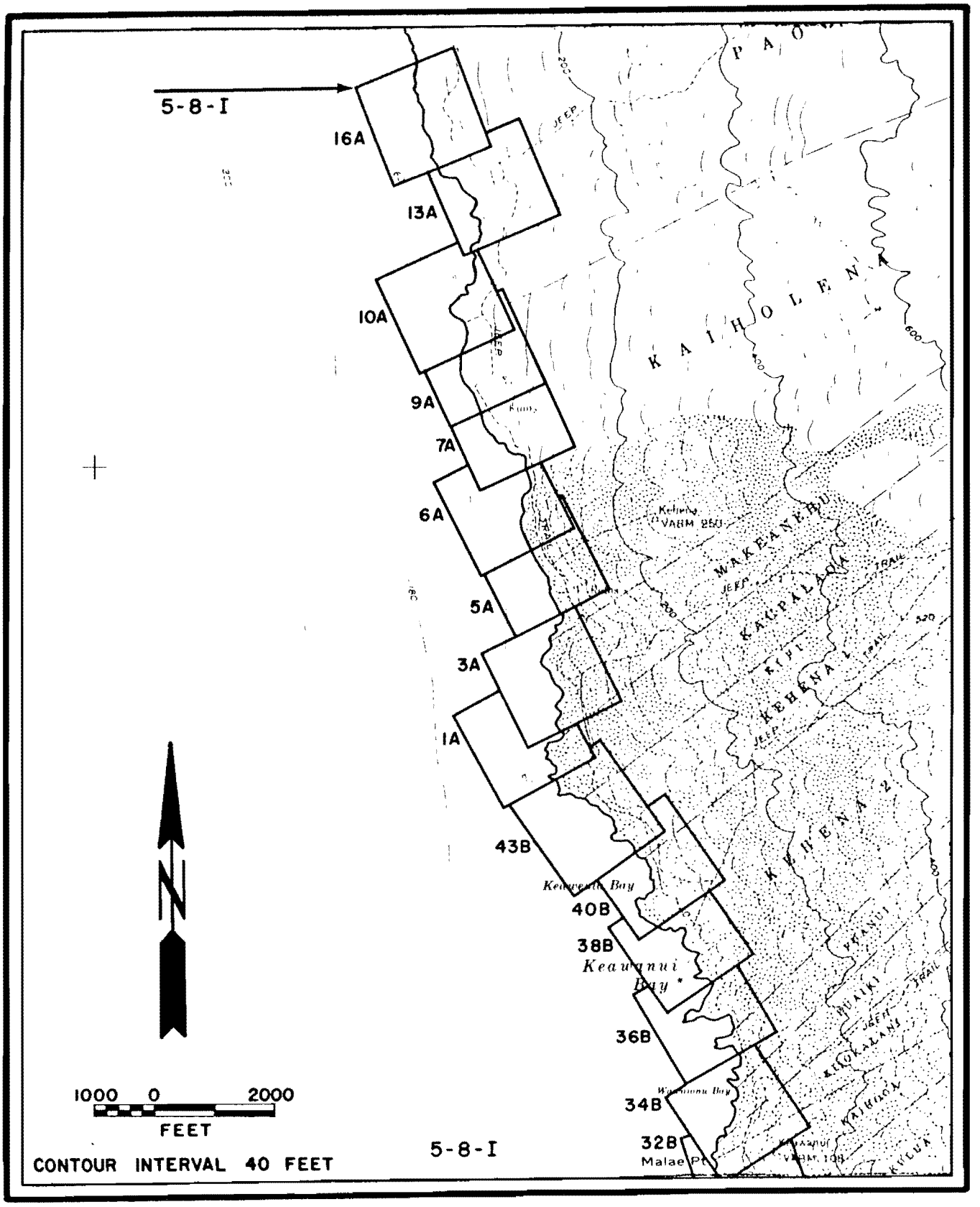

SUB-INDEX MAP NO. 3

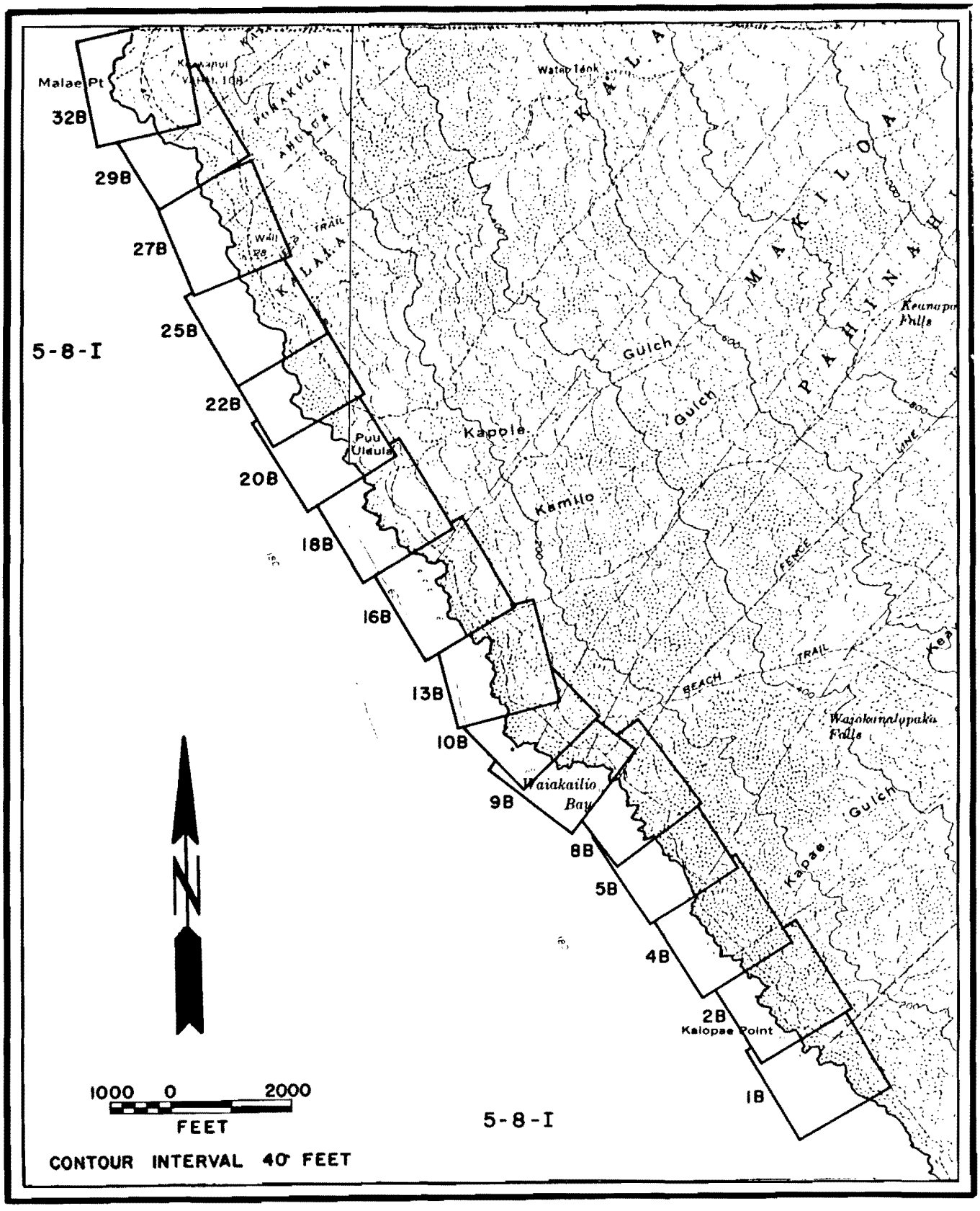

SUB-INDEX MAP NO. 4

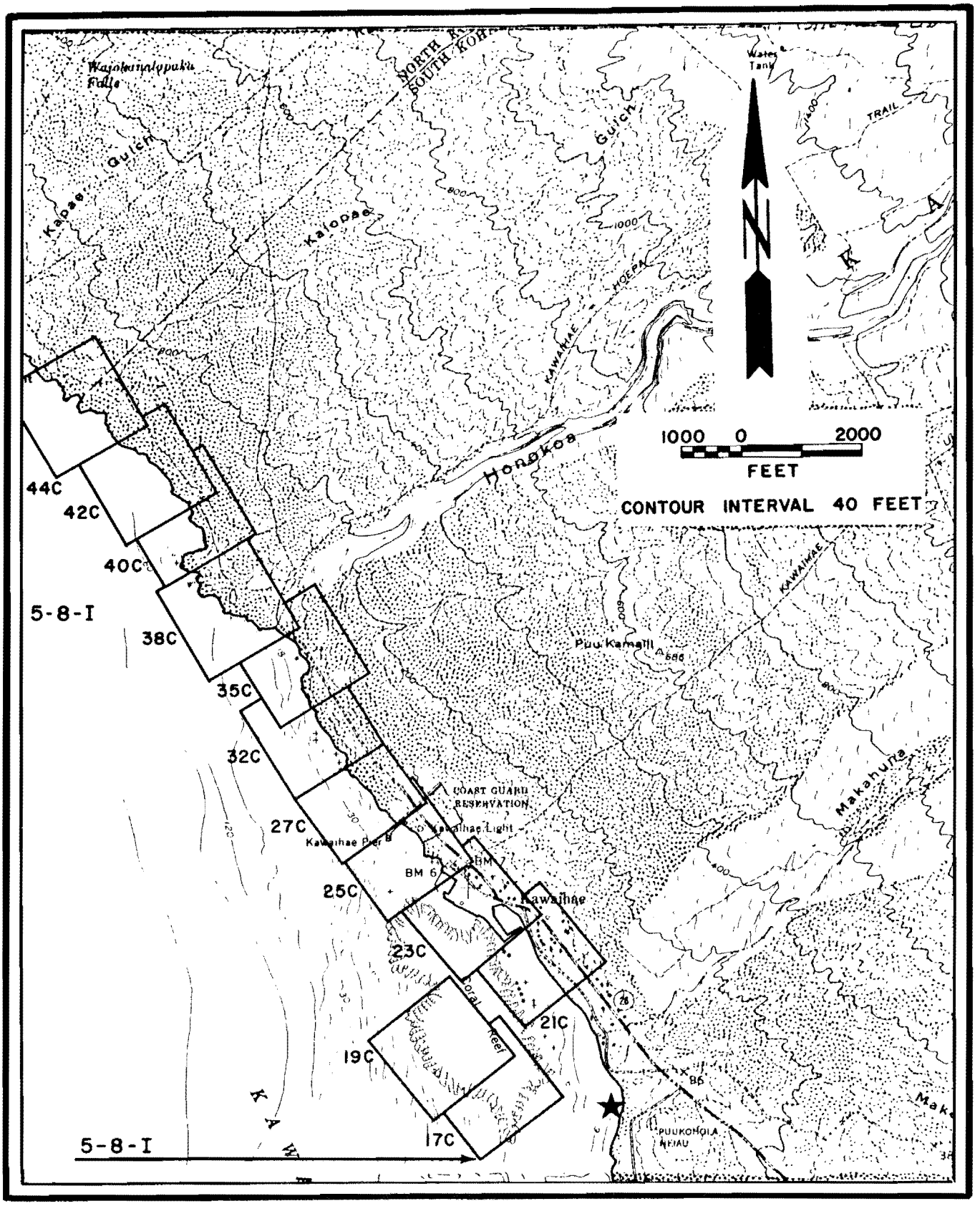

SUB-INDEX MAP NO. 5

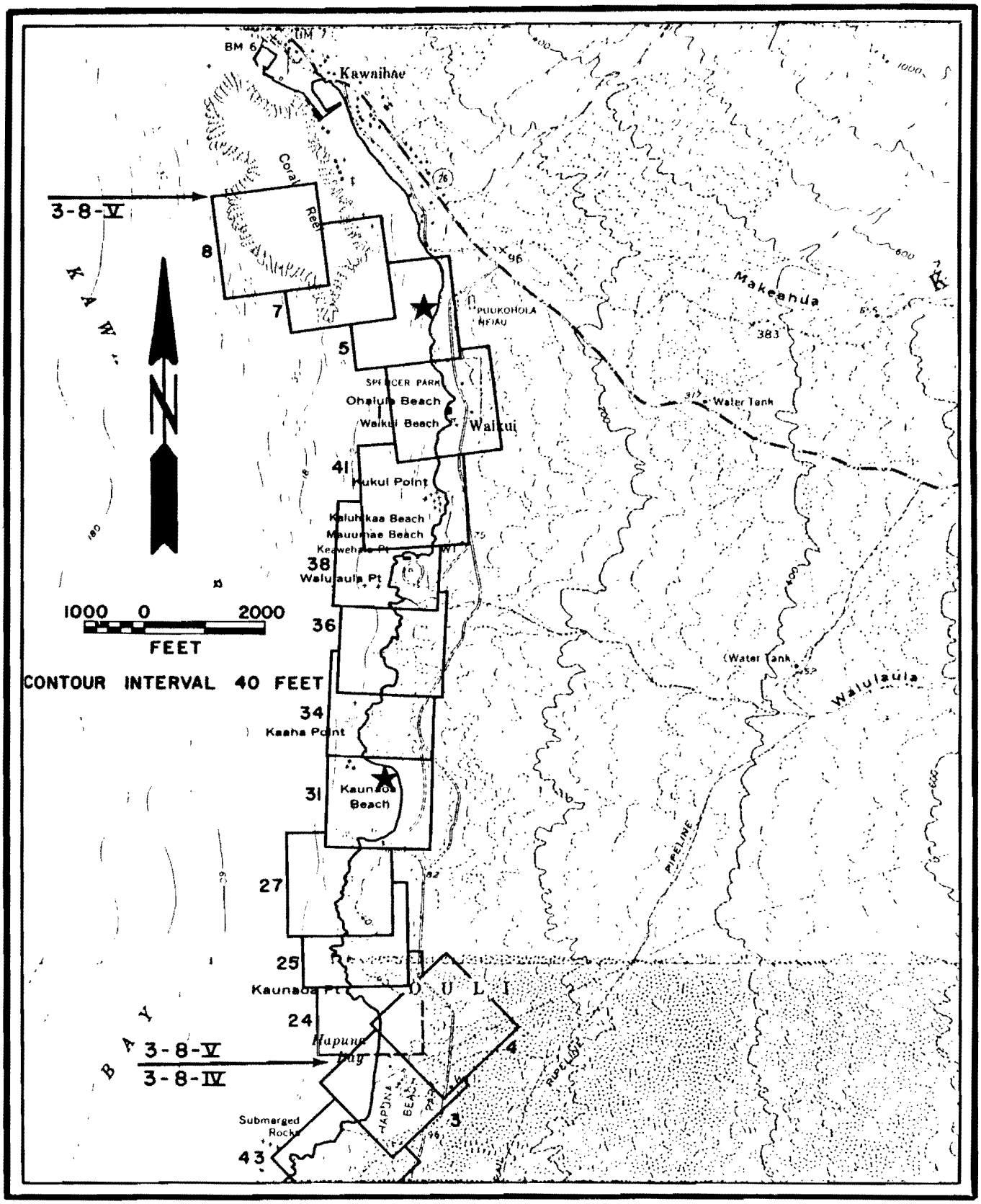

SUB-INDEX MAP NO. 6

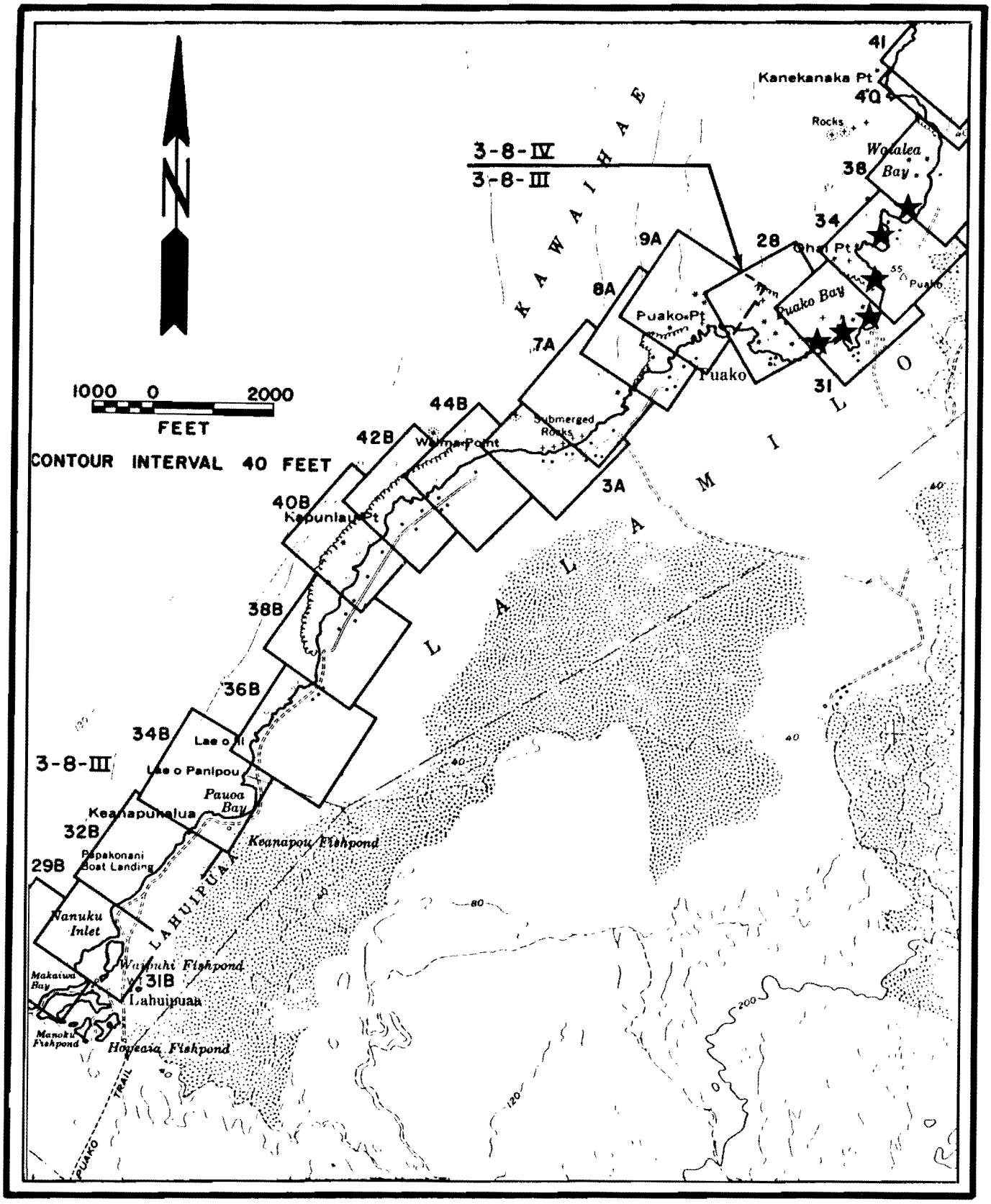

SUB-INDEX MAP NO. 7

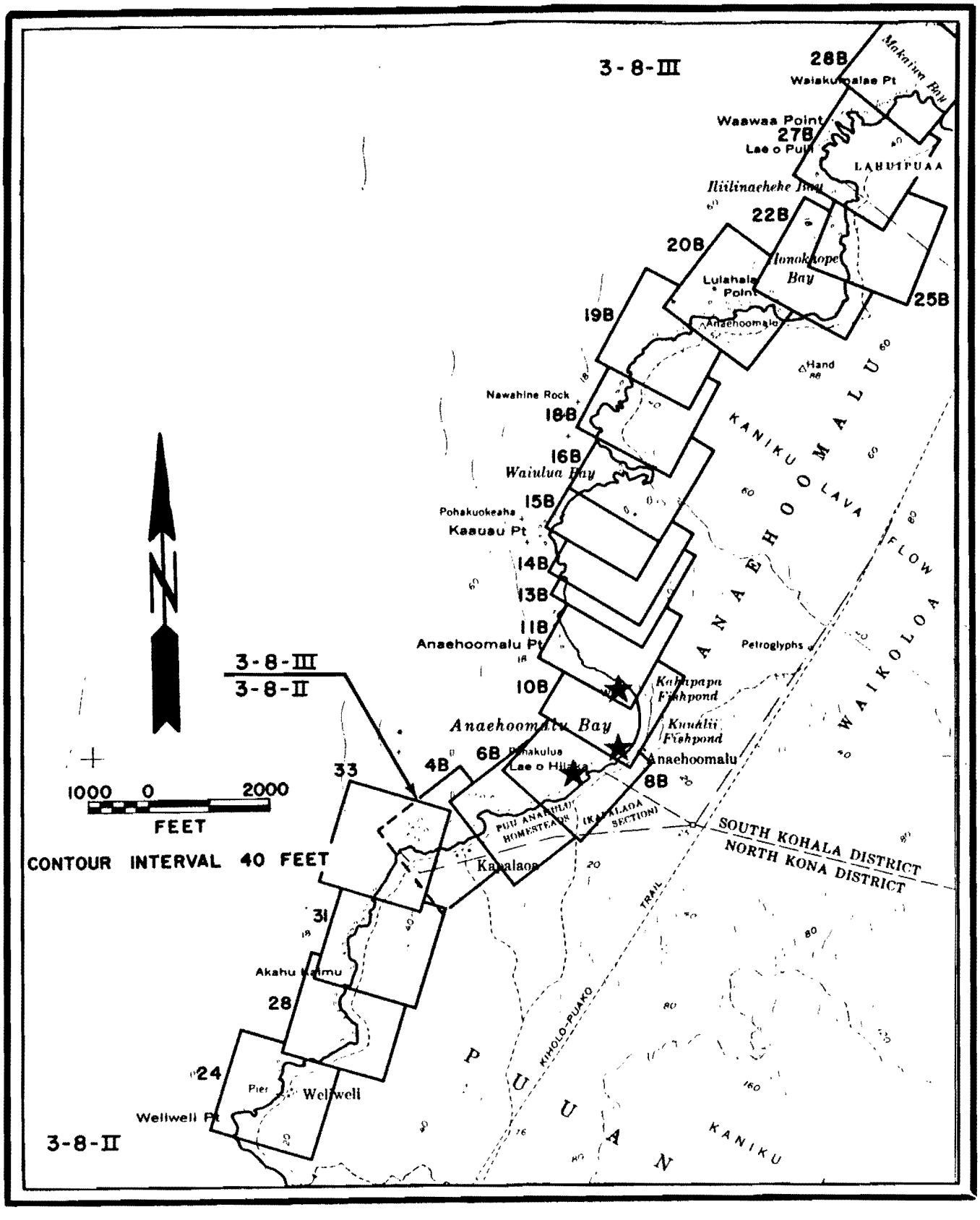

SUB-INDEX MAP NO. 8

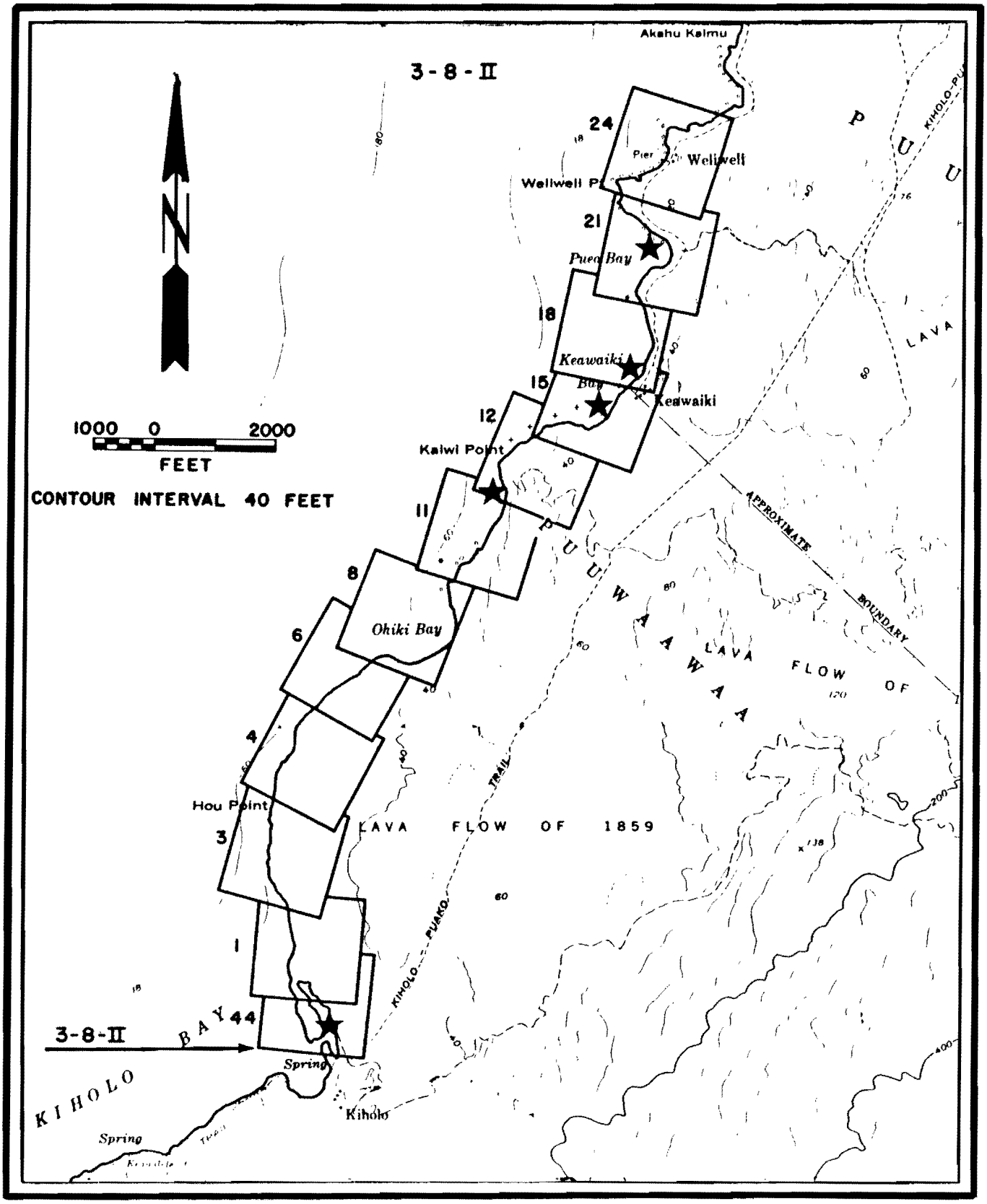

SUB-INDEX MAP NO. 9

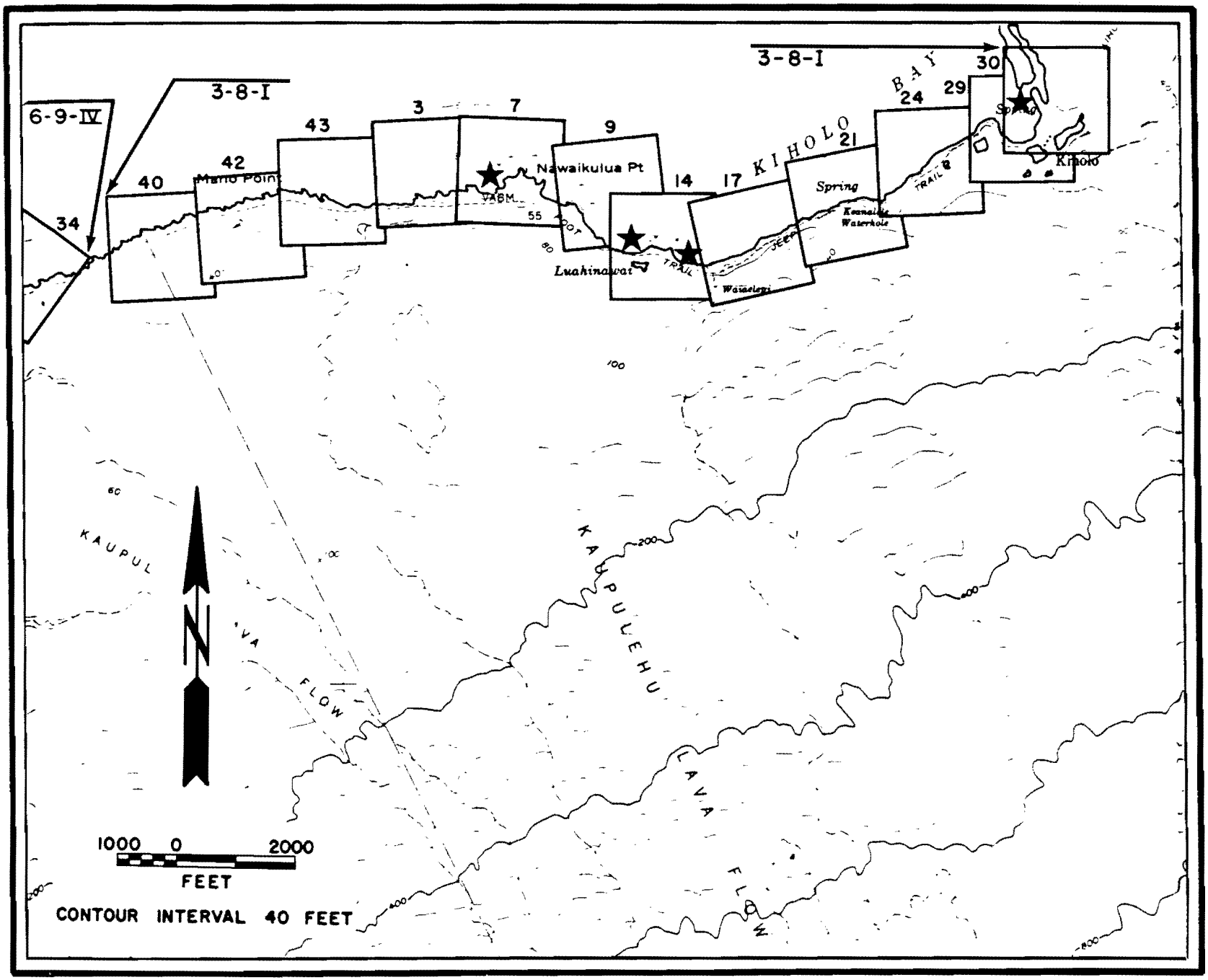

SUB-INDEX MAP NO. 10

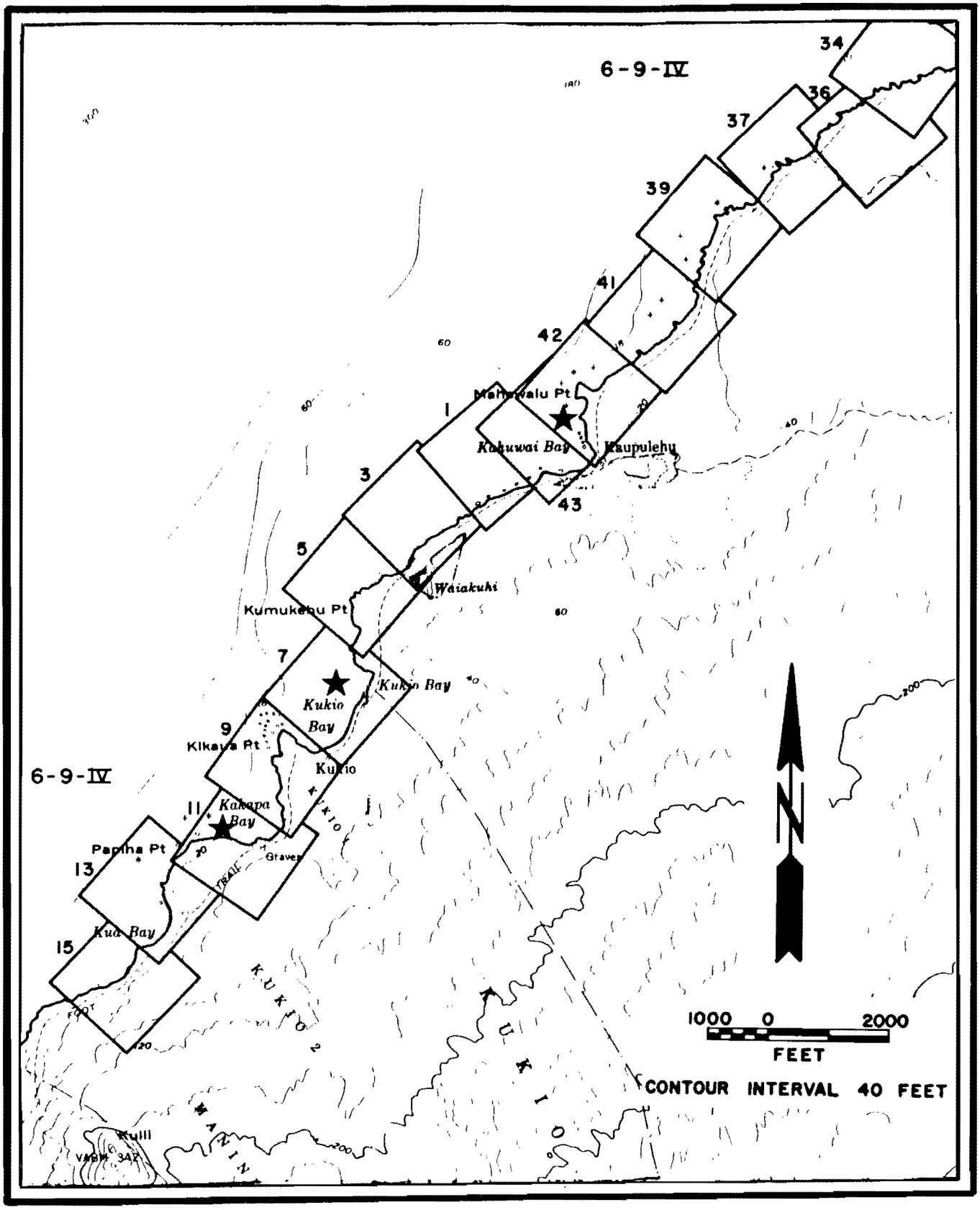

SUB-INDEX MAP NO. 11

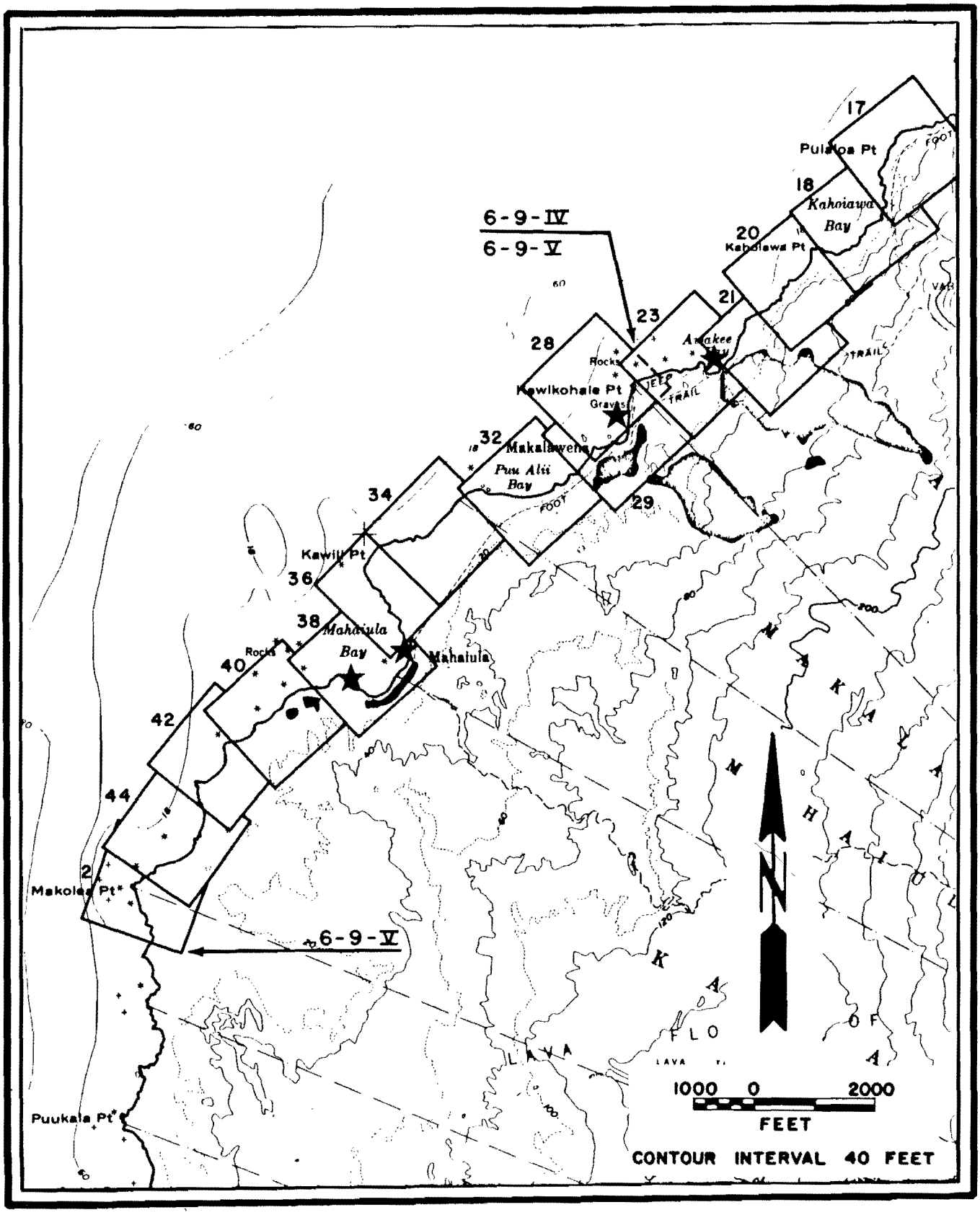

SUB-INDEX MAP NO. 12

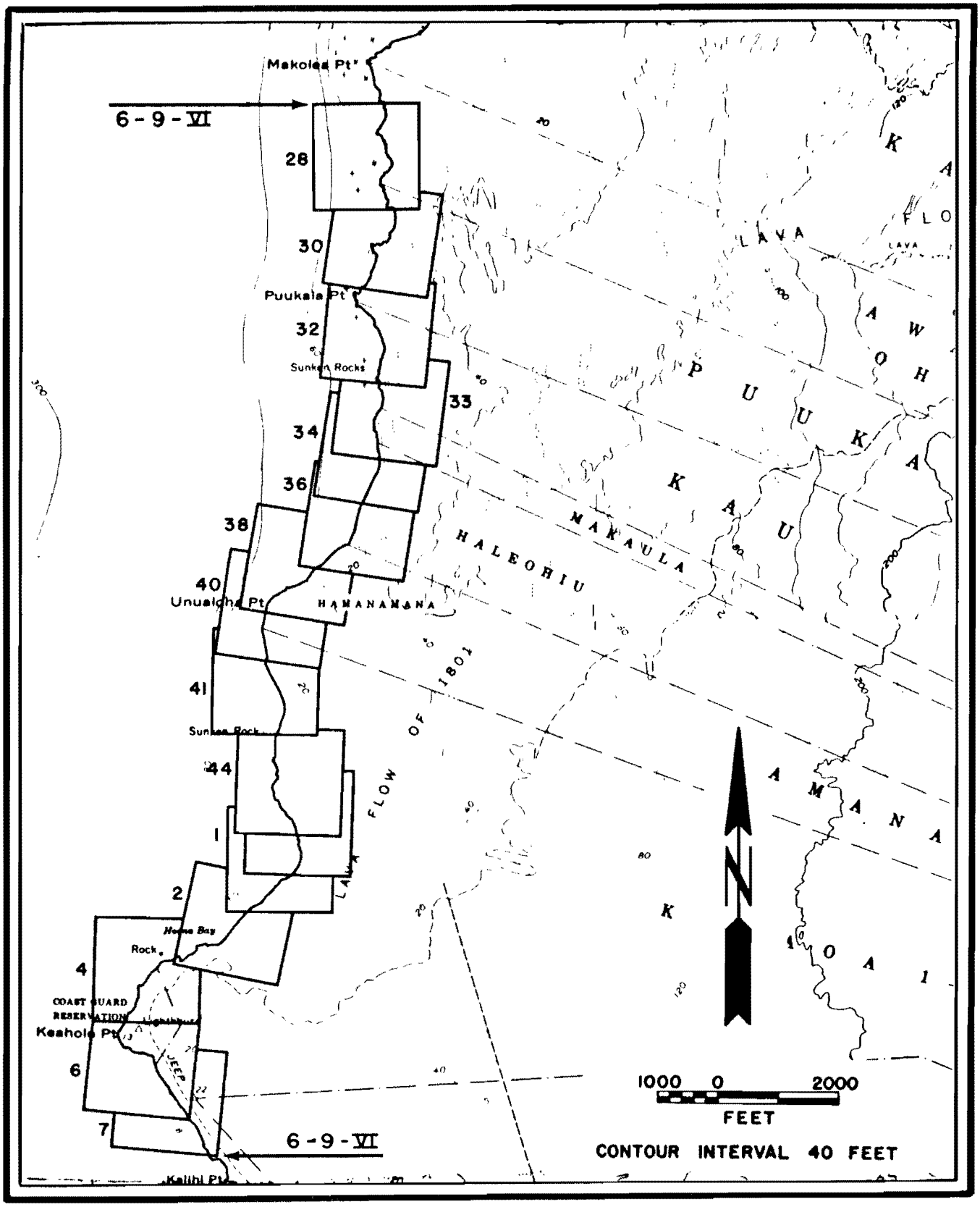

SUB-INDEX MAP NO. 13

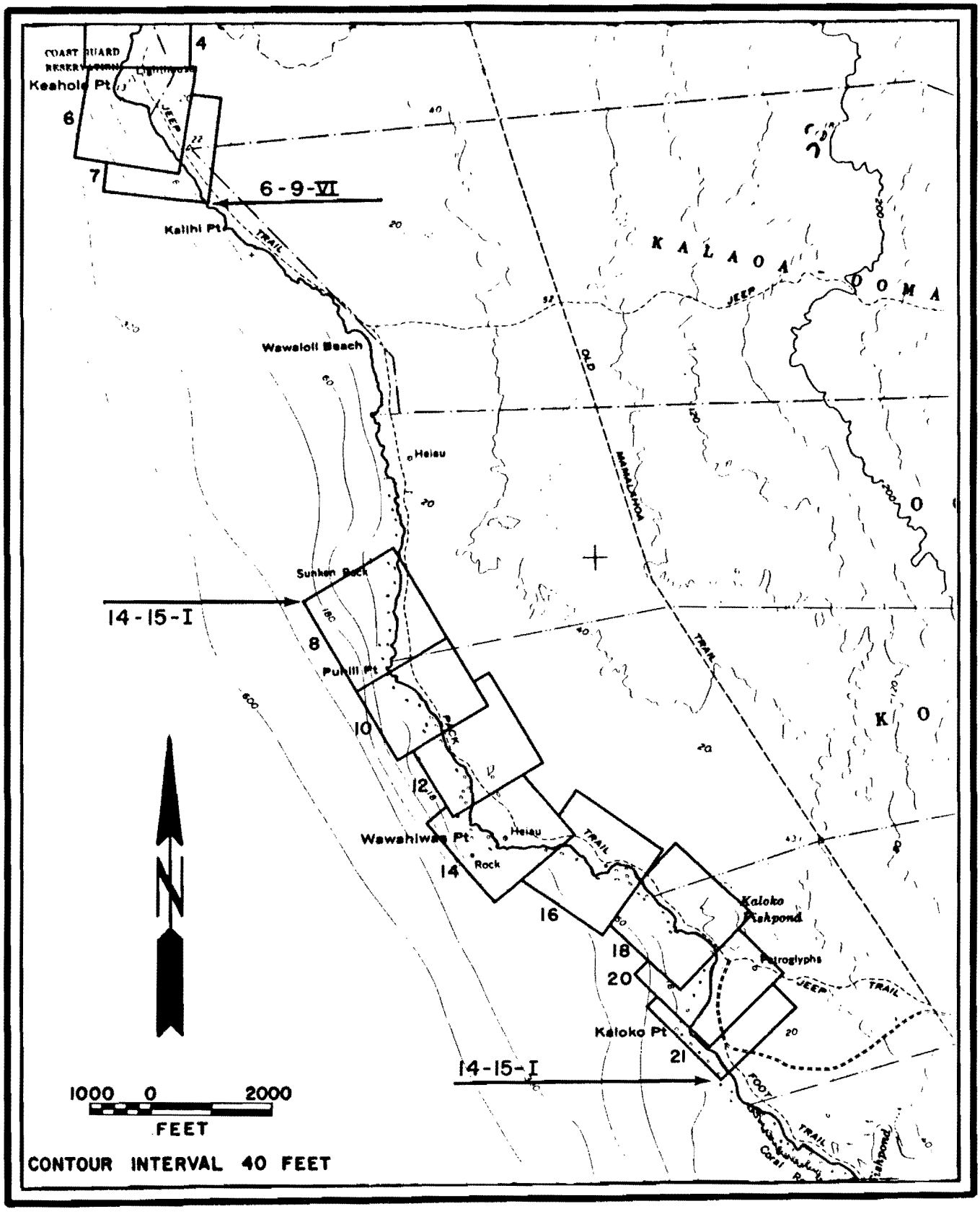

SUB-INDEX MAP NO. 14

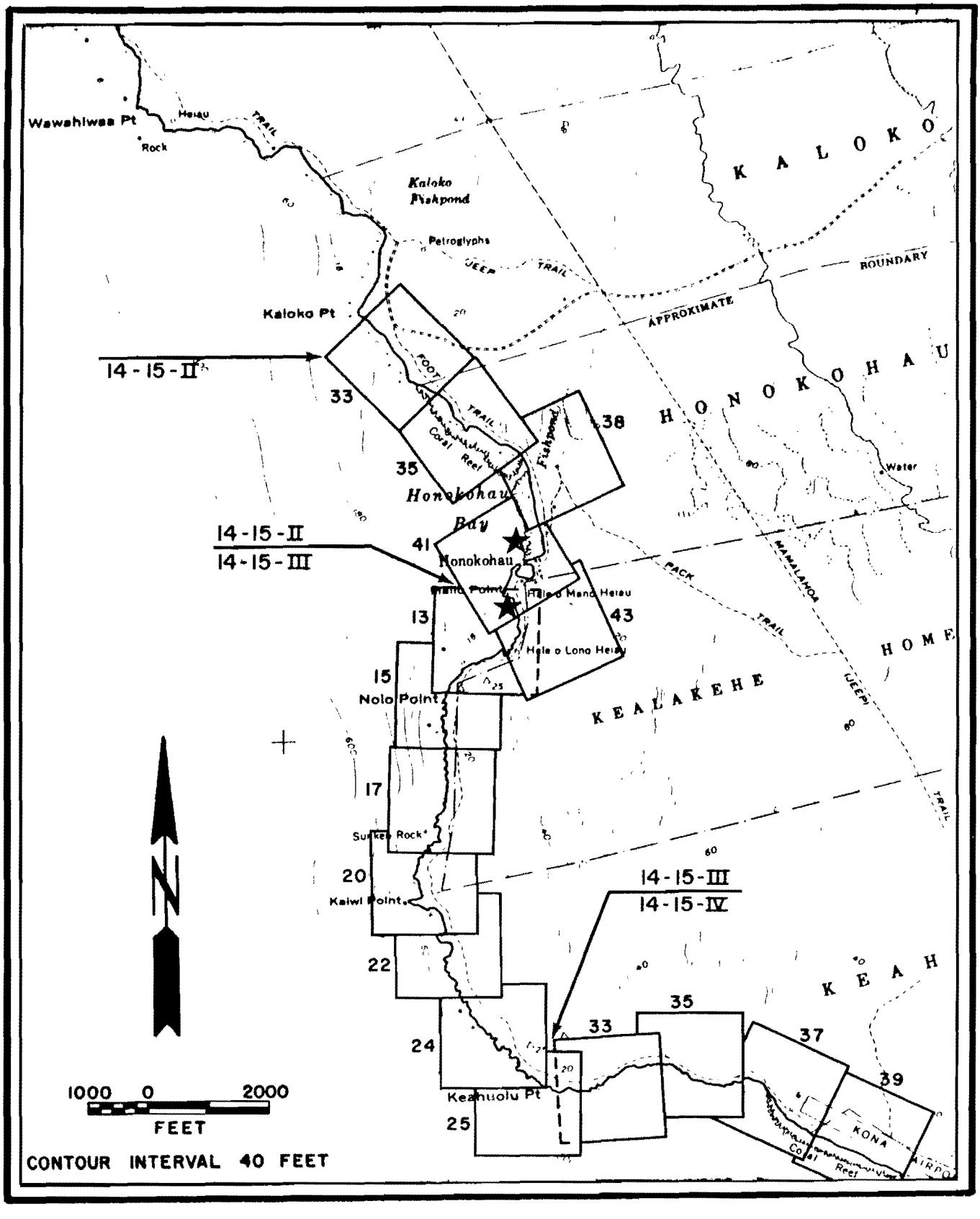

SUB-INDEX MAP NO. 15

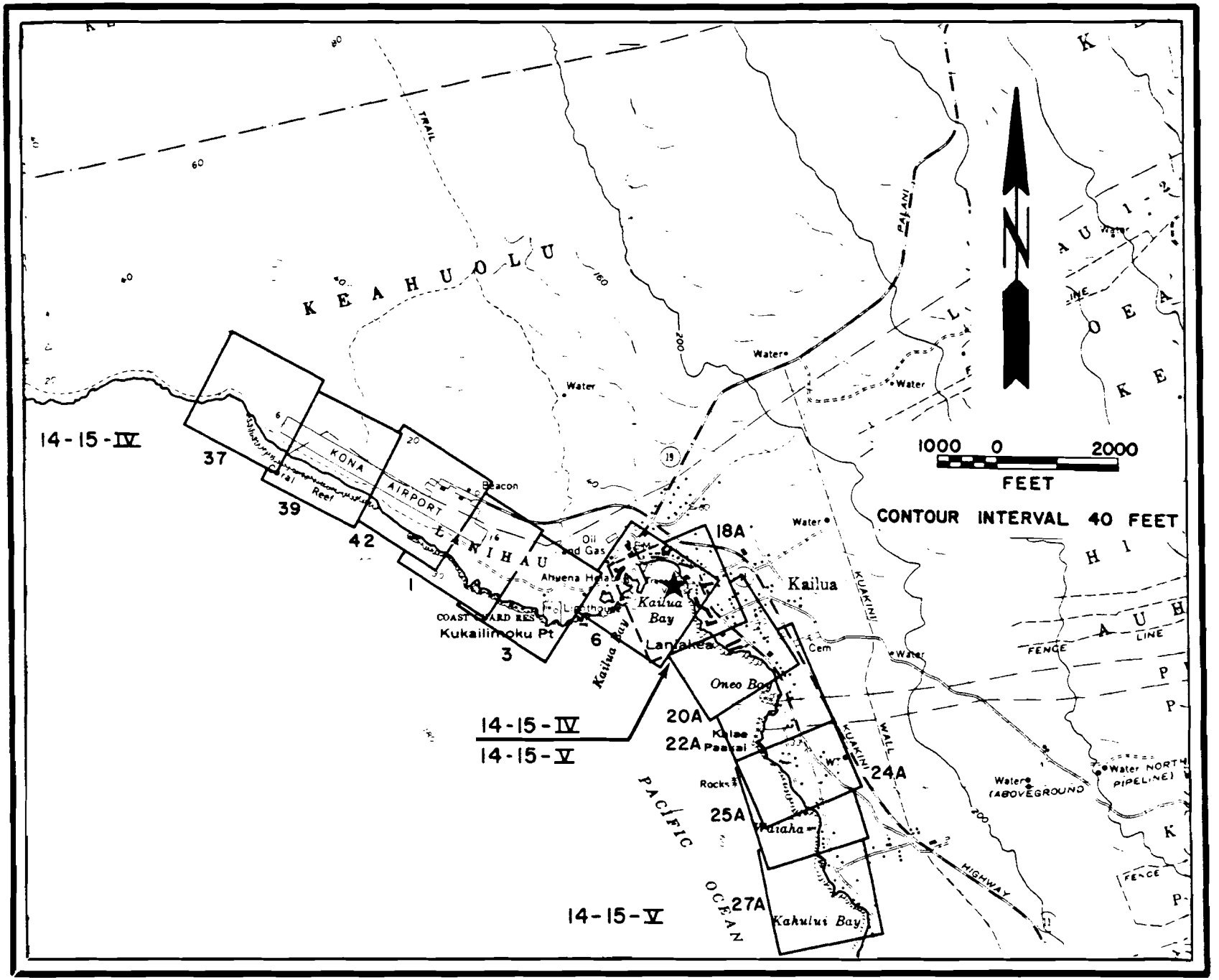

SUB-INDEX MAP NO. 16

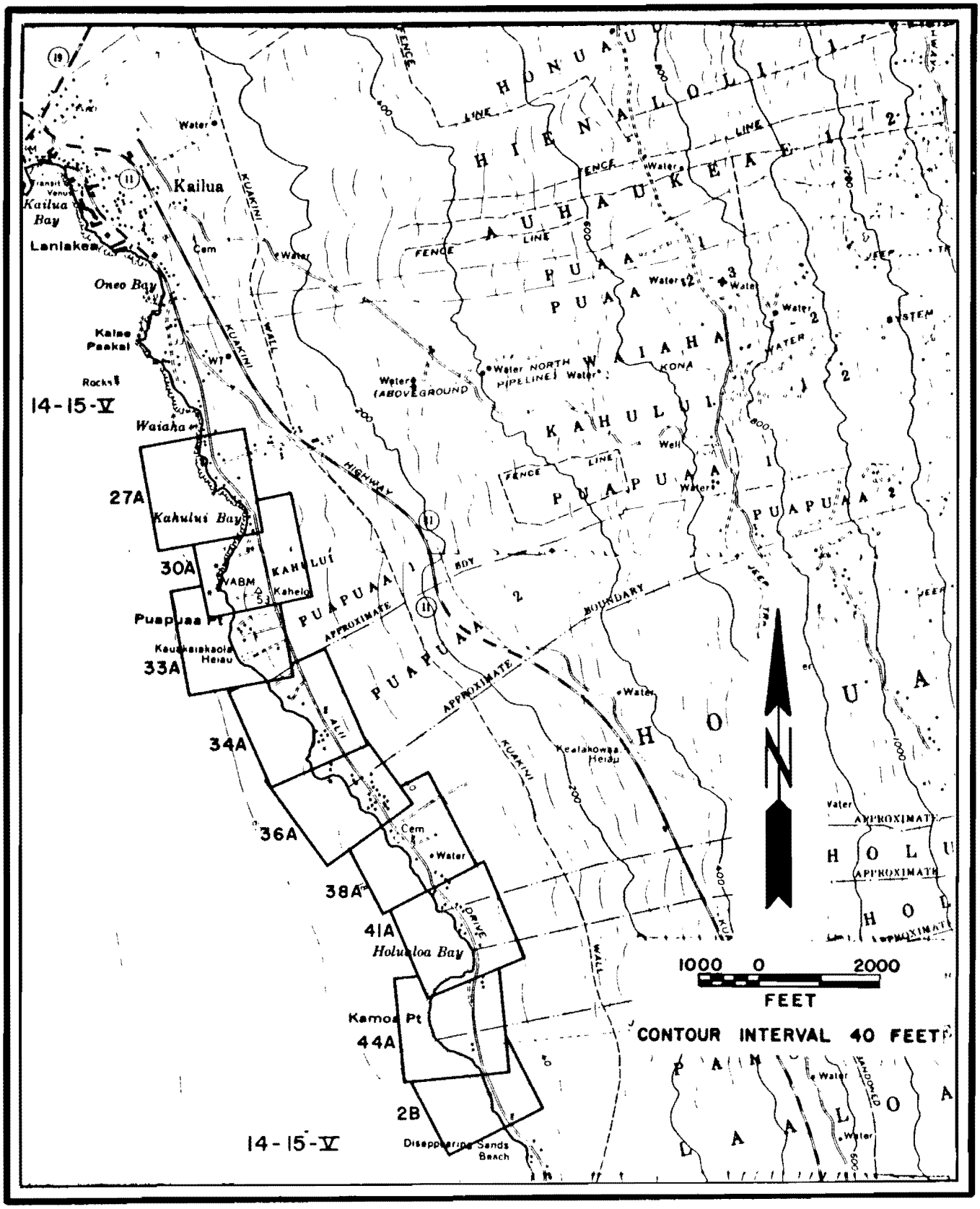

SUB-INDEX MAP NO. 17

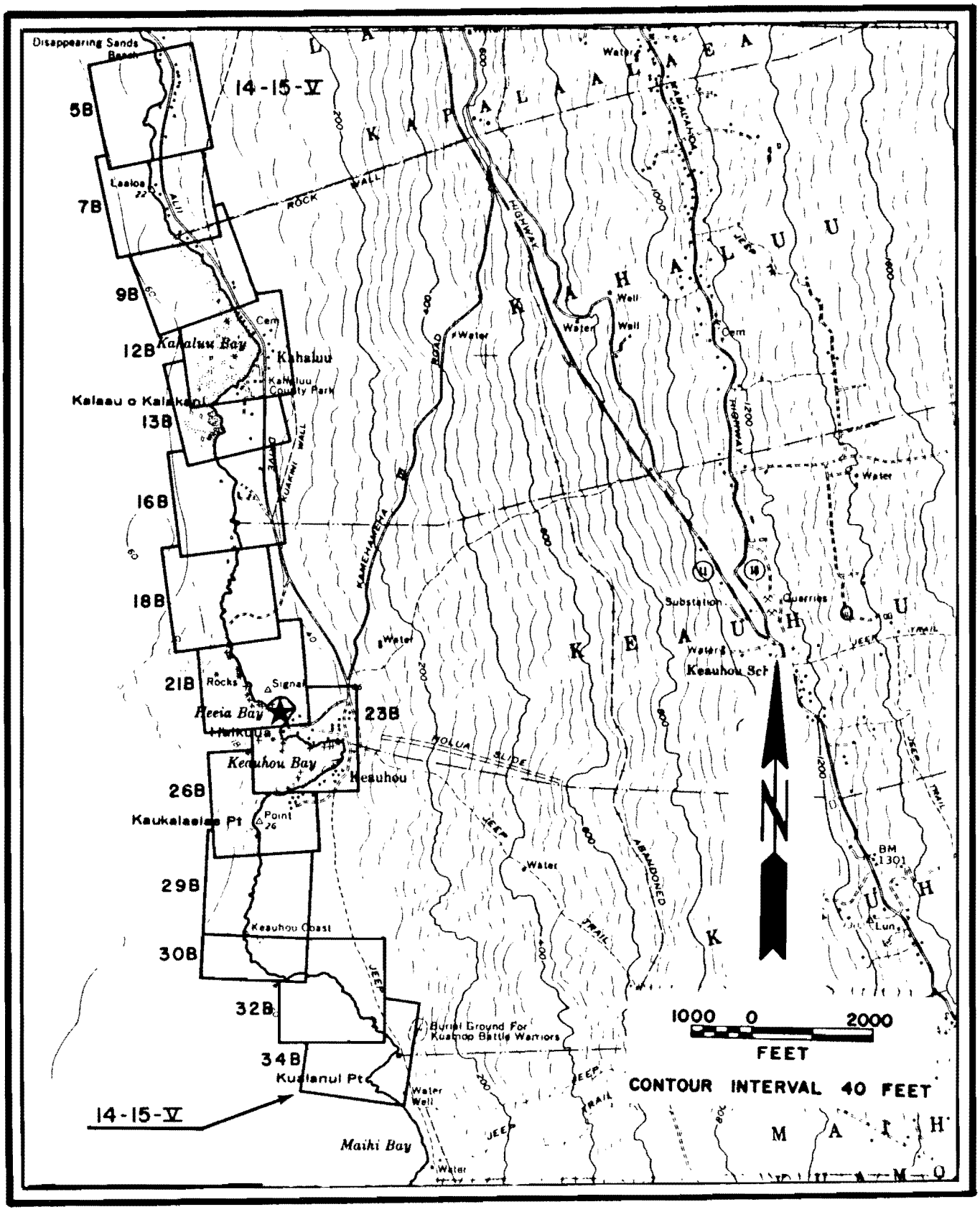

SUB-INDEX MAP NO. 18

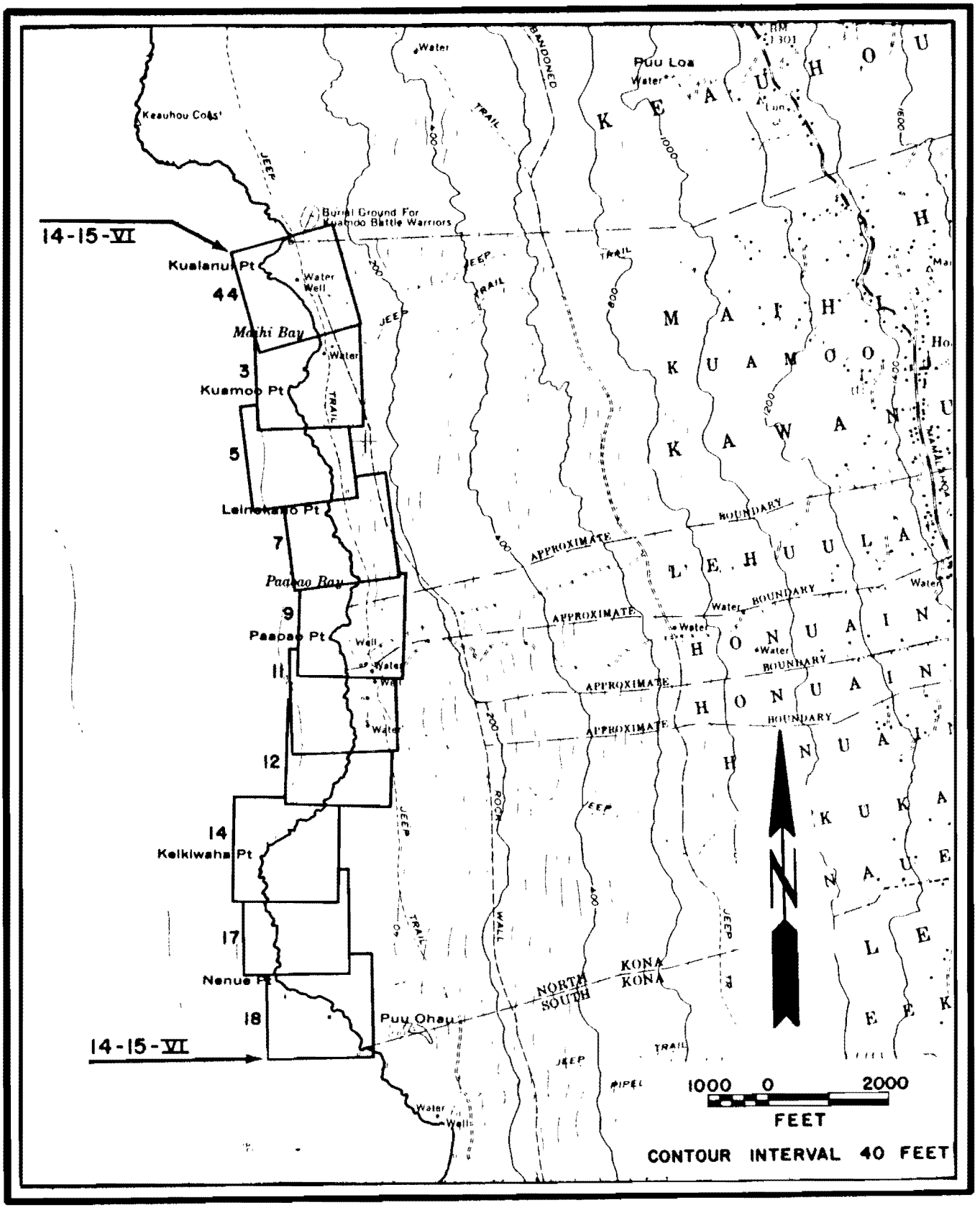

SUB-INDEX MAP NO. 19

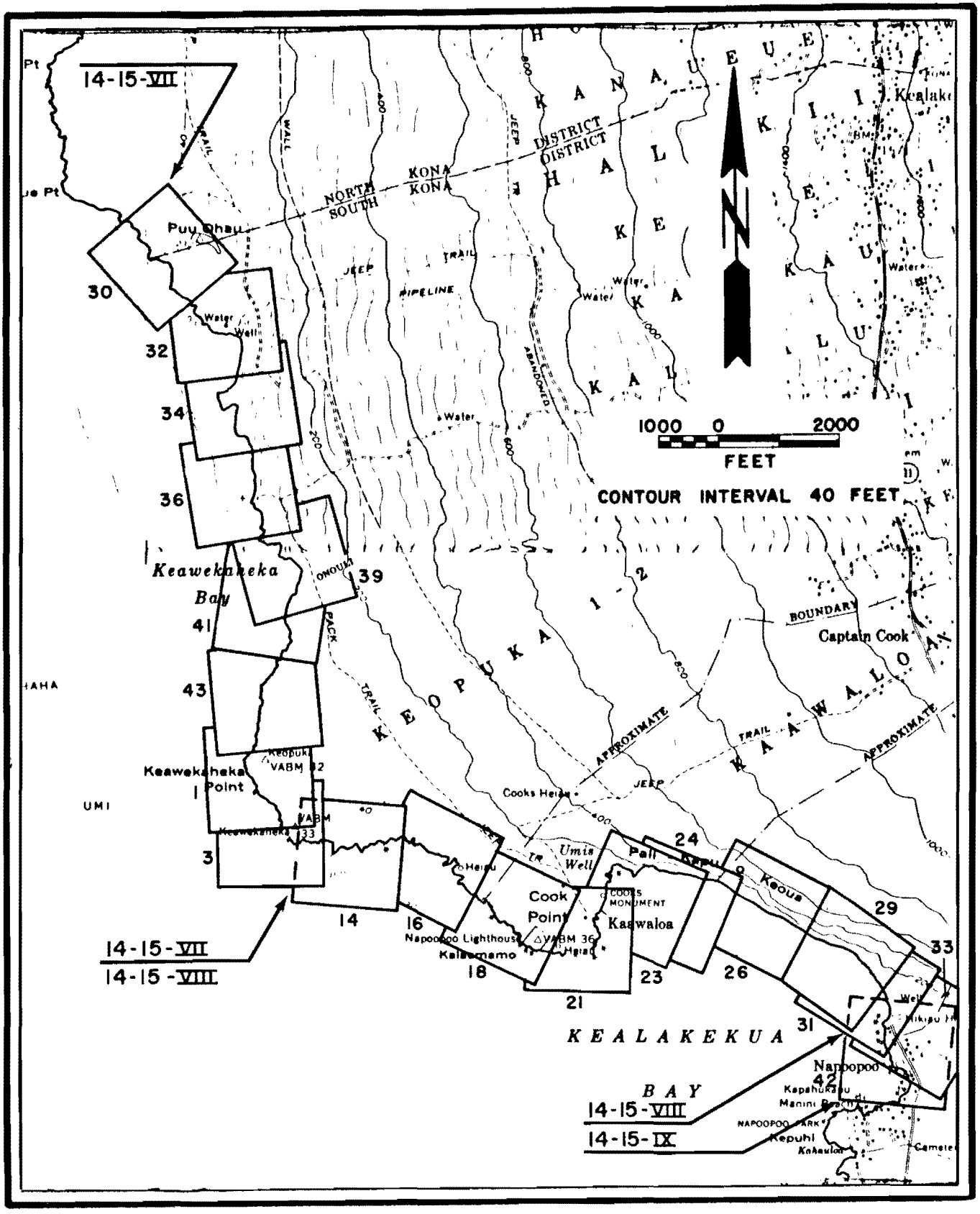

SUB-INDEX MAP NO. 20

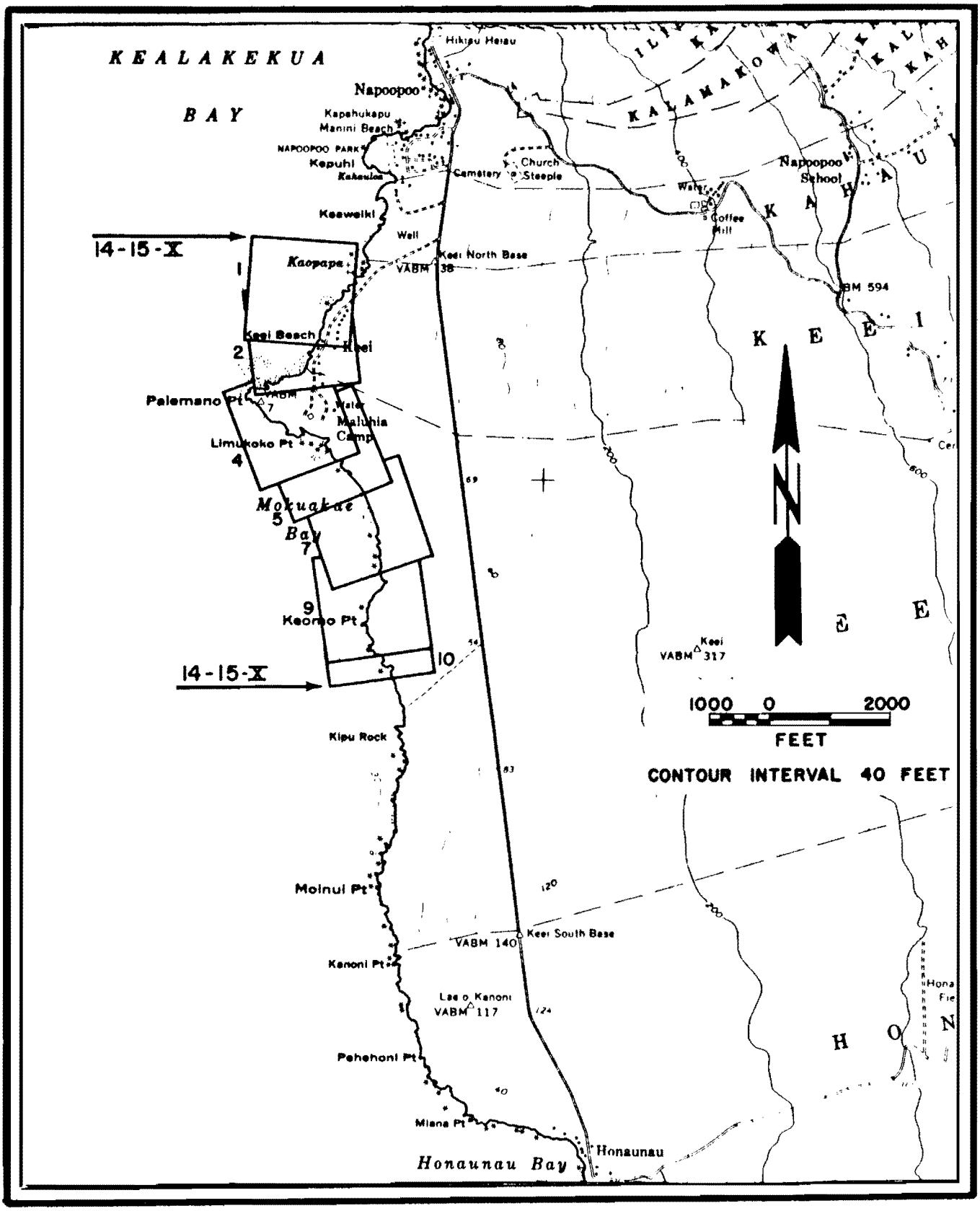

SUB-INDEX MAP NO. 21

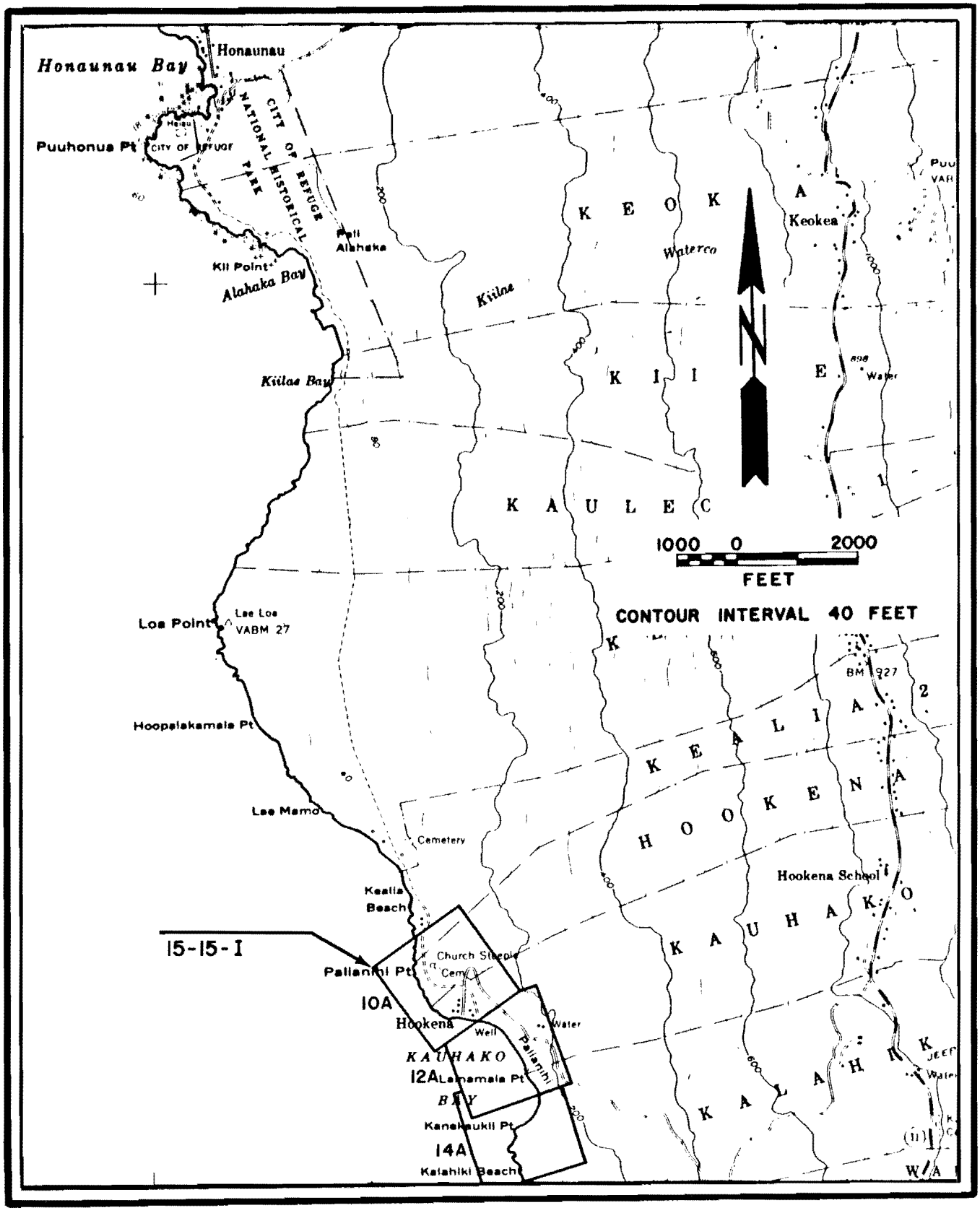

SUB-INDEX MAP NO. 22

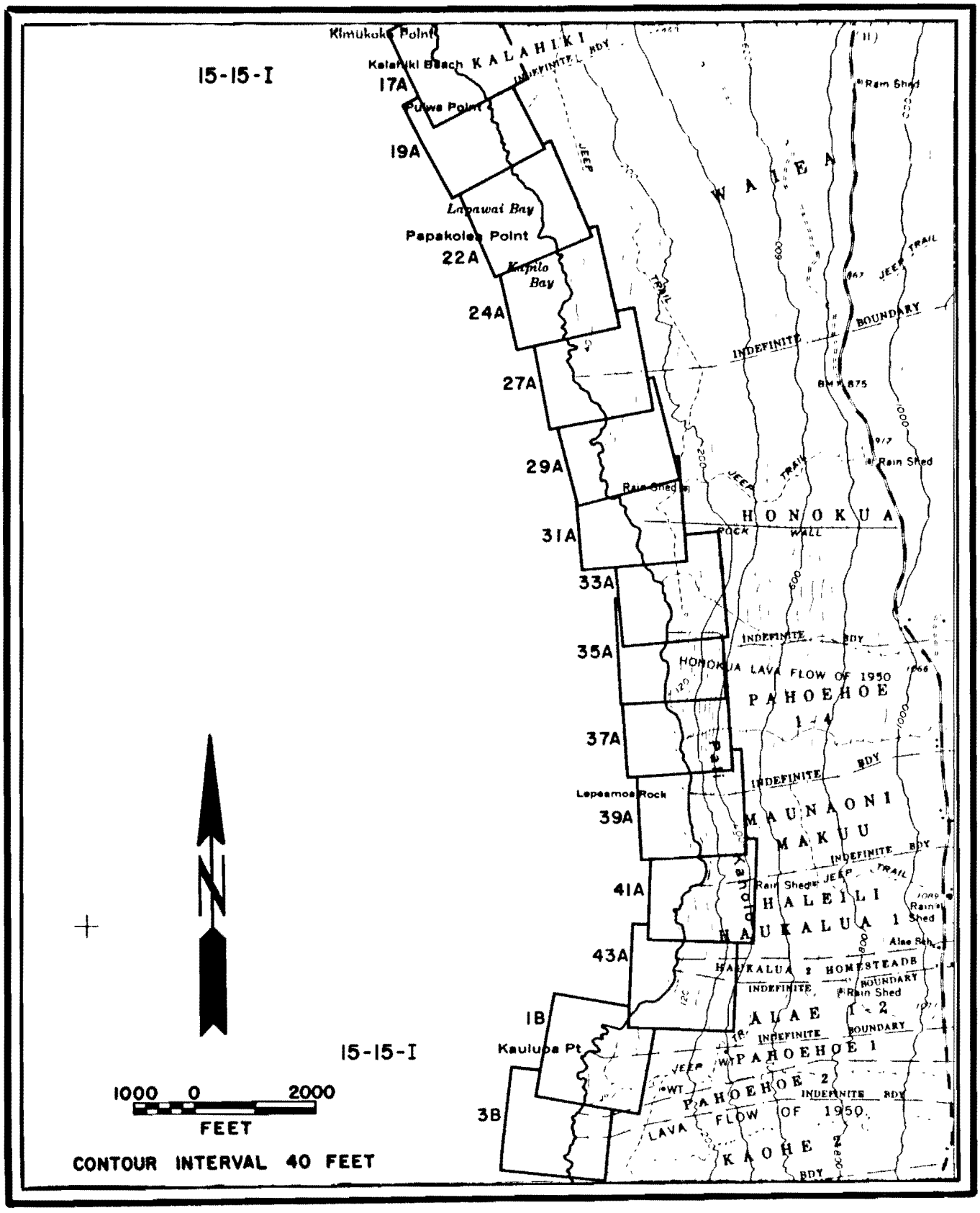

SUB-INDEX MAP NO. 23

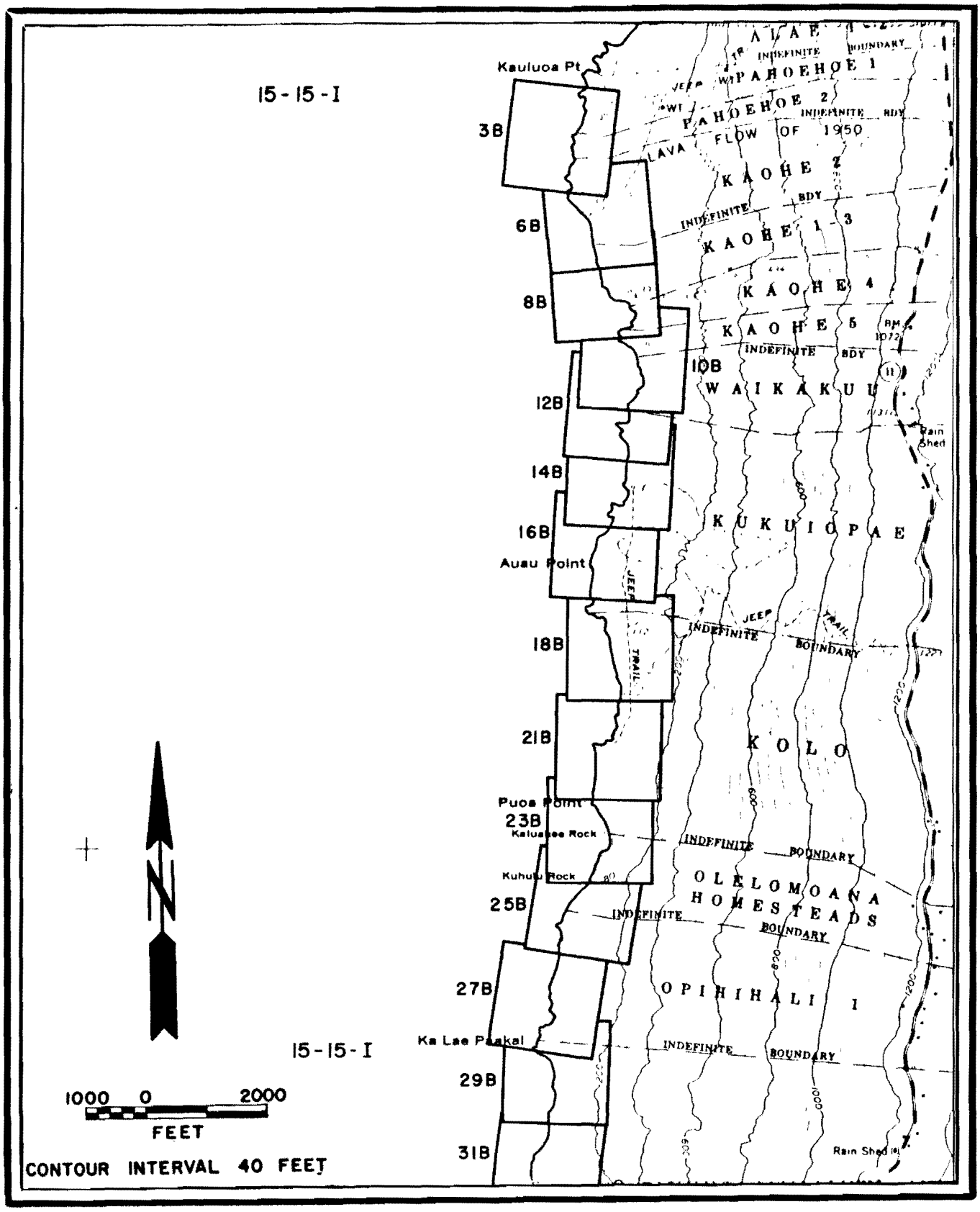

SUB-INDEX MAP NO. 24

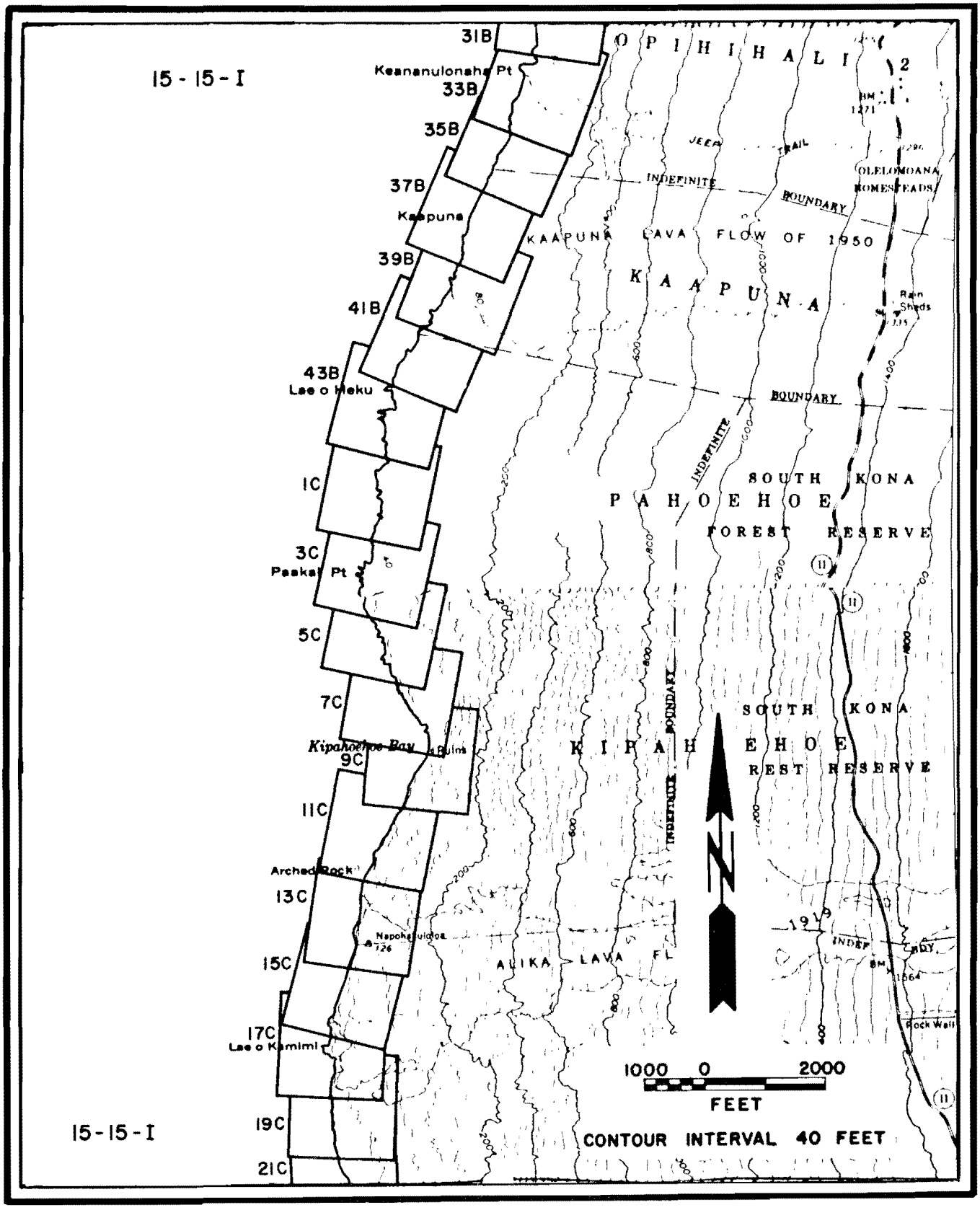

SUB-INDEX MAP NO. 25

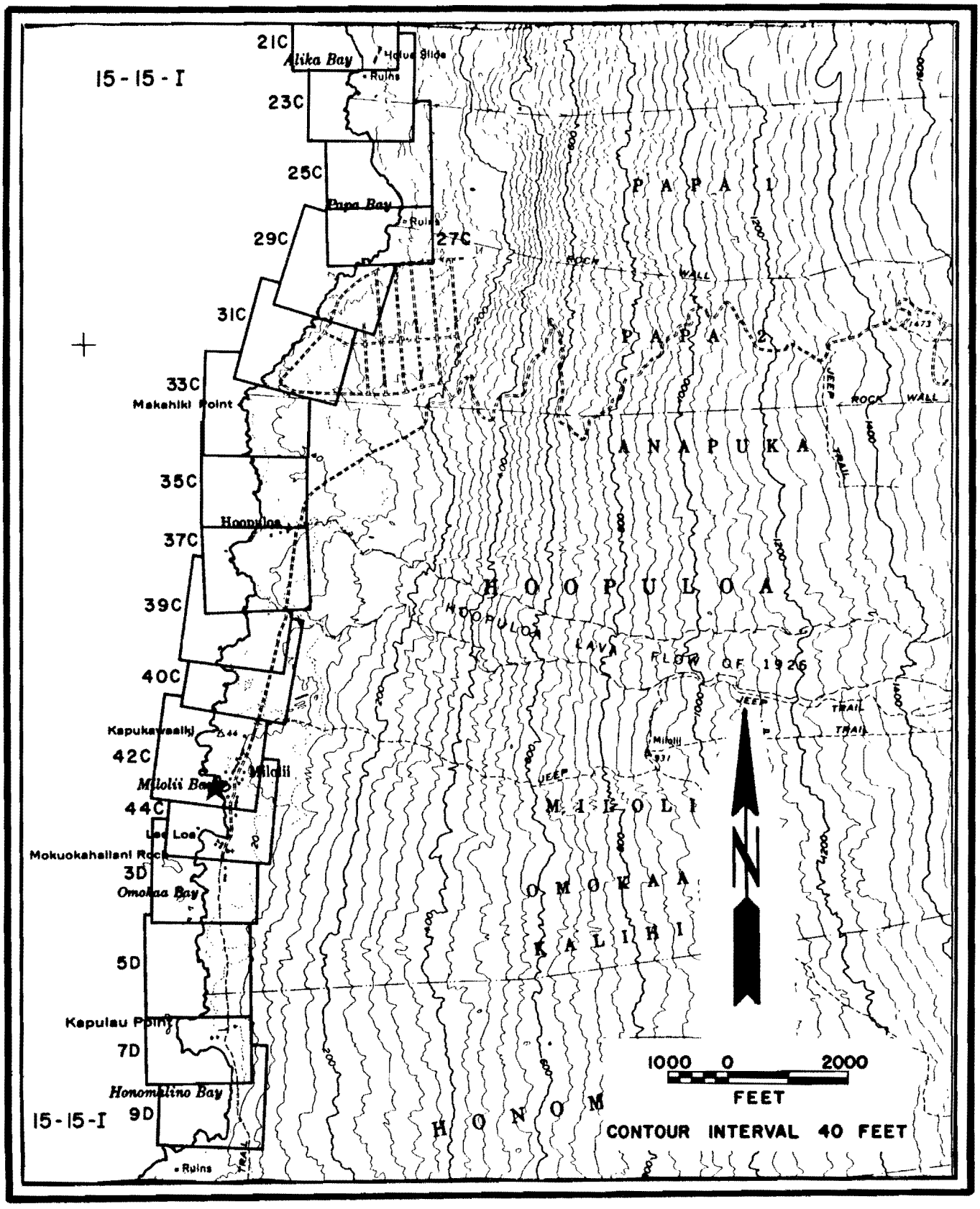

SUB-INDEX MAP NO. 26

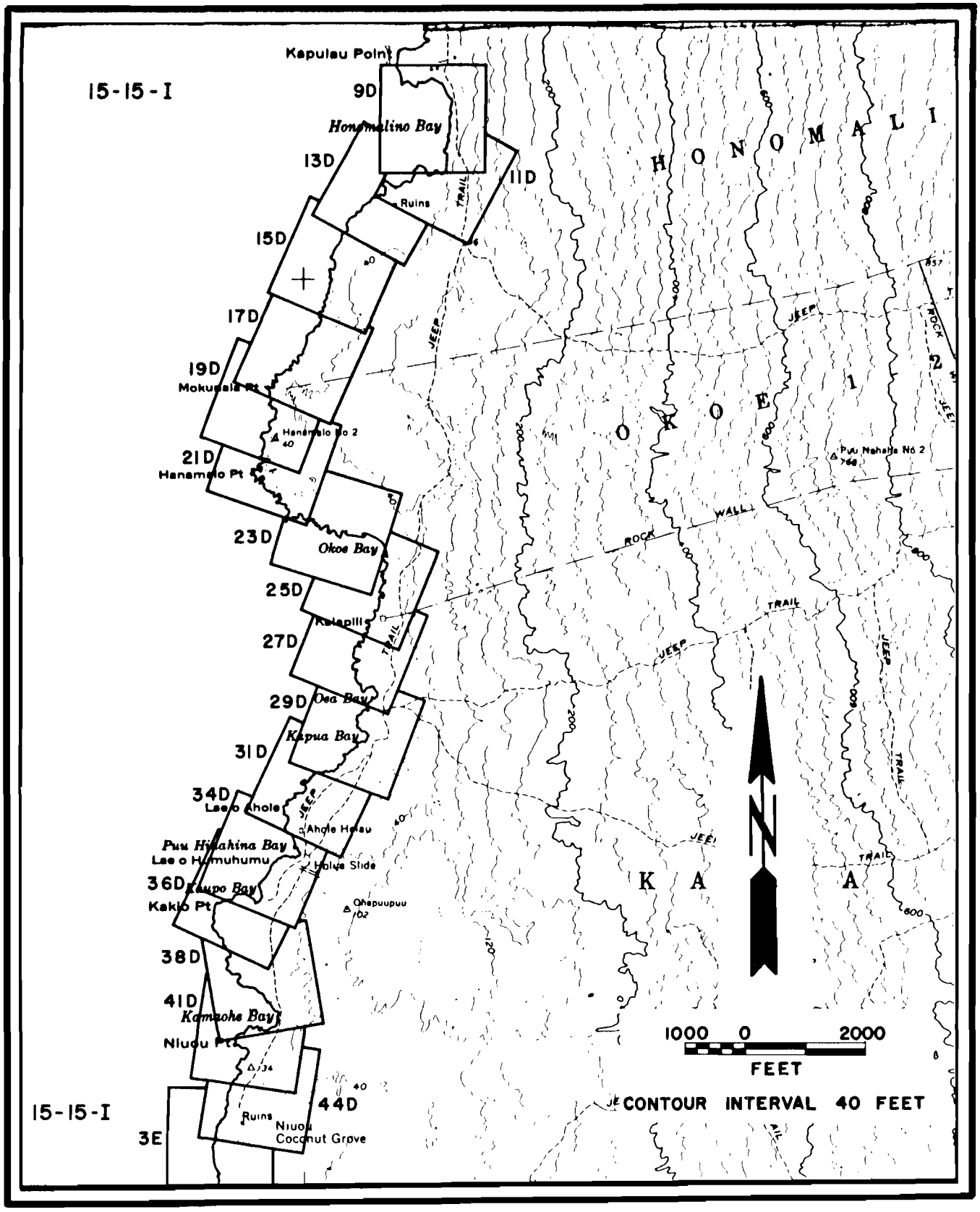

SUB-INDEX MAP NO. 27

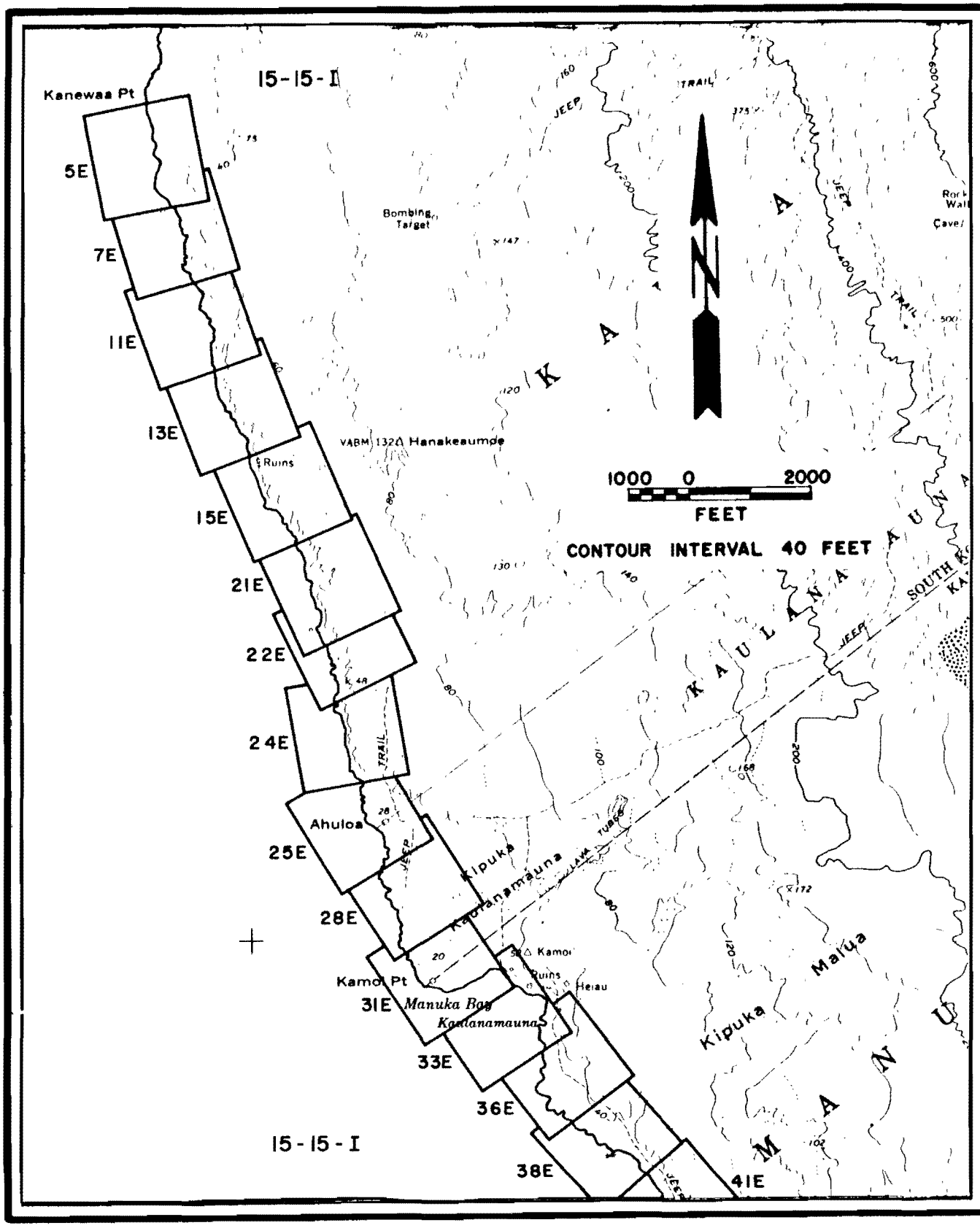

SUB-INDEX MAP NO. 28

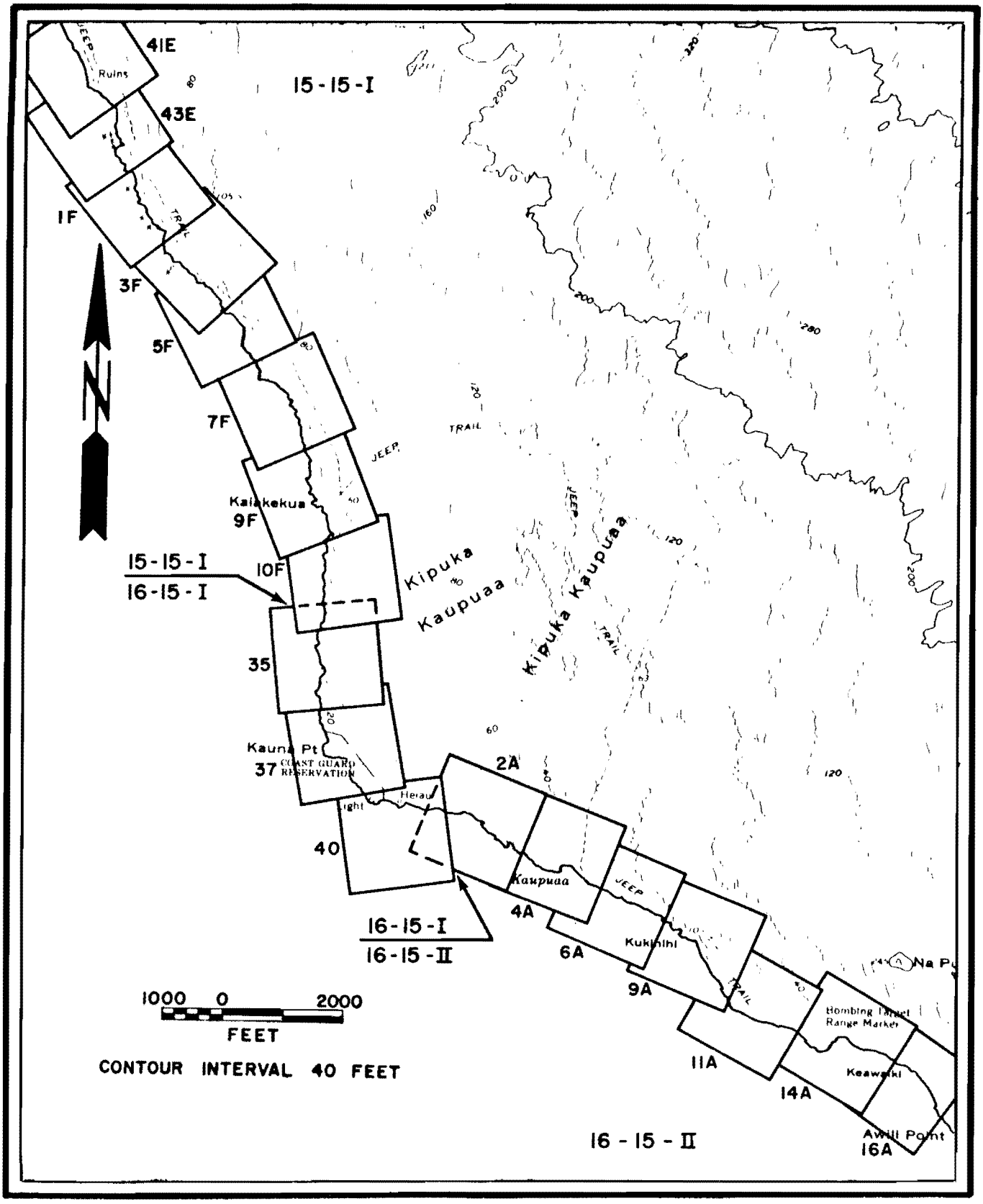

SUB-INDEX MAP NO. 29

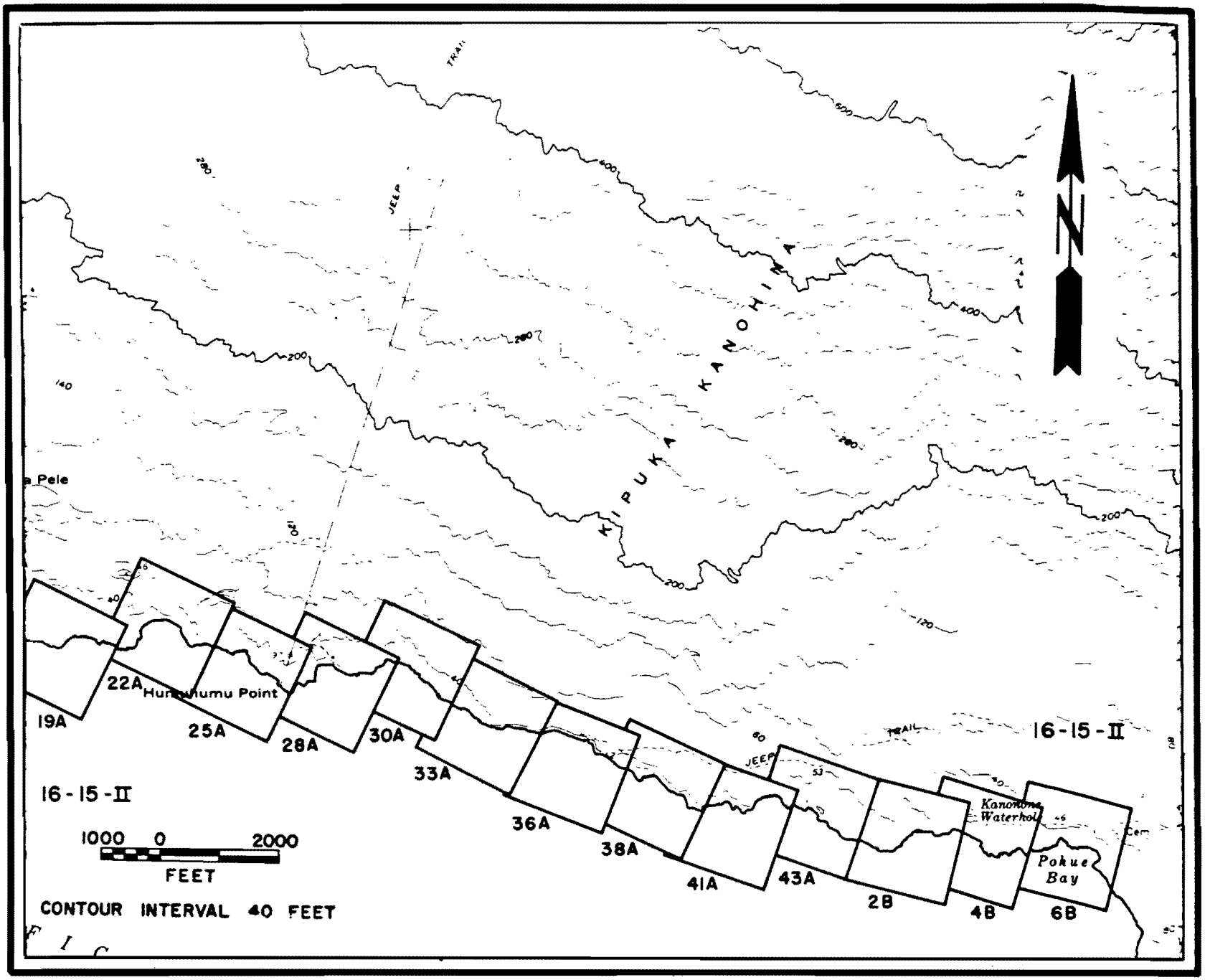

SUB-INDEX MAP NO. 30

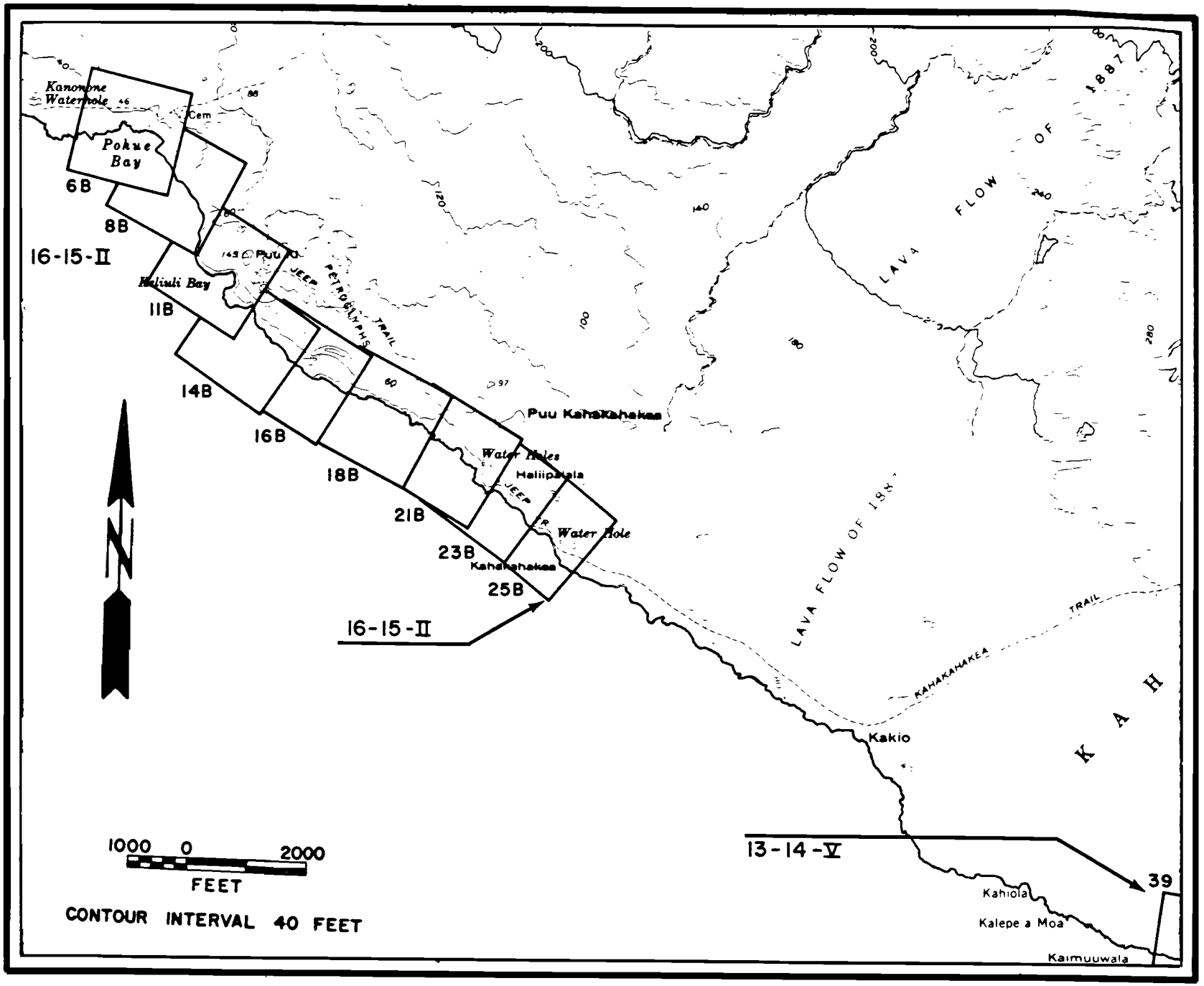

SUB-INDEX MAP NO. 31

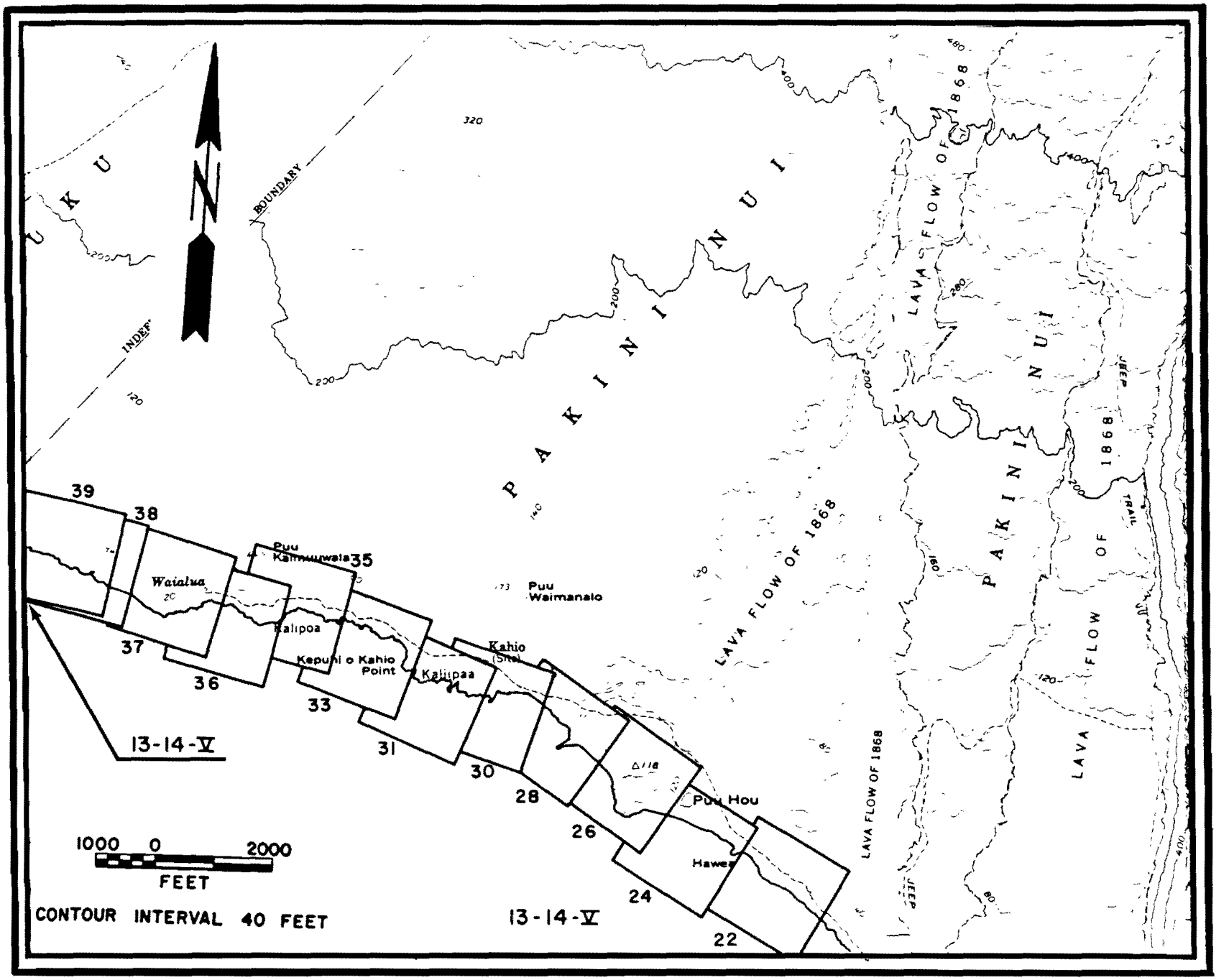

SUB-INDEX MAP NO. 32

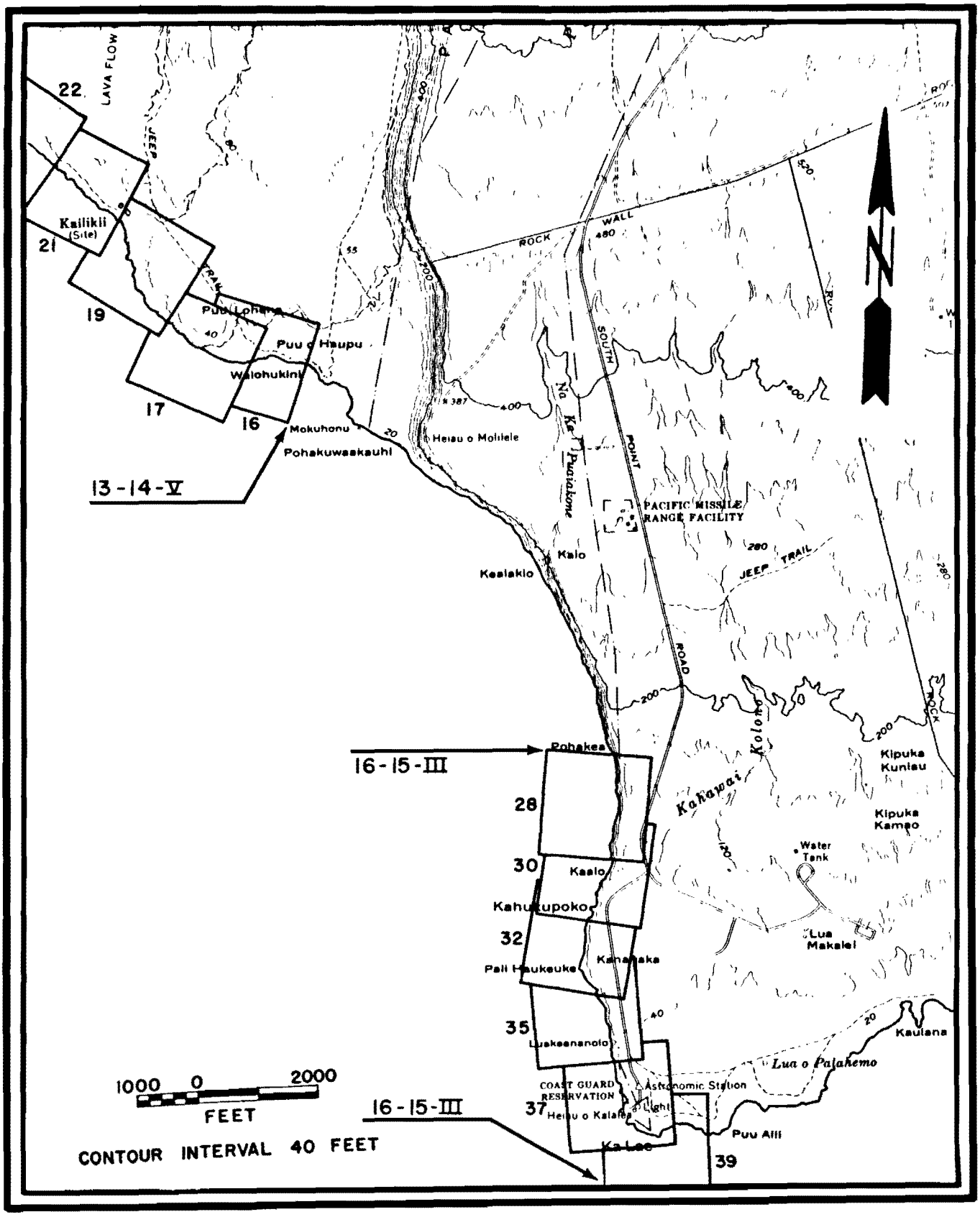

SUB-INDEX MAP NO. 33

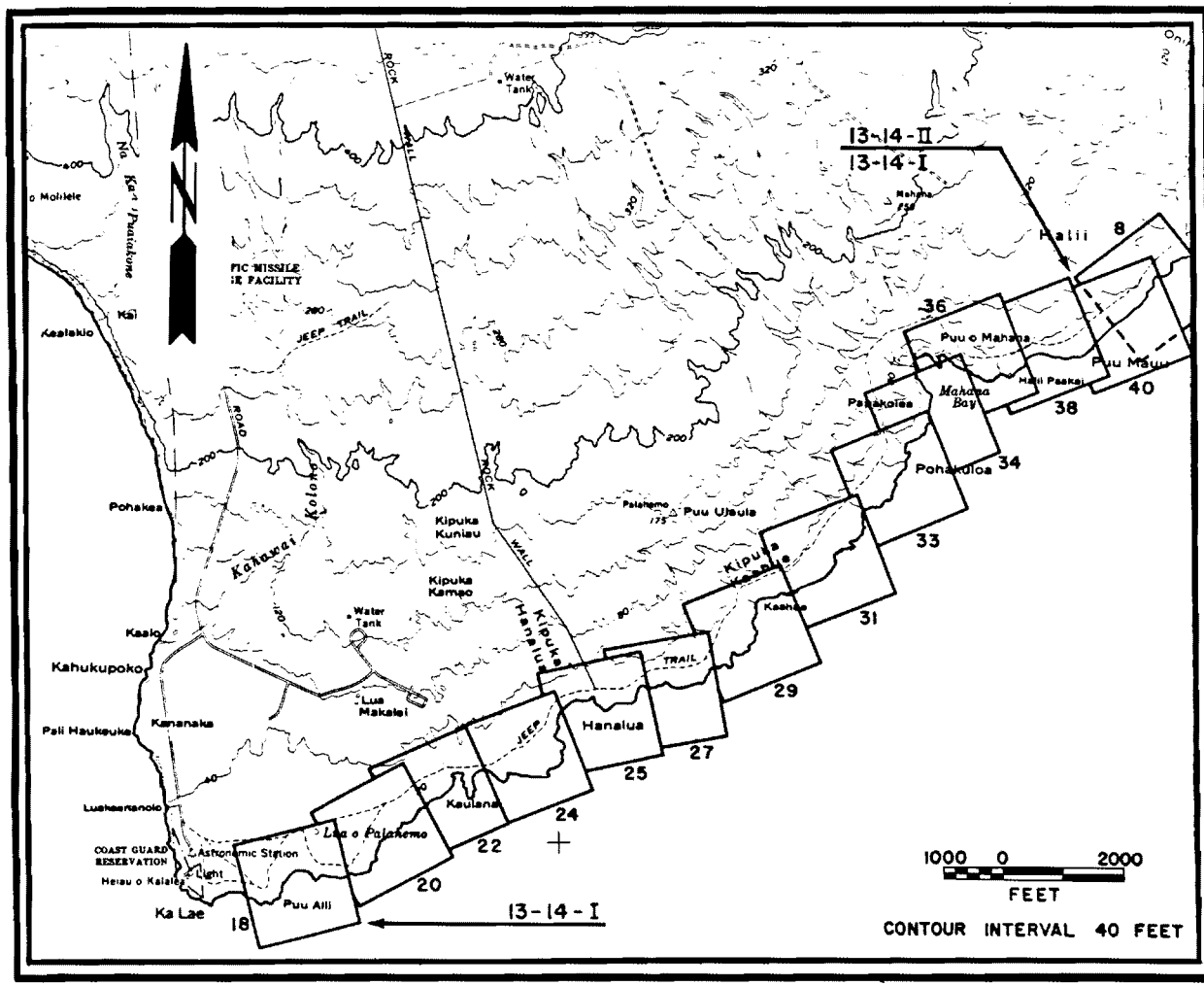

SUB-INDEX MAP NO. 34

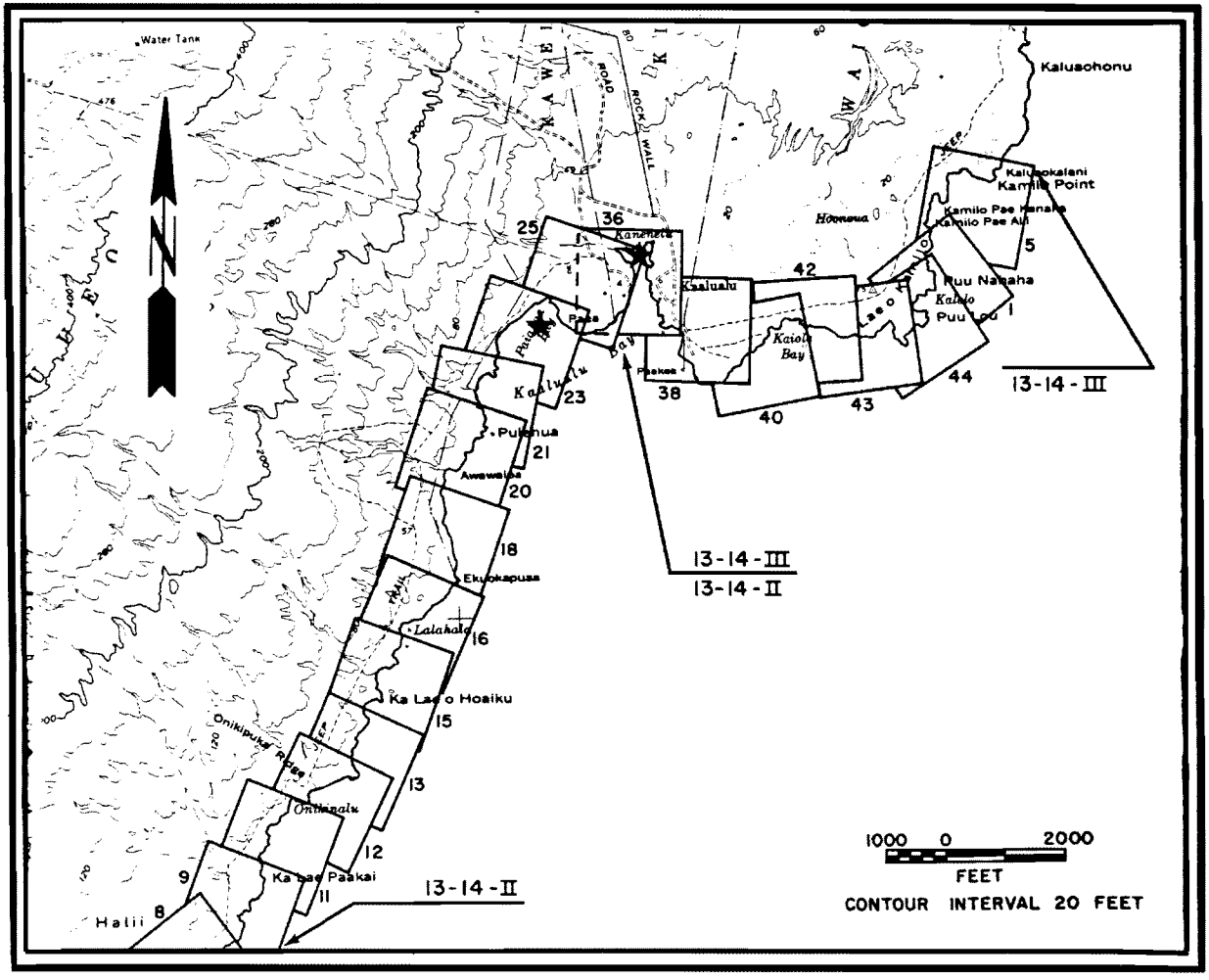

SUB-INDEX MAP NO. 35

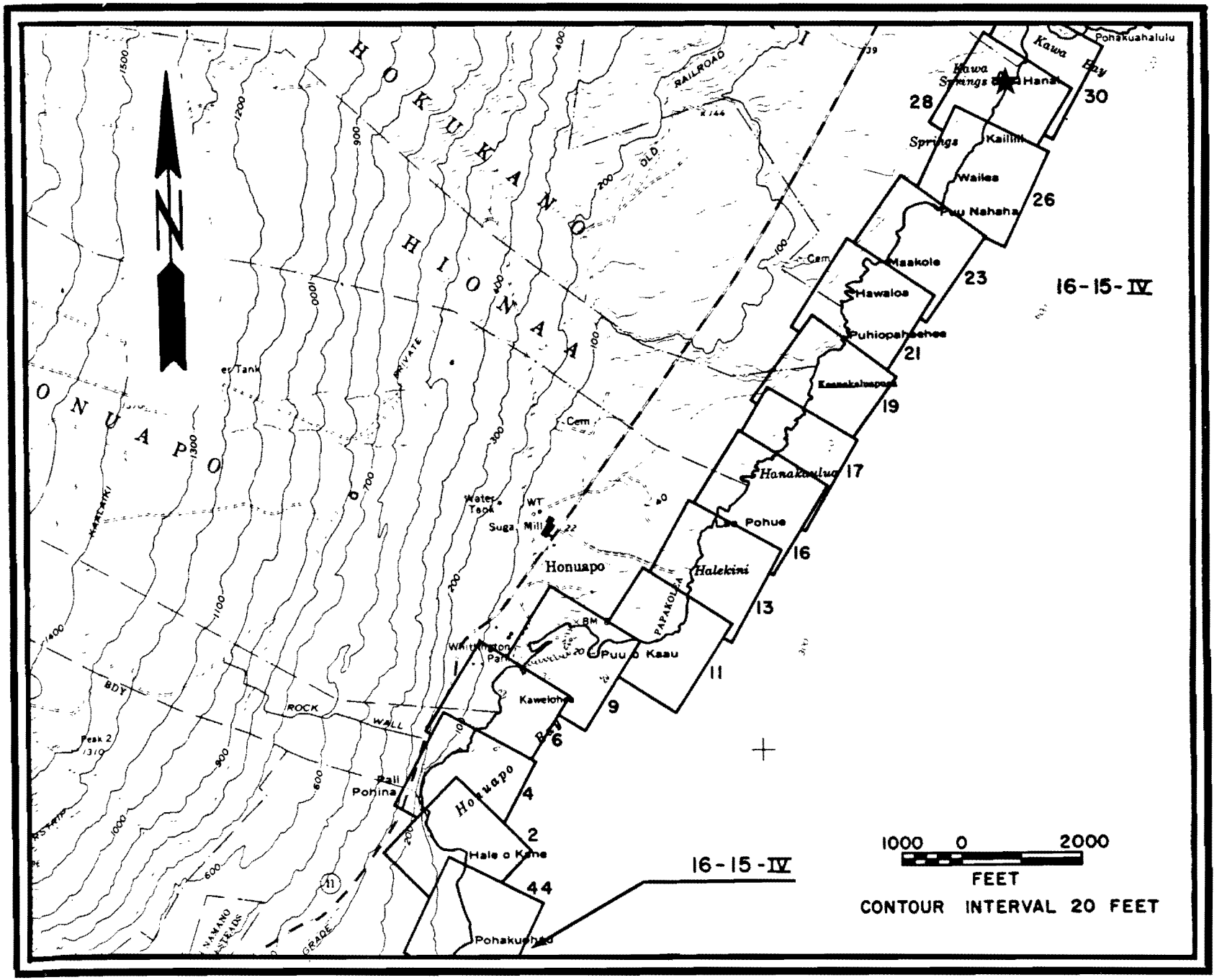

SUB-INDEX MAP NO. 36

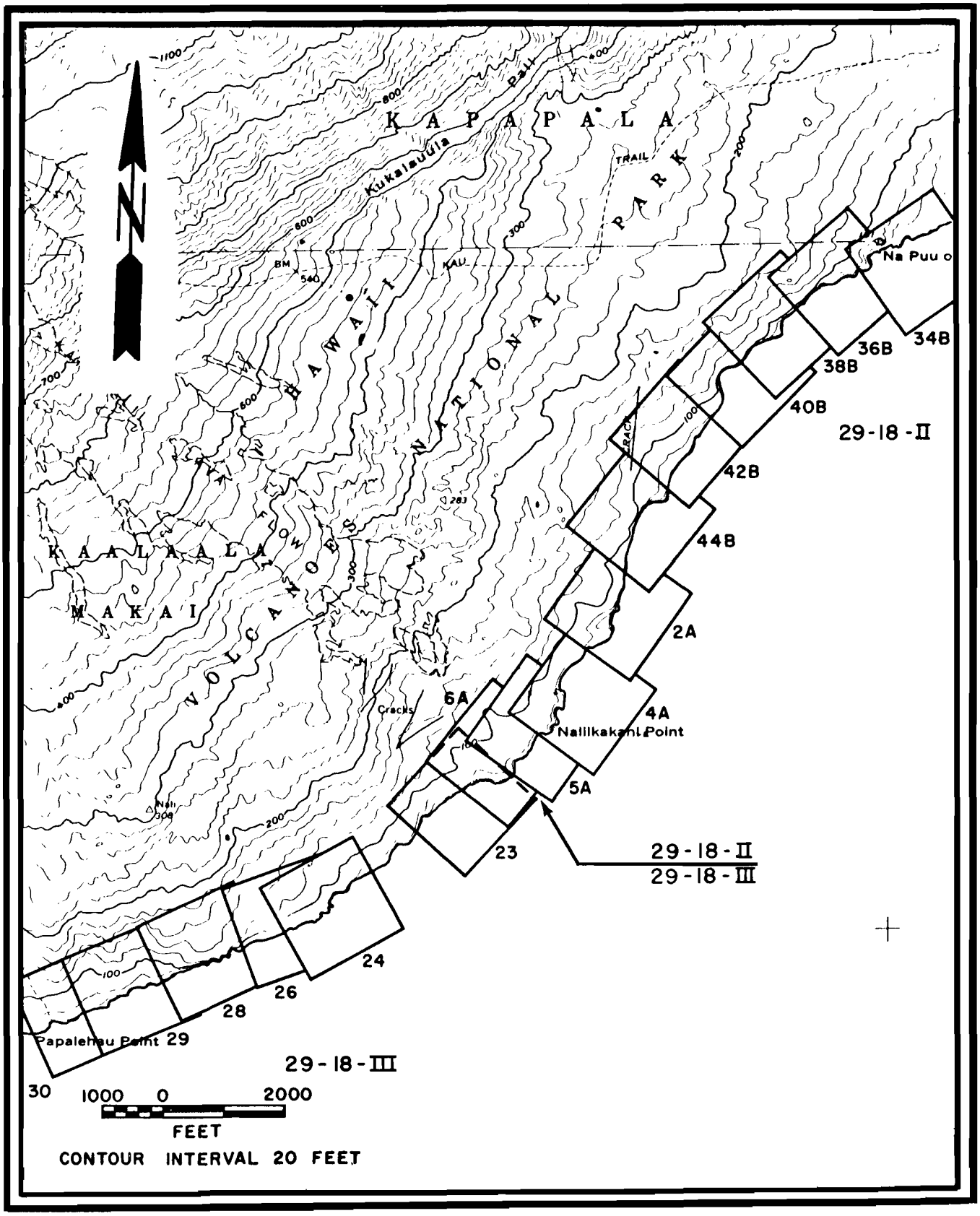

SUB-INDEX MAP NO. 37

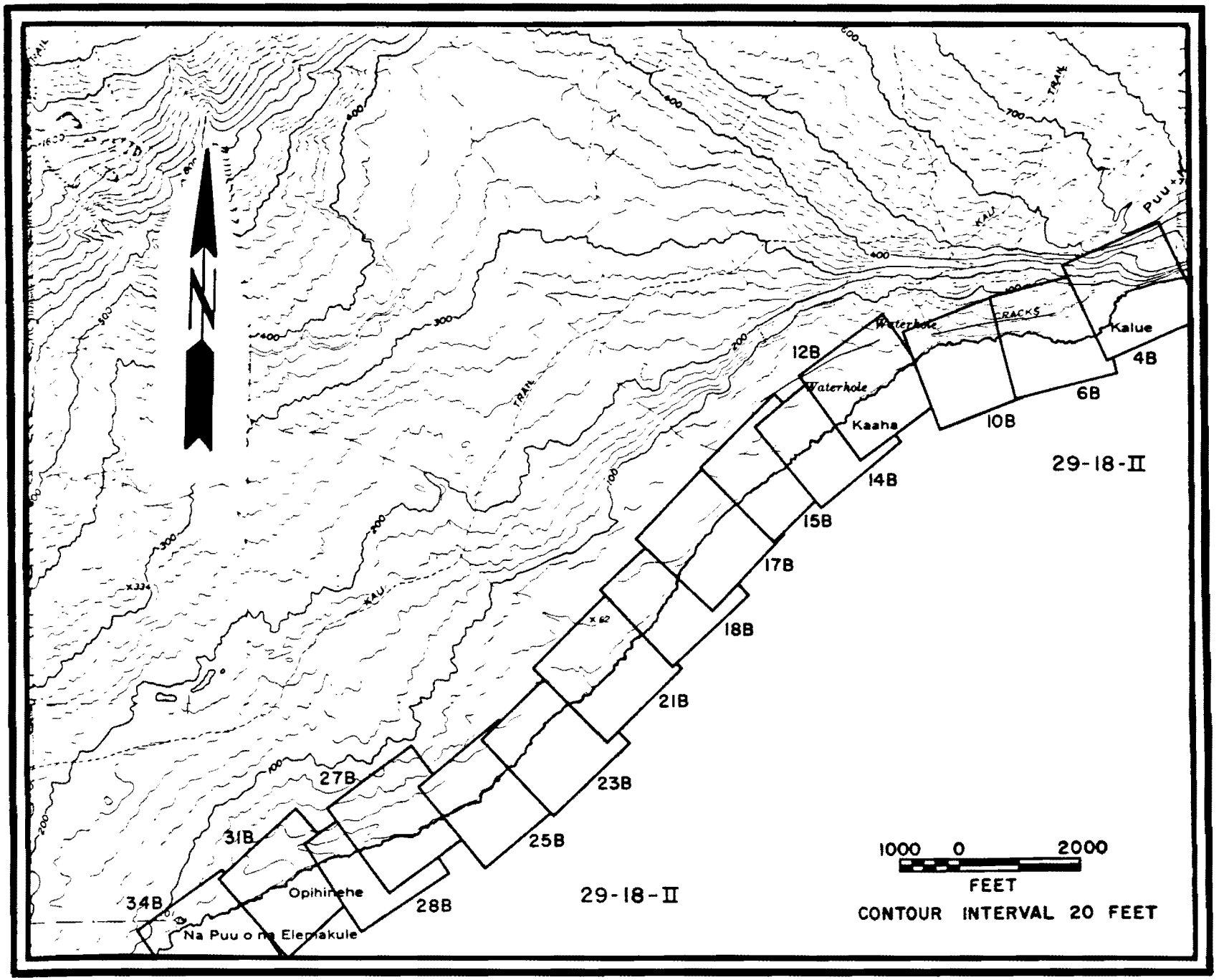

SUB-INDEX MAP NO. 38

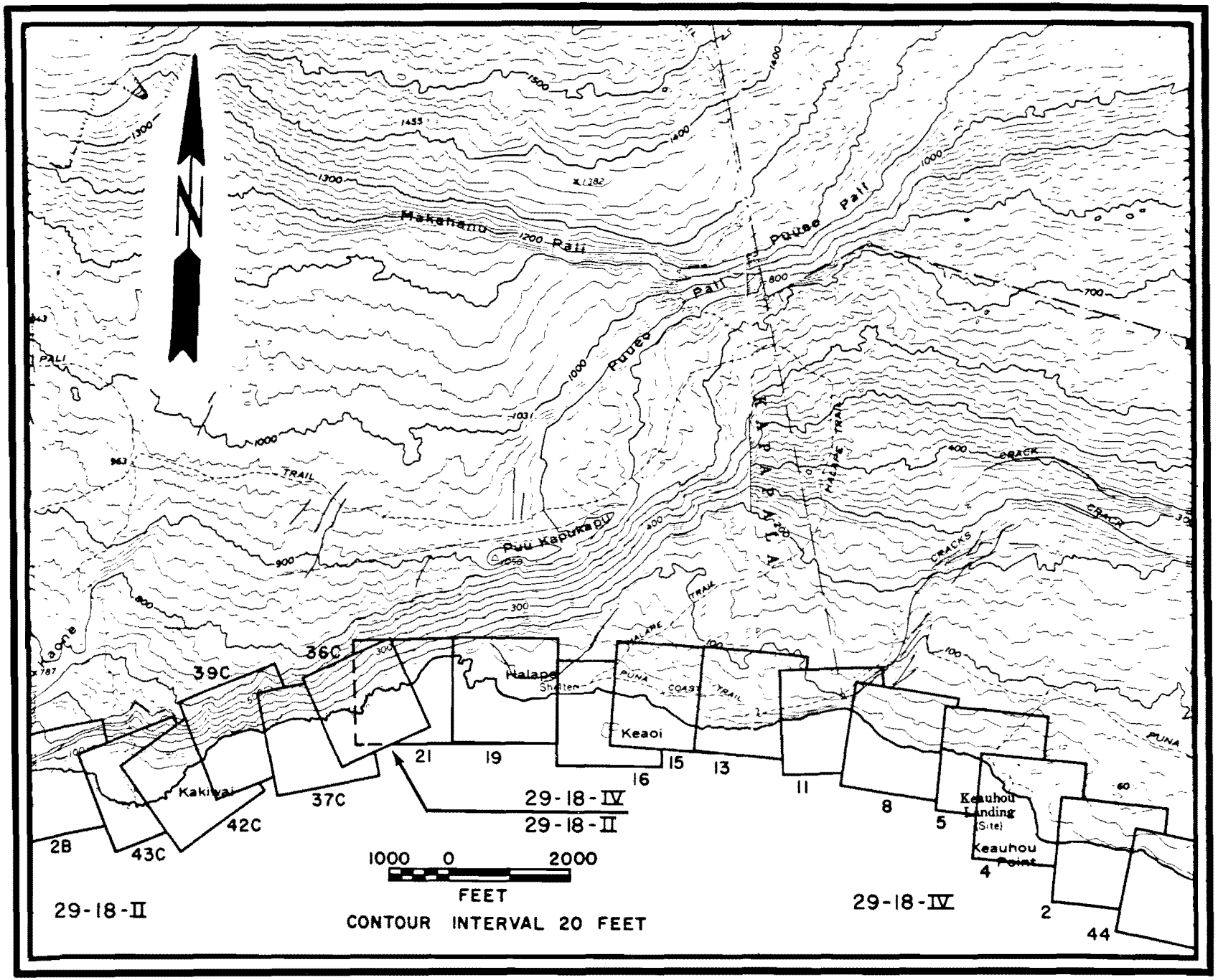

SUB-INDEX MAP NO. 39

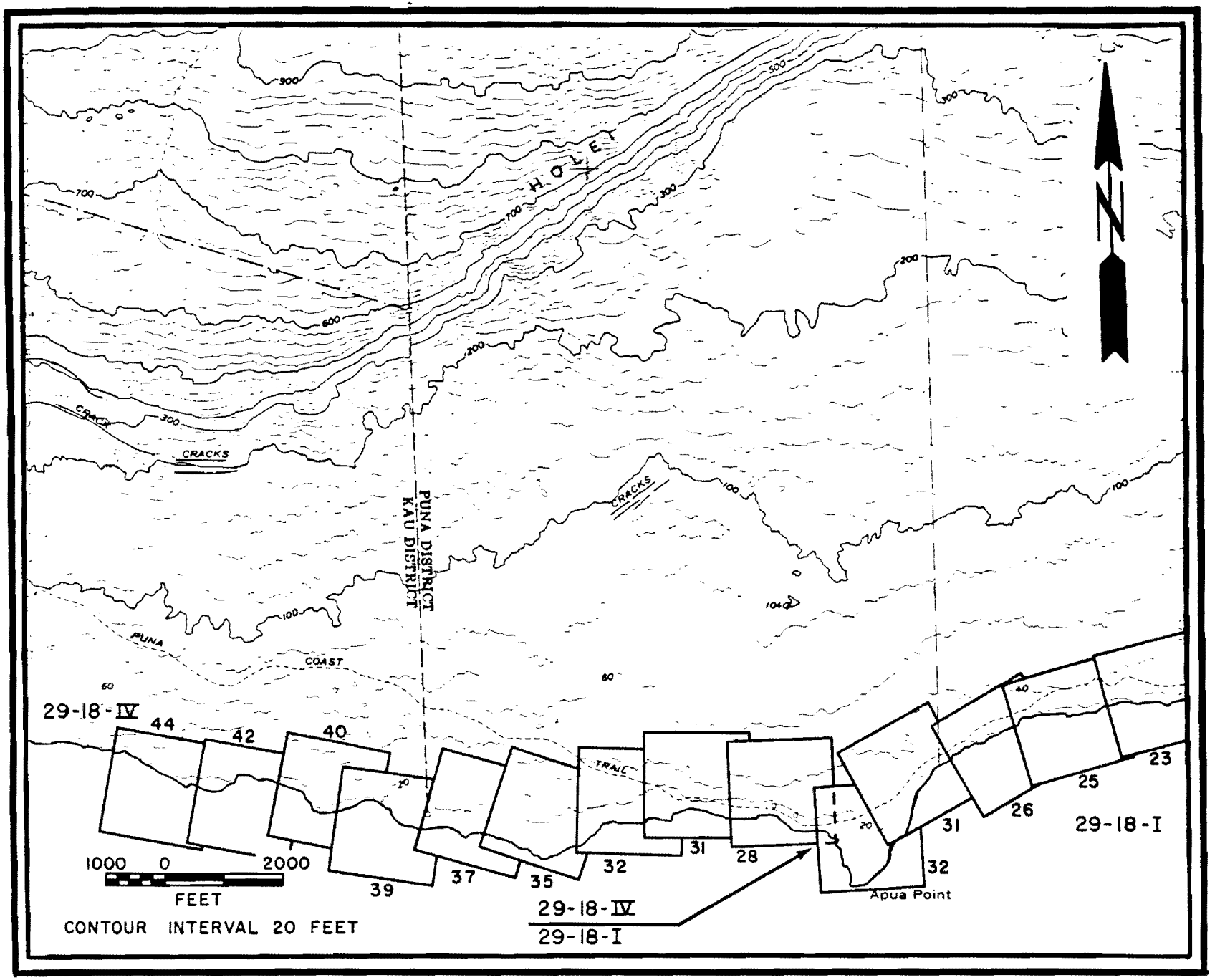

SUB-INDEX MAP NO. 40

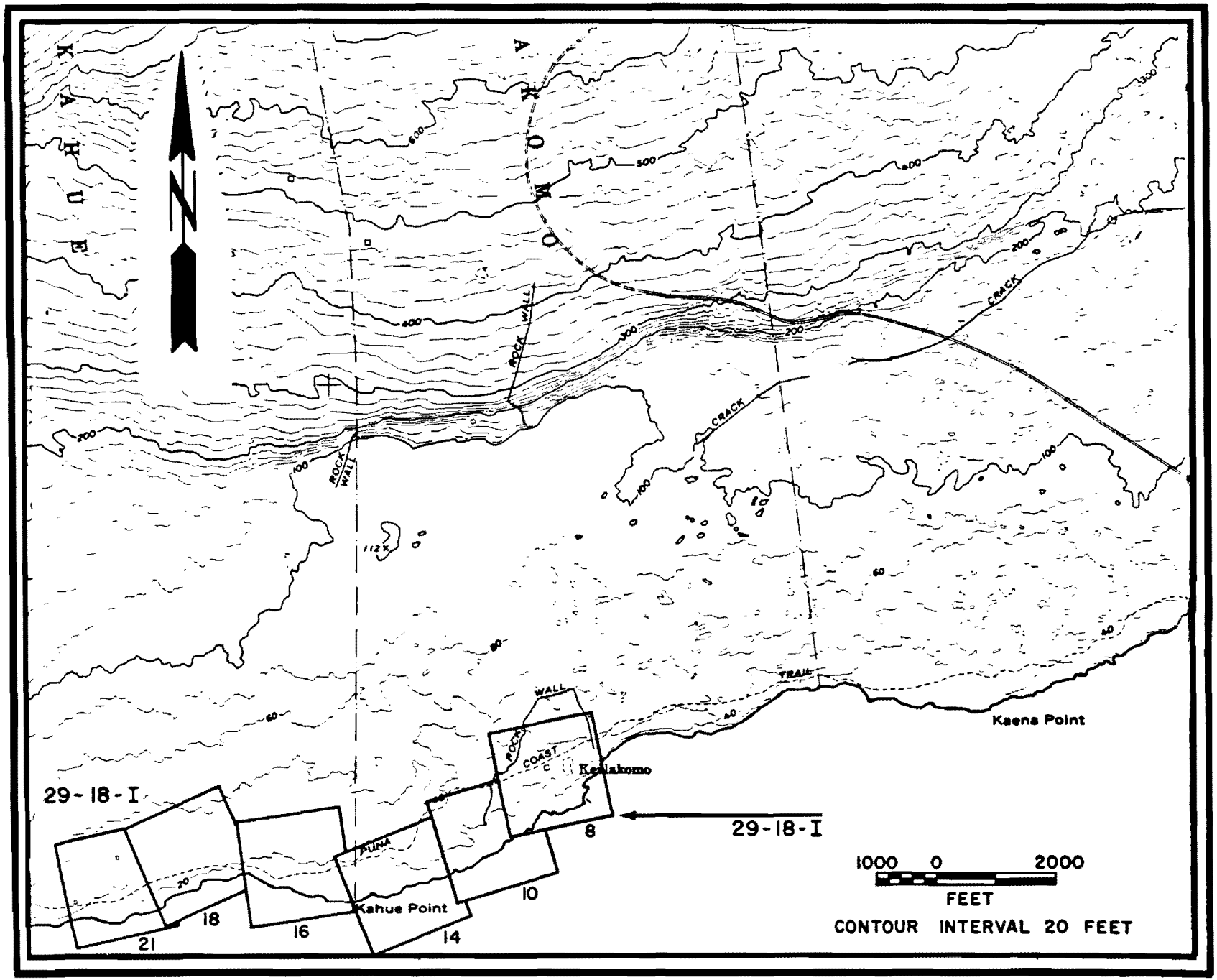

SUB-INDEX MAP NO. 41

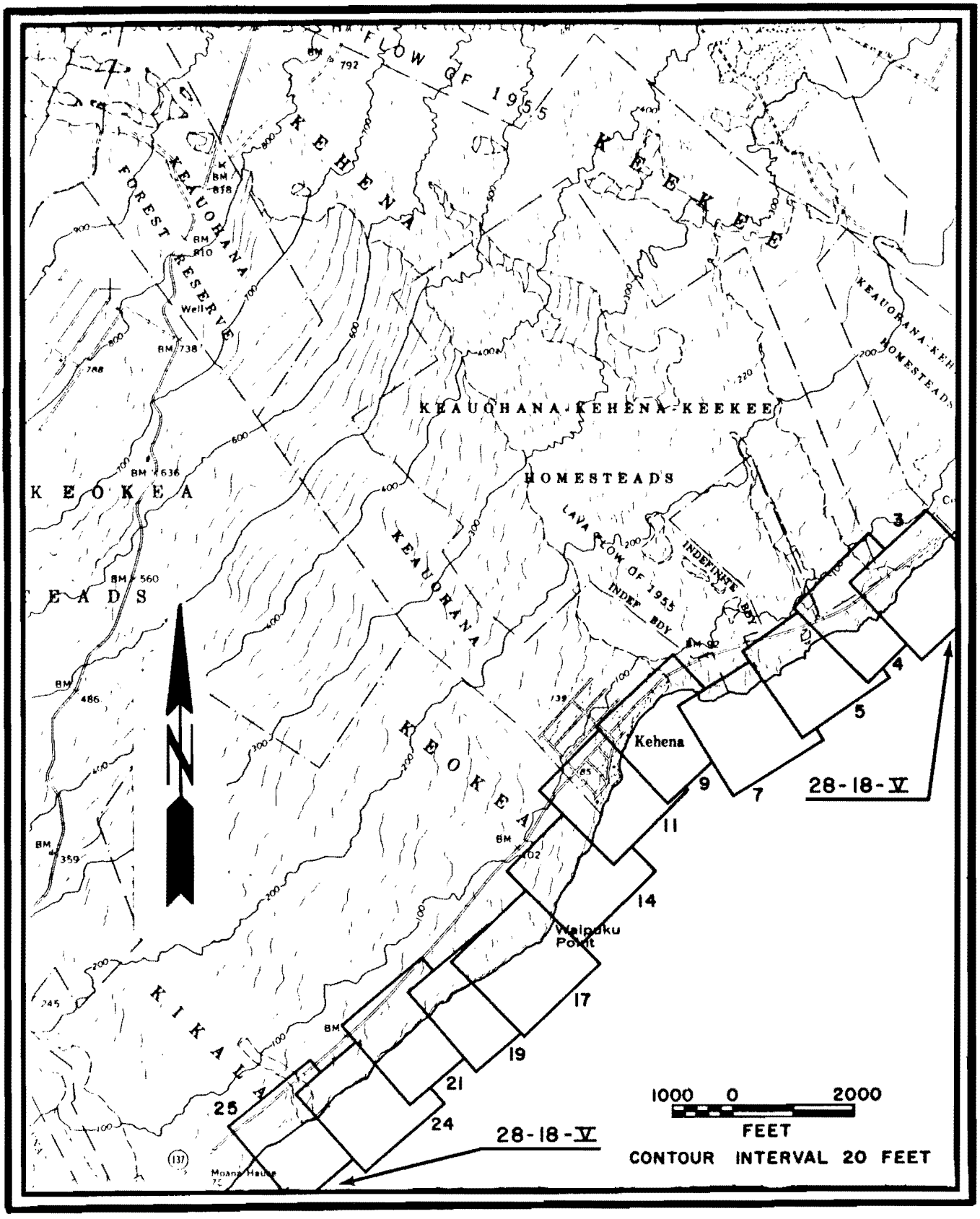

SUB-INDEX MAP NO. 42

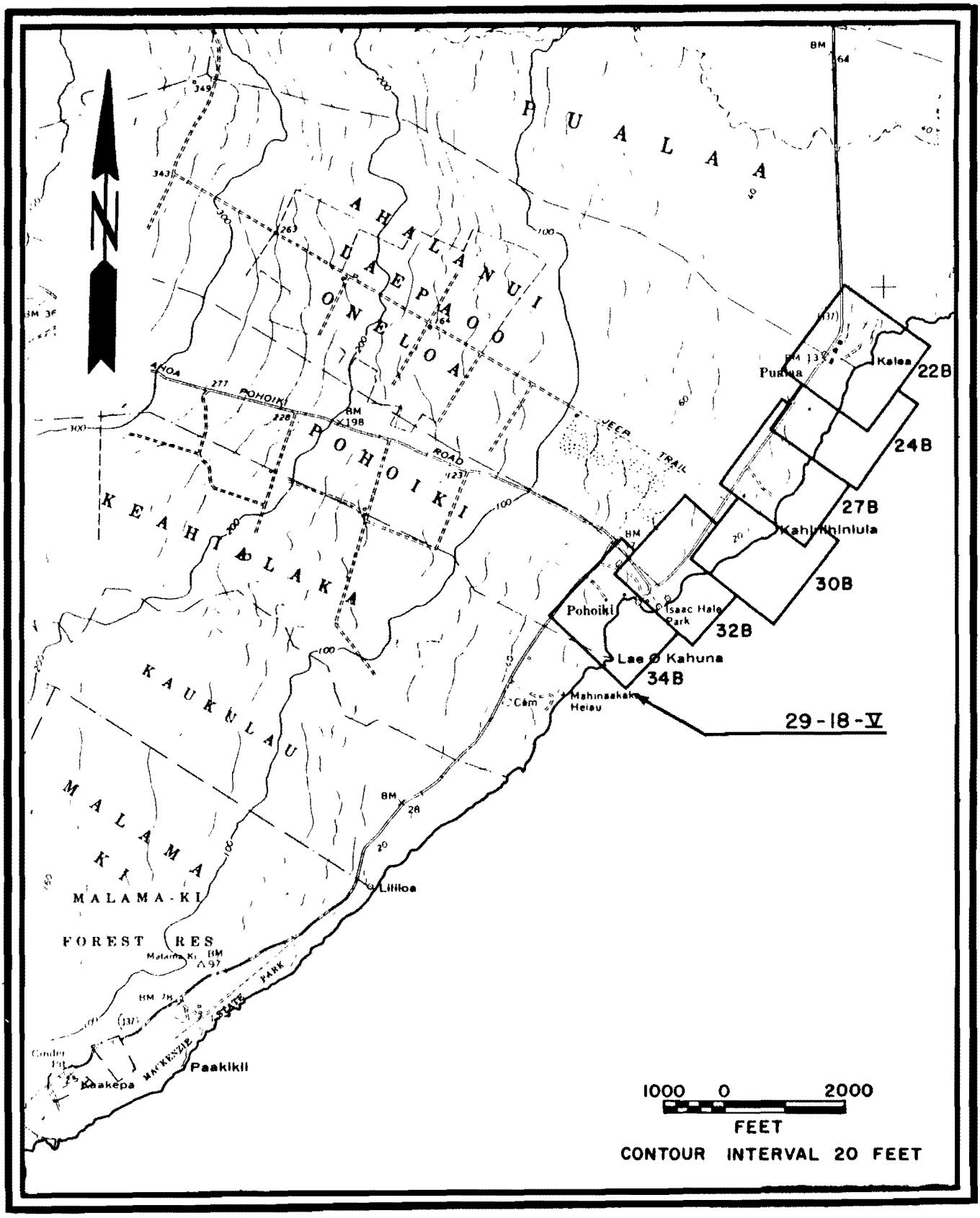

SUB-INDEX MAP NO. 43

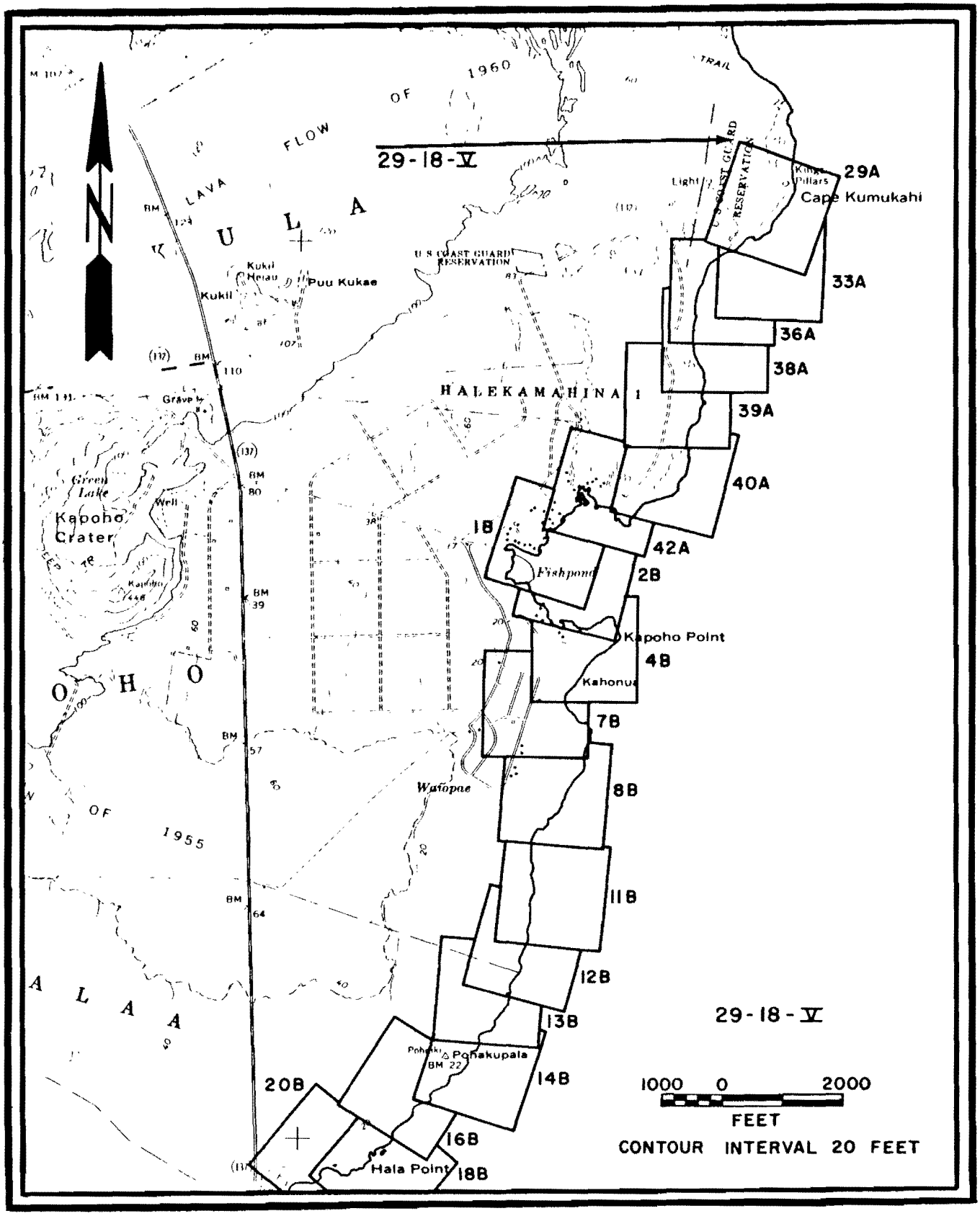

SUB-INDEX MAP NO. 44

AERO-MAGNETICS

SURENDRA P. MATHUR AND WILLIAM M. ADAMS

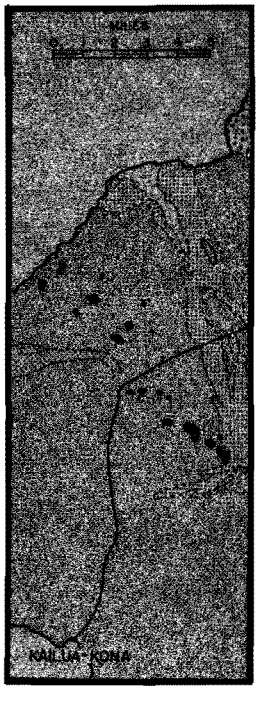

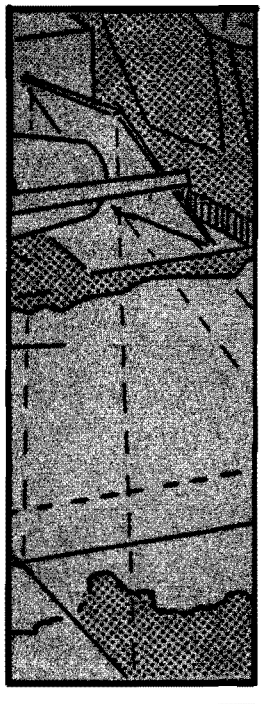

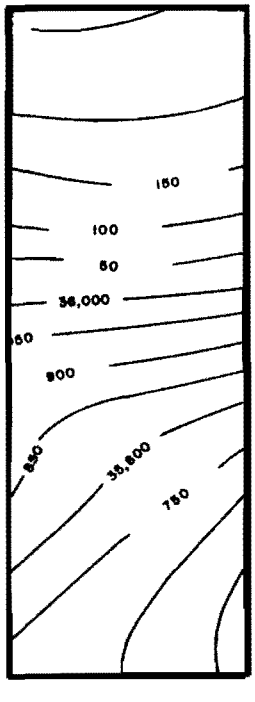

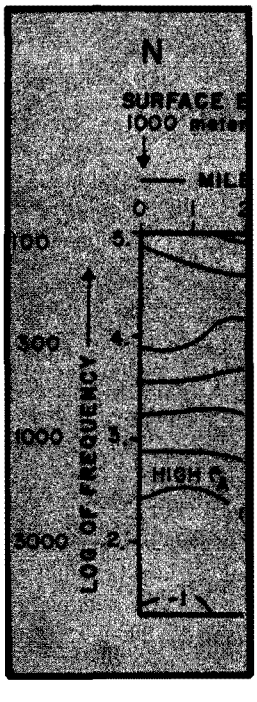

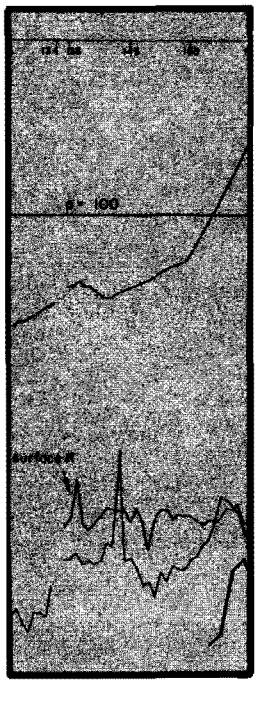

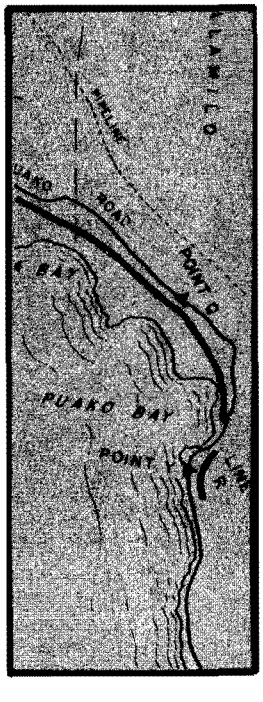

INTRODUCTION

The aerial magnetic survey effort attempted to delineate subsurface rock structures which might control the flow of ground water under the basaltic terrain of South Kohala between Kawaihae and Makolea Point along the NW coast of the island of Hawaii (Fig. 3.1).

INSTRUMENTS AND PROCEDURES

The total magnetic field observations were made by using an ELSEC Proton Magnetometer type 592/G (mfr. Littlemore Scientific Engineering Co., Oxford, England),towed by a Piper Apache twin-engined, 5-seater aircraft. The magnetometer units (Fig. 3.2) are transistorized and packaged for easy handling and maintenance.

The instruments were installed in racks mounted in the space made available behind the pilot's and co-pilot's seats by removing the two passenger seats. The interconnection of the battery, location camera, and various magnetometer units are shown in a block diagram (Fig. 3.3). The magnetometer sensing head, the "bird," which was stowed near the baggage door of the airfraft when not in used, was suspended through the baggage door by means of a braided polyprophylene rope through which the cable connecting the head to the recording instruments was passed. The door was closed after the 100-foot cable was fully extended. The end of the suspension rope was anchored to a ring welded to the instrument rack.

The procedure given in the brochure provided by the manufacturer was followed for operating the magnetometer. In brief, the steps to be taken are as follows:

1. Check the battery voltage and the circuit continuity.
2. Check the zeros and nines of the counters.
3. Set the tuning knobs properly for the ambient magnetic field strength.
4. Run the instrument on automatic fixed period polarization cycle.
5. Check the proper operation of the camera and the synchronization of the time marks on the chart.

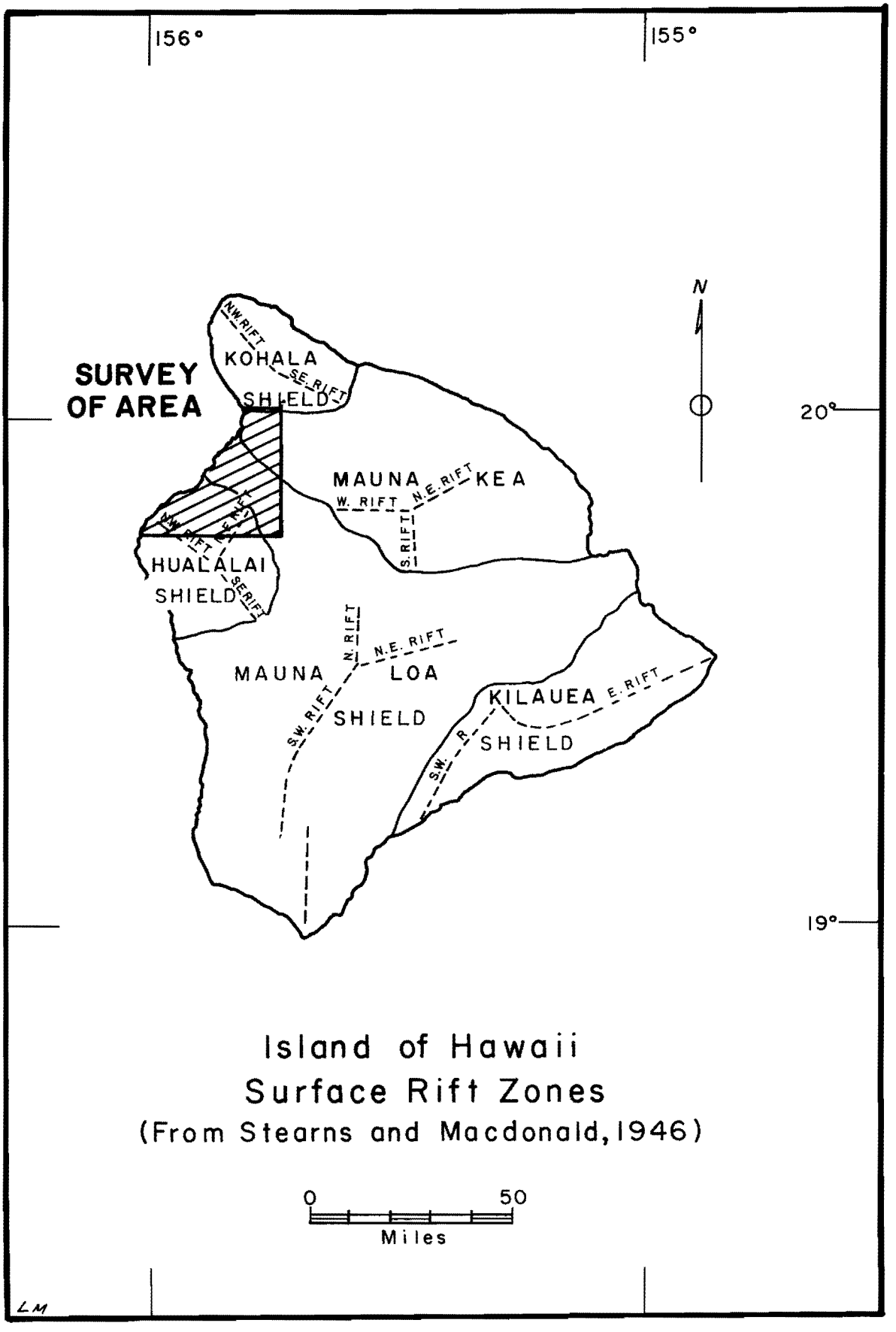

FIGURE 3.1. LOCATION MAP OF THE ISLAND OF HAWAII.

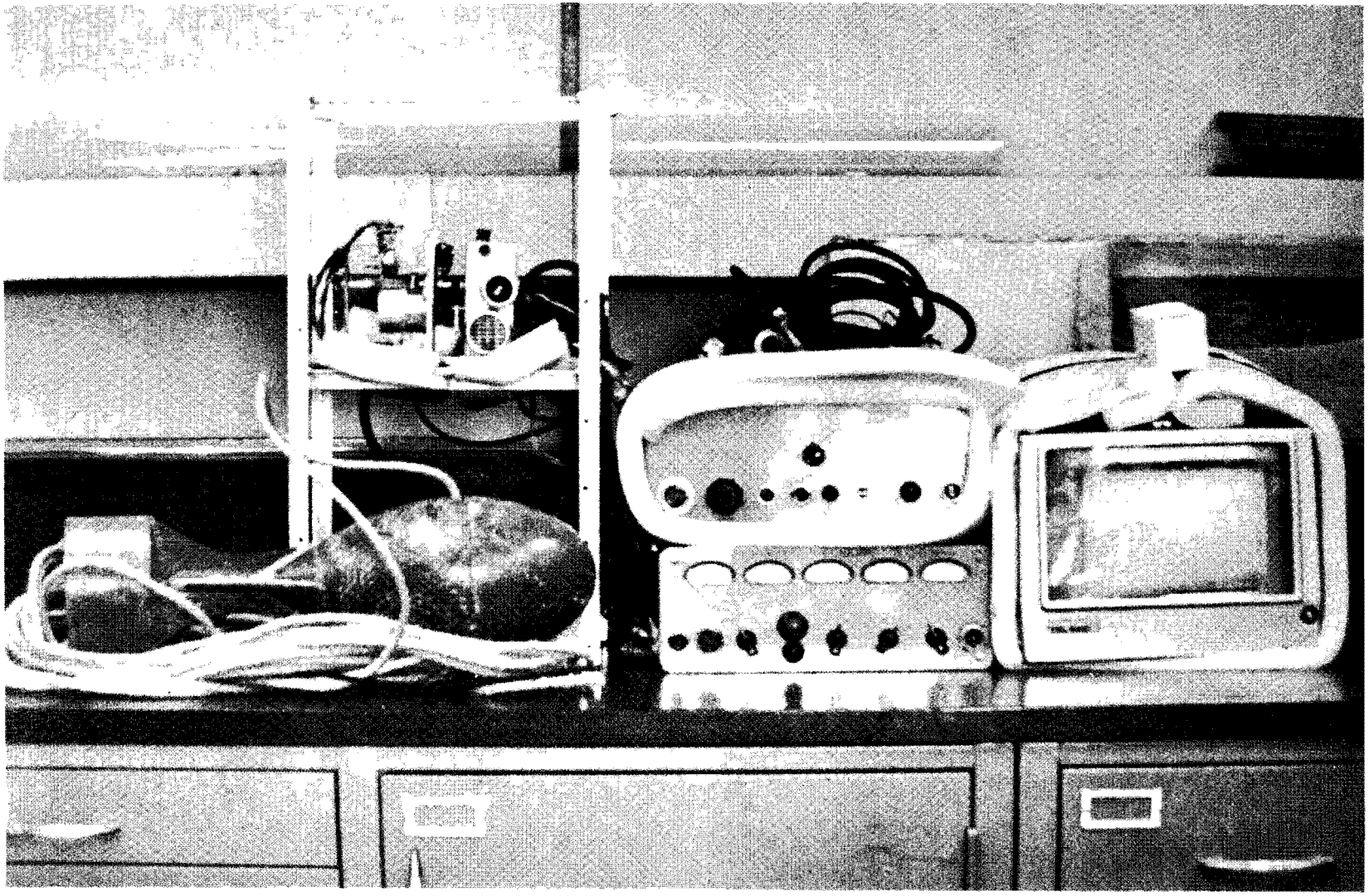

FIGURE 3.2. PICTURE OF THE INSTRUMENTS.

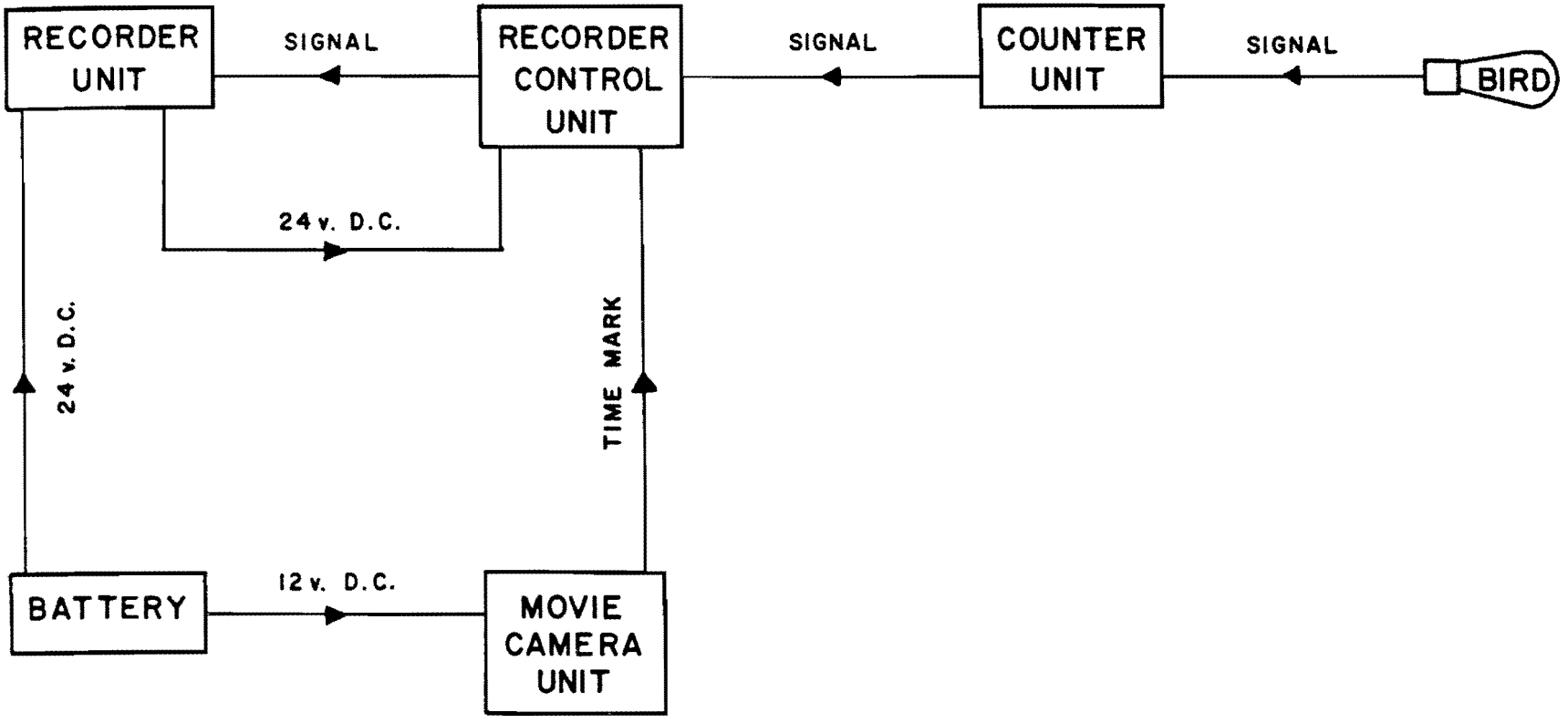

FIGURE 3.3. BLOCK DIAGRAM OF CABLE CONNECTIONS BETWEEN THE INSTRUMENT UNITS.

Magnetic storms during flight cause the magnetometer to become erratic and,hence, the nearest magnetic observatory should be contacted for weather information before and after each flight.

A 16-mm Bell and Howell movie camera, Model 200EE, was mounted vertically on a rack (as shown in Fig. 3:2) to enable the camera to take color photographs of the ground in flight through a port in the floor of the aircraft. The camera was triggered electrically at a speed of 1 frame/second. A synchronous time mark on the chart in the recorder unit provided a means of correlating the camera and the recording chart. Additional correlation was obtained by holding a light colored filter in front of the camera lens for a few seconds and marking the corresponding position on the chart. The power for both the magnetometer and the camera units was supplied by a 24-volt battery accumulator which lasted for 12 hours of continuous operation.

The aircraft was flown at speeds of about 100 mph. Polarization cycling periods of 6.4 or 2.6 seconds were chosen for the recording of the magnetic field,depending on the magnetic gradients encountered. At a speed of 100 mph the 6.4-second period permitted a surface sampling interval of about 800 feet.

All the flight lines in the Kawaihae-Kiholo Bay area were run from east to west from the high mountainous terrain to the east to the coastline to the west. On January 24, 1969, the lines were flown at about 4,000 feet above sea level and covered the area between Kawaihae and Anaehoomalu Bay wih an a-line spacing of about 1 mile. On March 29, 1969, the aircraft was flown at about the 3,000-foot altitude and a closer spacing of about 1/2 to 1 mile in the area south of Anaehoomalu Bay to Makolea Point in an effort to get a more detailed picture of the magnetic field.

The operations were greatly hampered by the amount of air turbulence encountered when flying on land near the coasts. The turbulence prevented the aircraft from flying any lower than 3,000 to 4,000 feet or maintaining the intended heading or spacing of the flight lines and also caused the aircraft altitude to fluctuate by as much as 500 feet.

Rapid and large changes were encountered in the magnetic field. Low altitudes made it difficult for the observer to manually mark at the right moment the hundred-digit value of the counter reading. Only the unit and the ten-digit values were automatically recorded on the

chart. Figure 3.4 is an example of the records where the hundred-digit values have been added with the possibility of large errors. Still another difficulty occurred because of poor time synchronization mechanism, *i.e.*, the triggering of the camera to produce the tick marks recorded on the chart, it was difficult to correlate correctly the pictures with the chart readings. This could have introduced an error of as much as ±5 seconds (*i.e.*, 700 feet) in the matching of pictures with the magnetic readings.

RESULTS AND DISCUSSIONS

The total magnetic field as mapped at about 4,000 feet in the Kawaihae to Anaehoomalu Bay area is shown as Figure 3.5 and that mapped at about 3,000 feet from Makolea Point to Anaehoomalu Bay is shown as Figure 3.6. The two maps were not combined because the altitudes in the two cases differed by about 1,000 feet. However, the small area east of the Anaehoomalu Bay, overlapped by the two surveys, shows similar anomaly features in the two figures.

For comparison, the regional magnetic field map of the island of Hawaii by Malahoff and Woollard (1965) is reproduced here as Figure 3.7. As expected, the Figures 3.5 and 3.6 show a higher value of the field strength and greater details of the anomalous features than the Figure 3.7, although the general pattern of the field remains the same.

The main features of Figure 3.5 are:

1. A magnetic high in the north-central area which is a part of the Kohala dipole field. Its southern extension (A) is rather pronounced and has a closure of about 150 gammas and is elongated in an east-westerly direction.
2. A small plateau area (B) with two small (50 gammas) closures on the southwest flank of the high (A).
3. Steep gradient on the southeast flank of the high (A) towards the regional low (C) of the Mauna Kea dipole field.

South of Anaehoomalu Bay the magnetic field pattern continues into Figure 3.6. The field steadily decreases in strength southwards and shows the following features:

1. A second plateau area (D) east of Keawiaki Bay with a small

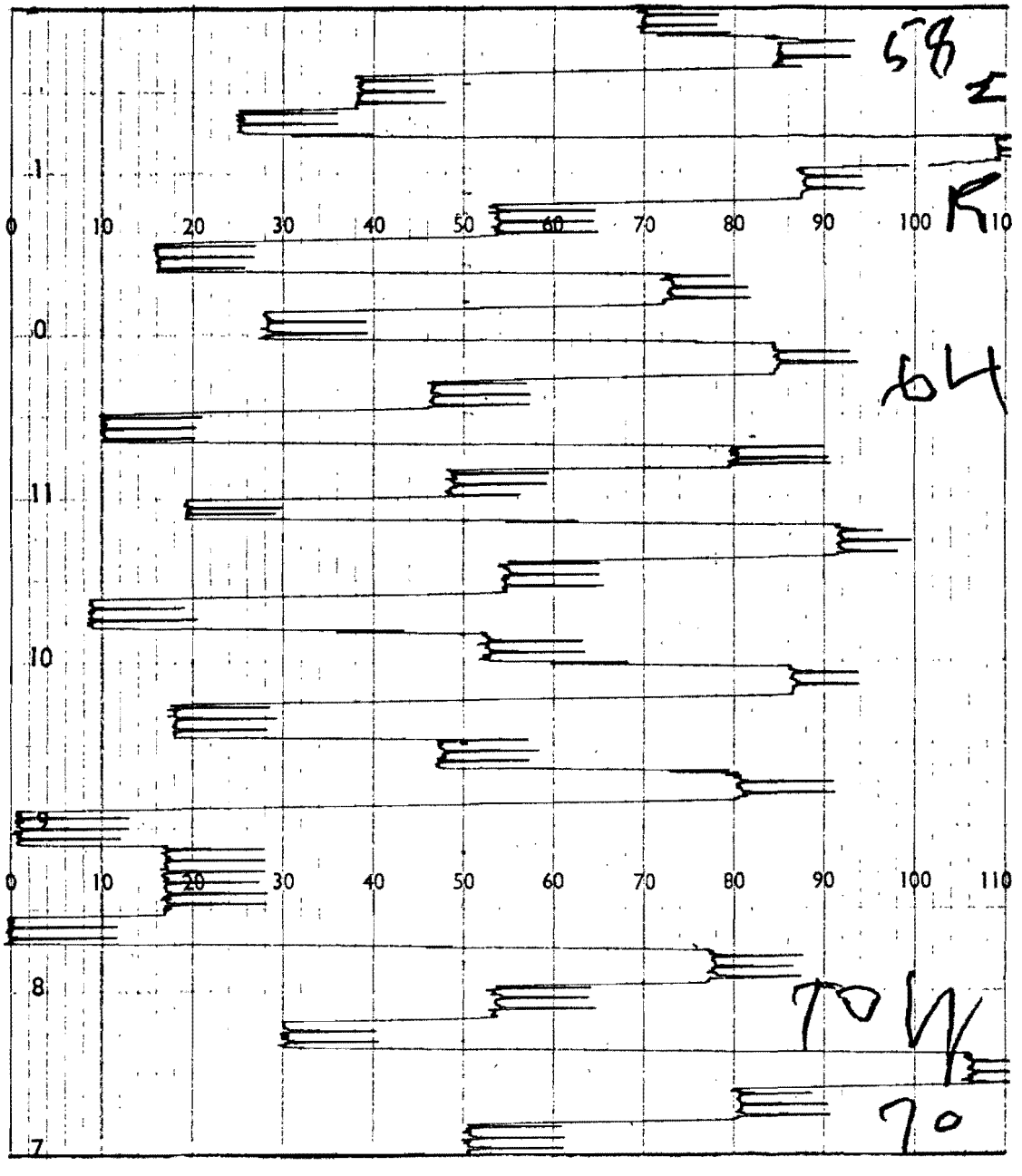

FIGURE 3.4. SAMPLE OF CHART SHOWING THE RAPID VARIATIONS IN THE FIELD OBSERVATIONS.

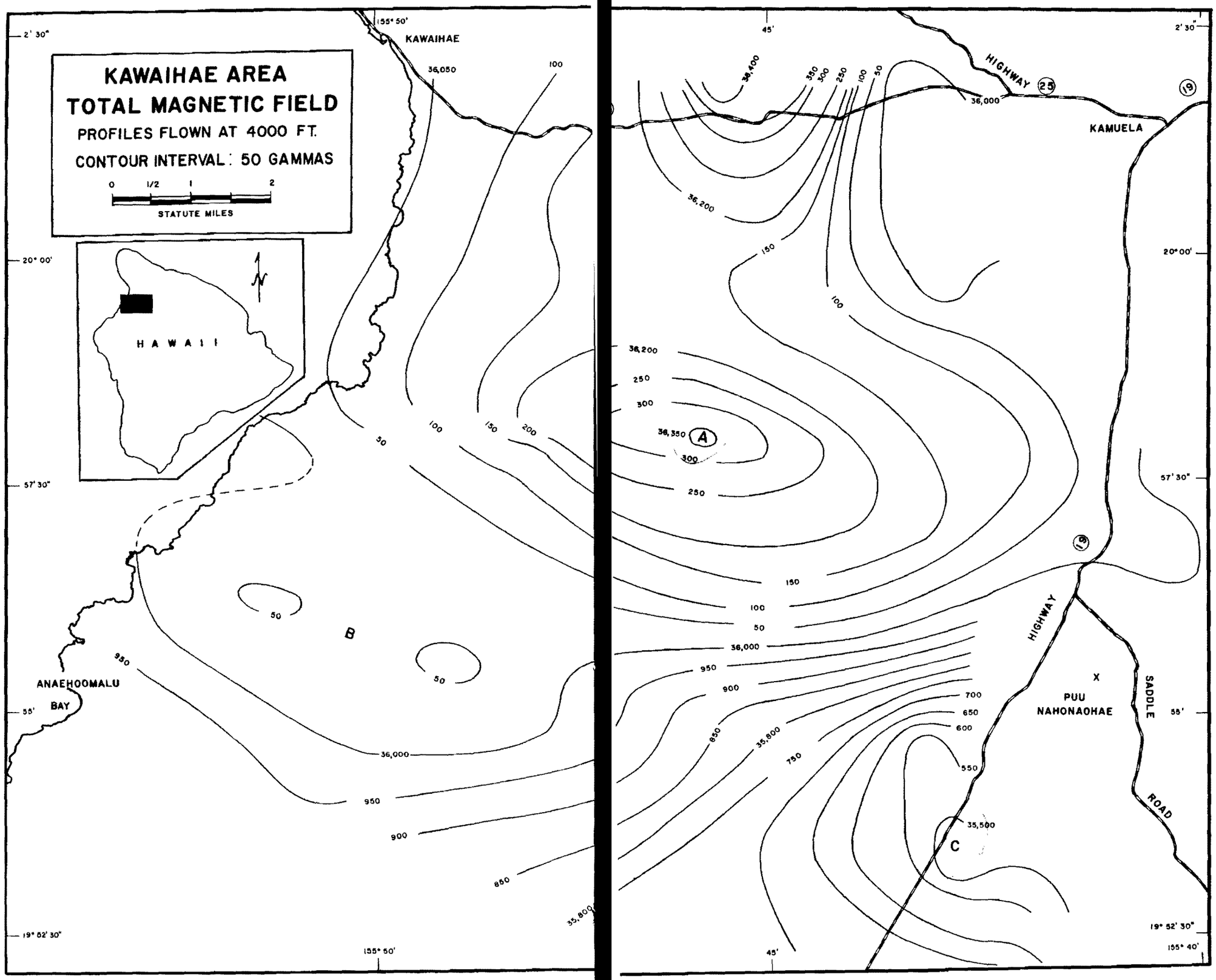

FIGURE 3.5. TOTAL MAGNETIC FIELD MAP OF KAWAIHAE AREA.

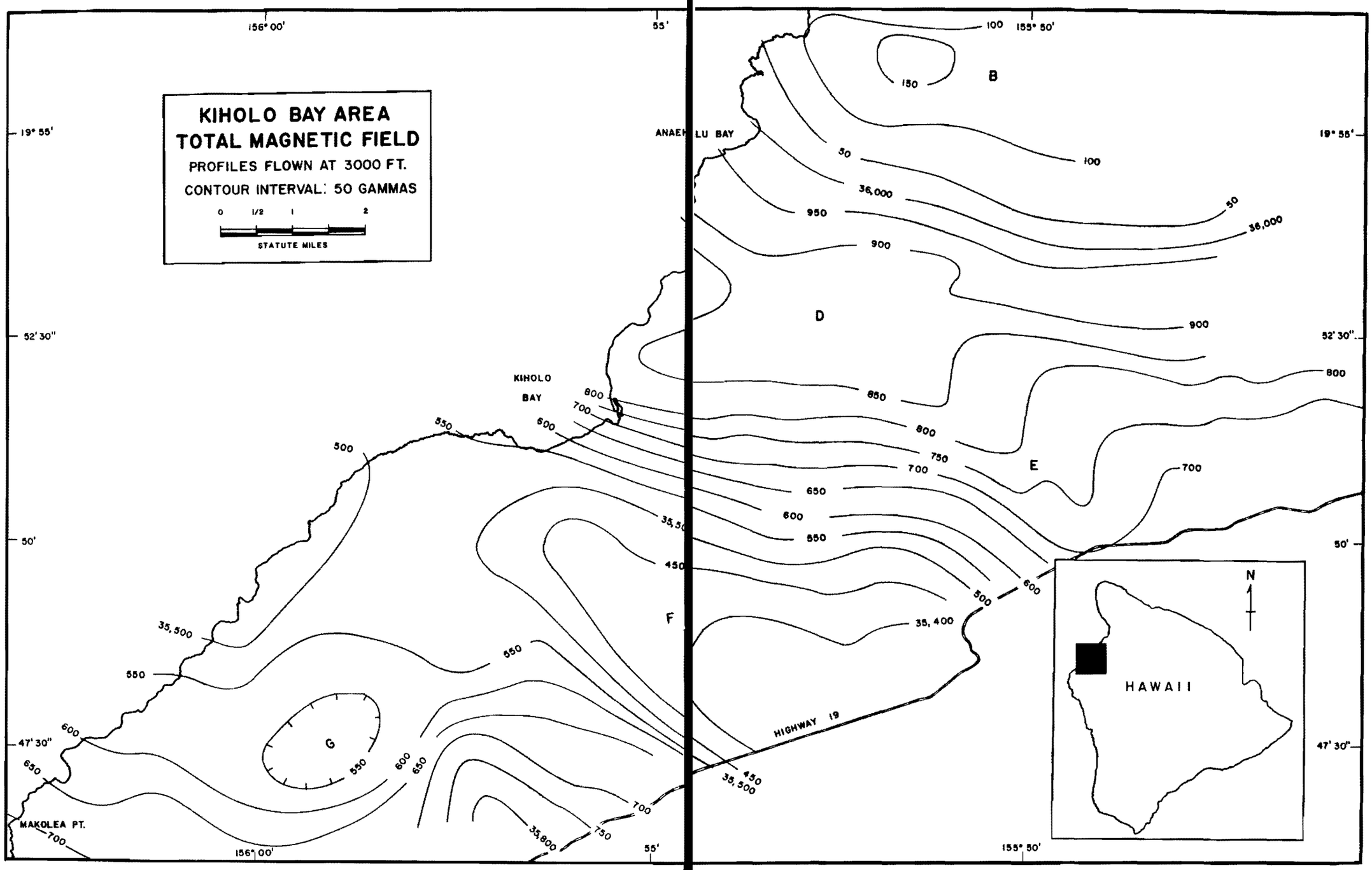

FIGURE 3.6. TOTAL MAGNETIC FIELD MAP OF KIHOLO BAY AREA.

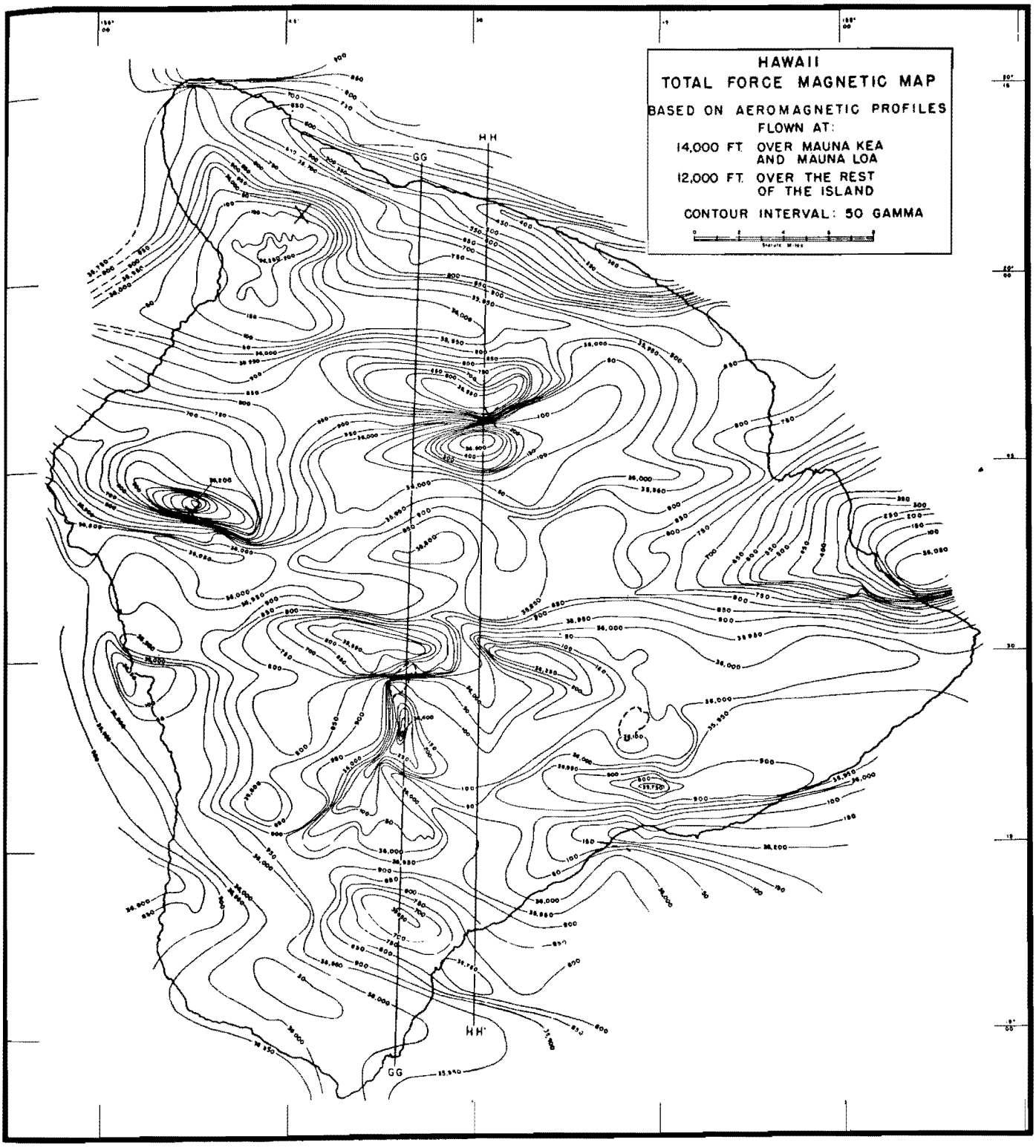

FIGURE 3.7. TOTAL MAGNETIC FIELD MAP OF THE ISLAND OF HAWAII (FROM MALAHOFF AND WOOLLARD, 1965).

nose-like feature (E) protruding towards the southeast.

2. A pronounce NW-SE trending low valley (F), southeast of Kiholo Bay.
3. A flat low area (G) on the southwestern flank of the valley (F).

All the above features, except the regional pattern and the effect of the Kohala and Mauna Kea dipole fields, have been delineated as a result of the low-level and closely-spaced aeromagnetic profiles.

The steep gradient in the magnetic field between the high (A) and the regional low (C) in Figure 3.5 could be due to an east-west dike or intrusive-filled rift zone and it corresponds to a sharp break in the apparent resistivity profile along the Waimea to Kailua-Kona Road (Lepley and Adams, 1969). The audiomagnetotelluric (AMT) survey there shows high resistivity to the northern side and low to the south. The zone of steep gradient towards the valley (F) seems to indicate a northwest extension of the Hualalai rift-zone,as proposed by Stearns and Macdonald (1946), and is picked up as a resistivity low in the AMT profile.

ACKNOWLEDGEMENTS

The assistance of messieurs Clifton Warren, Charles Dorigan, Frederick Duennebier, and Steve Hammond during the flight observations, of messieurs Howard Ishida and Roy Araki in assembling the camera rack and of Charles Dorigan in drafting the figures is gratefully acknowledged. Thanks are also due to messieurs Larry K. Lepley and Richie Huber for helpful discussion of the results.

Instruction on operation of the magnetometer was graciously provided by Dr. Alexander Malahoff. Mr. Ken Culler helpfully showed procedures to be used for efficiently working in the airplane with the pilot.

BIBLIOGRAPHY

Malahoff, Alexander and George P. Woollard. 1965. *Magnetic Surveys over the Hawaii Ridge*. HIG-65-11. Hawaii Institute of Geophysics, University of Hawaii.

Stearns, Harold T. and Gordon A. Macdonald. 1946. *Geology and Ground-Water Resources of the Island of Hawaii*. Bulletin 9. Hawaii Division of Hydrography.

AUDIO-MAGNETO-TELLURICS

LARRY K. LEPLEY
W. M. ADAMS

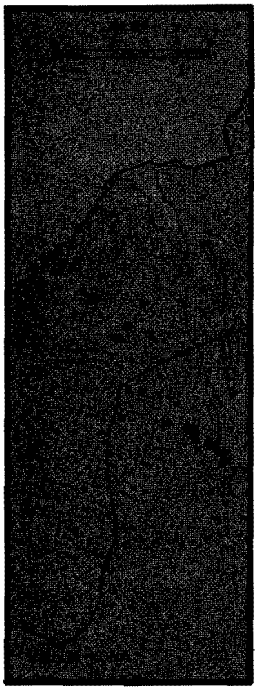

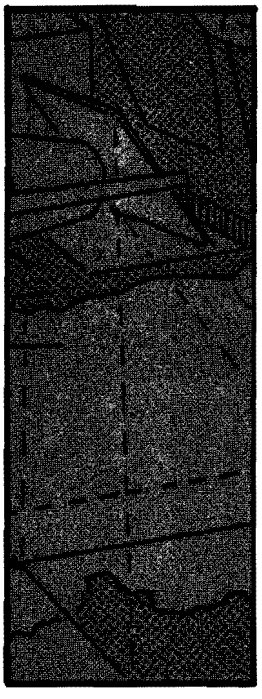

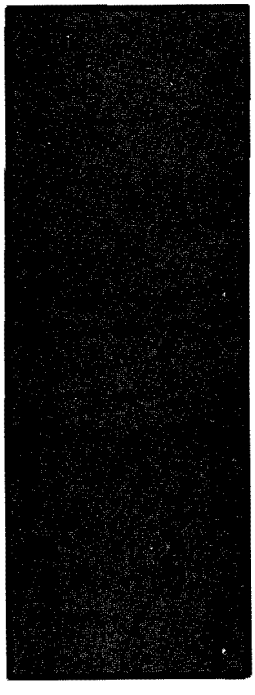

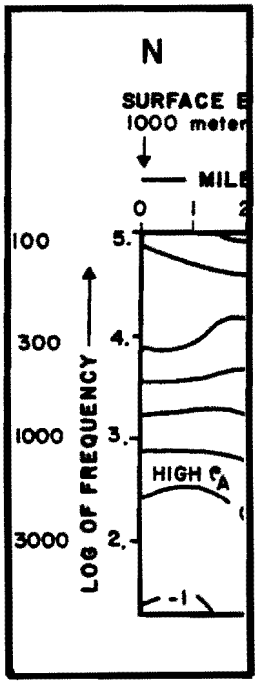

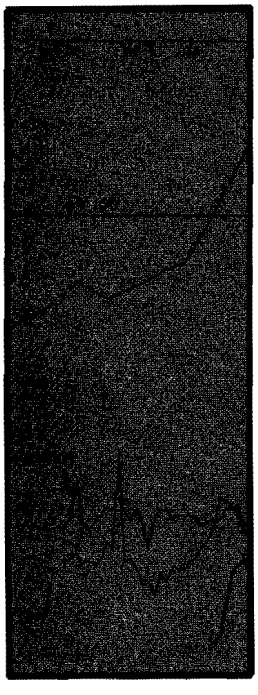

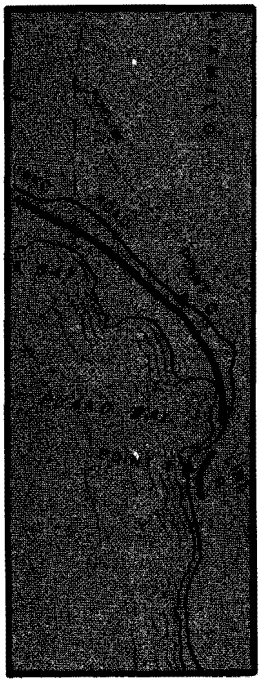

INTRODUCTION

The magnetotelluric method is a geophysical procedure for the determination of earth resistivity described in Keller and Frischknecht (1966). The prefix, audio, describes the frequency range used, from 20 to 100,000 cps. The purpose of the method is to obtain crude electrical resistivity logs without drilling. Assuming plane parallel beds, a resistivity log would indicate the depth, through volcanic rocks having high resistivity, to the sea-water interface having low resistivity.

The audiomagnetotelluric (AMT) method consists of finding the impedance normal to the earth's surface by measuring the mutually perpendicular horizontal components of electric and magnetic vectors of the magnetotelluric field. The magnetotelluric field is a naturally-occurring field usually considered to be electrical noise. In the audio section of the spectrum the source of energy is distant lightning.

The locations of the survey stations for the study are shown on the map in Figure 4.1. The purpose of the survey was to locate the depth to the sea-water interface or to locate dikes buried by subsequent lava flows.

THEORY

The main sources of the AMT fields are the electromagnetic waves generated by lightning discharges in electrical storm centers located principally in Africa, South America, and the East Indies (Keller and Frischknecht, 1966). The field can be assumed to be plane waves propagating vertically into the earth because the enormous propagation contrast between air and earth causes the waves to be refracted downward regardless of incidence angle. Another fortunate aspect of the AMT field is its large scale uniformity which permits us to be concerned with local effects (Neves, 1957).

At audio frequencies, another source of energy can be current flowing through power mains. The wavelengths measured in the earth (drastically shorter than those in air) range from a few hundred meters to a few kilometers. The assumption of plane-wave behavior is valid when the sources of energy are more than a few wavelengths away. At audio frequencies, lateral changes in resistivity distort the results if they occur within a half wavelength of the measuring site. Current flow across

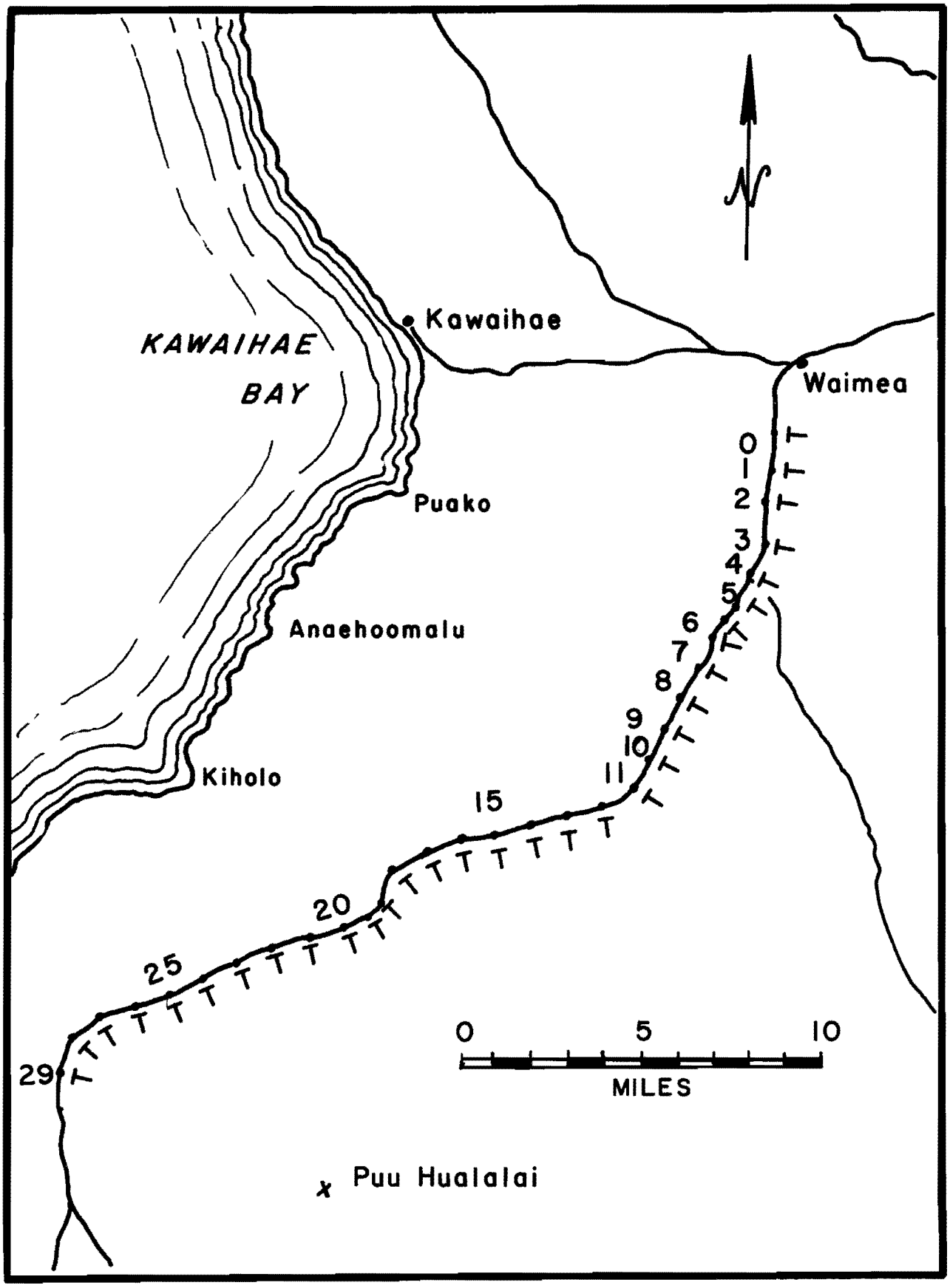

FIGURE 4.1. STATION LOCATIONS ON AMT PROFILE.

the earth's surface is negligible. Therefore, if telluric current flow is perpendicular to the strike of a dike, the magnetic field is constant or monotonically changing with frequency or distance from the dike. If, on the other hand, the current flow is parallel to the strike, then the electric field is constant or monotonic. While the one-dimensional problem treated by Cagniard (1953) needed only a spectrum of frequencies at one location for a two-dimensional structure (*i.e.*, dikes, etc.), measurements along a line perpendicular to the strike is needed so that both the vertical and horizontal changes in conductivity may be detected.

In the Cagniard method, the impedance of the earth's surface is related to the ratio of the intensities of the electrical and magnetic fields:

$$\rho_A \sim \frac{1}{\mu\omega} \left(\frac{E_x}{H_y}\right)^2 \tag{1}$$

or, according to Yungel (1968):

$$\rho_A = \frac{0.2}{f} \left(\frac{E_x}{H_y}\right)^2 \tag{2}$$

where:

E = electric field in volts per meter,

H = magnetic field in amperes per meter,

μ = magnetic permeability (assumed to be 1. for geologic material) in H per meter,

ω = frequency in radians per second,

f = frequency in cycles per second (cps), and

ρ_A= apparent resistivity in ohms per meter.

The apparent resistivity is sampled over one-half of the frequency-dependent skin depth ρ:

$$\frac{1}{2}\rho = \frac{1}{2}\sqrt{\frac{\rho_A}{\mu\omega}} \tag{3}$$

For a given depth, attenuation is stronger at higher frequencies. Therefore, the measurement of E/H at decreasing frequencies samples resistivities

at increasing depths.

Yungel (1968) has published a catalogue of apparent resistivity curves for the one-dimensional (horizontal isotropy) case. The important conclusion that can be drawn from Yungel's computations is that, for horizontal, isotropic bedding, the slope of the curve, ρ_A, versus frequency on log-log plot *cannot exceed* ±*1* for the two-layer model. For the three-layer case, the slope can approach ±2.

Neves (1957) has presented an analytical solution to the problem of dipping beds and arbitrary two-dimensional geometries. Charles Swift's (1968) curves of measured ρ_A at a single frequency versus distance over a vertical contact show an abrupt discontinuity of the perpendicular E field ($E_{\perp}$) over the contact and a monotonic curve of the parallel E field ($E_{||}$).

INSTRUMENTATION AND FIELD PROCEDURE

The electric field component was detected by heavy metal rods driven into the ground or placed on lava rock 31 meters apart. The contact resistance between the electrode pairs varied from 1,000 ohms in soil near the Kamuela airport (Fig. 4.1) to 200,000 ohms on aa lava flows.

The horizontal component of the magnetic field at right angles to the electrode line was detected with a calibrated induction coil consisting of 30,000 turns of wire on a square frame enclosing 1.2 m^2 of air core. Figure 4.2a is a photograph of the equipment and Figure 4.2b shows the operation of the equipment in field.

The outputs of the pair of electrodes and the induction coil were analyzed and measure with two General Radio null meters, which are high-gain amplifiers having narrow band-pass variable-frequency filters and a meter. Between the input leads (from the coil and the electrodes) and their respective meters are variable attenuators with linear dial settings (Fig. 4.3).

At the first station, the gain setting on the two amplifiers were equalized each day by adjusting the gains for equal meter readings when the electrode output was connected to both null meters in parallel.

At each station, the leads from the electrodes were connected to the left attenuator and the coil to the right attenuator. The attenuators

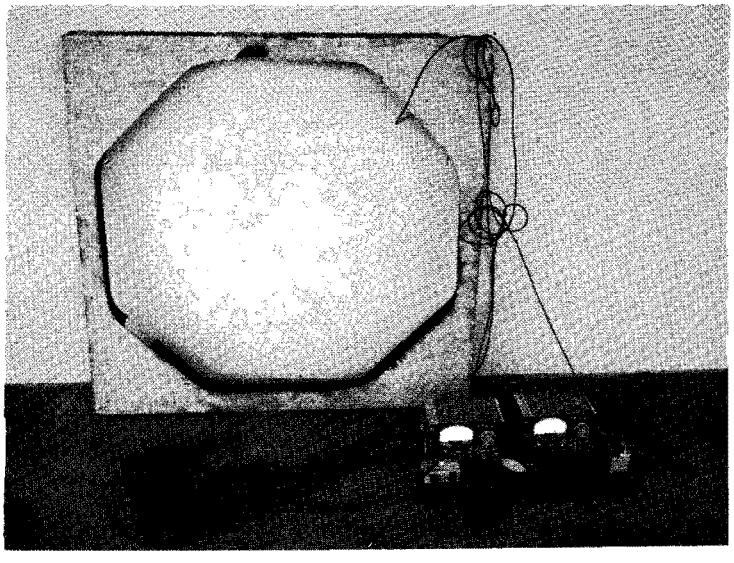

FIGURE 4.2a.
PHOTOGRAPH OF THE
AMT EQUIPMENT.

FIGURE 4.2b.
OPERATION OF THE
AMT EQUIPMENT IN
THE FIELD.

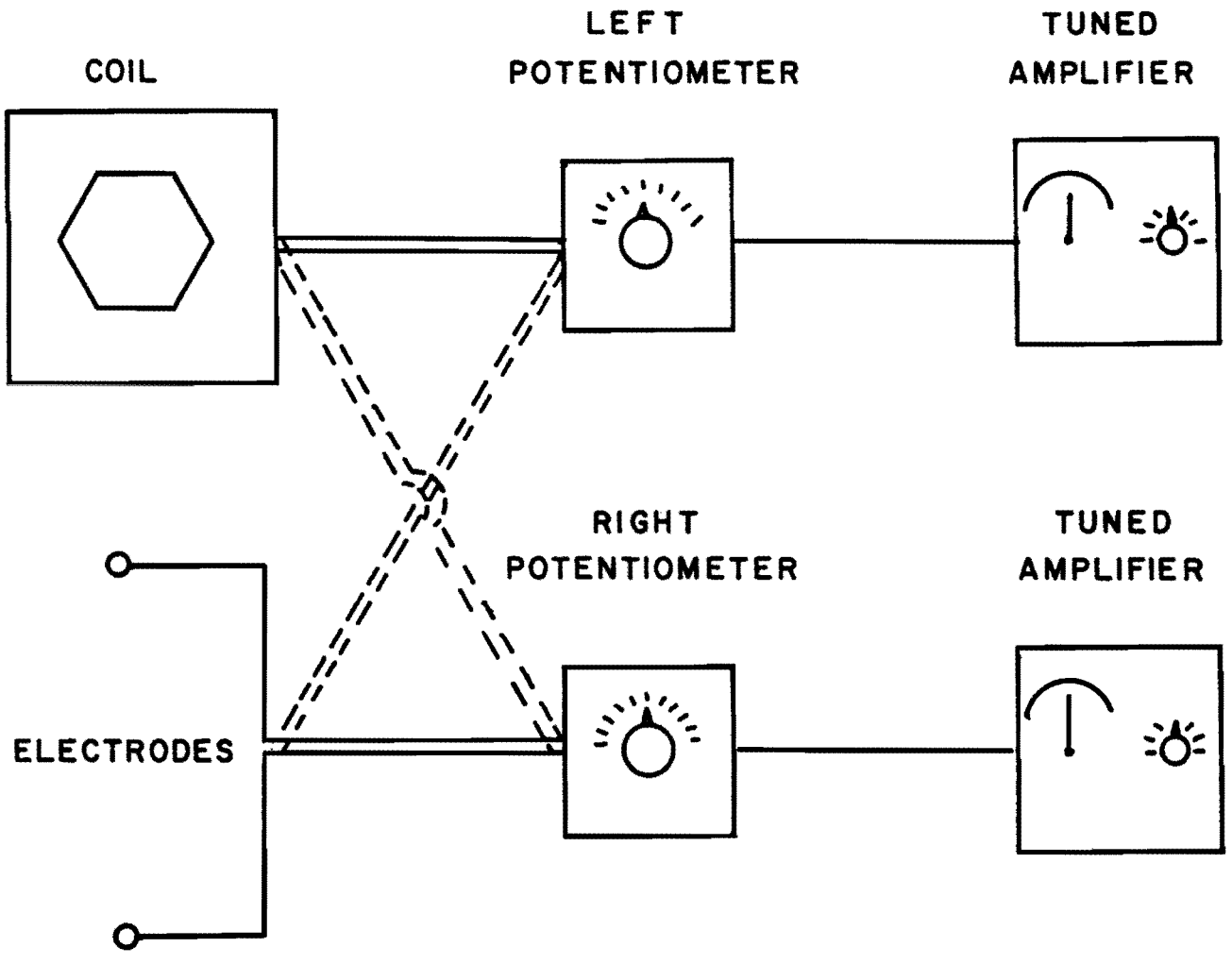

FIGURE 4.3. BLOCK DIAGRAM OF CIRCUITRY USED FOR AMT FIELD MEASUREMENTS.

(potentiometers voltage dividers) were then adjusted so that the simultaneous meter readings are equal and the attenuator dial settings are recorded as $\frac{1}{E_L}$ and $\frac{1}{H_R}$ for the electrodes and coil, respectively. (L is for left meter; R, for right meter). Then the leads were reversed. Opposite attenuator-meter combinations were used and the new attenuator settings were recorded as $\frac{1}{E_R}$ and $\frac{1}{H_L}$. The reverse setting corrected electronic asymmetries. The meters were tuned to the next predetermined frequency and the measurement repeated. After the entire frequency scale was transversed, the electrodes and coil were reset at the same station at right angles to their previous orientation and all measurements repeated and recorded separately.

The null meters were not intended to be used as voltmeters, but only as null indicators to enable the measurement of the ratio of electric to magnetic fields and not the absolute magnitudes. The electrode resistance was also measured with an ohmmeter at each station.

The orientations of the electrode pairs is indicated on Figure 4.1 as line-pointer segments beside each station number. The stations were located on the Kamuela to Kailua-Kona highway at approximately one-mile intervals and numbered so that the station numbers indicate the mileage south of station number 0.

REDUCTION OF FIELD DATA

Computation of resistivity was based on the Cagniard expression:

$$\rho_A = \frac{1}{\omega\mu} \left(\frac{E_x}{H_y}\right)^2 , \qquad (4)$$

where H is the magnetic field component in amperes per meter, E is the electric field component in volts per meter, ω is the angular frequency in radians per second and μ is $4\pi \times 10^{-7}$.

However, the voltage drop, V, between the electrodes, separated by 31 meters, was actually measured,

$$V \text{ (volts)} = 31 \text{ (meters) } E \left[\frac{\text{volts}}{\text{meters}}\right]$$

In the survey area, the electrode resistance was appreciable when compared to the input resistance of the potentiometer circuit and the

voltage which passed through the attenuator was less than the voltage, V, at the electrodes:

$$Va = \left[\frac{R_i}{R_i + R_g}\right] V \quad , \tag{5}$$

where R_i is the input resistance of the circuit and R_g is the resistance of the electrodes in the ground.

The magnetic field, measured by the induction coil producing an electromotive force (the ideal coil has no resonance or capacitive effects), is:

$$EMF = -nA\mu\omega H, \quad , \tag{6}$$

where n is the number of turns in the coil and A is the area in square meters. A correction must be made to the output voltage of the non-ideal coil. On coil calibration, the voltage output is larger than predicted for an ideal coil near the coil resonance and less for frequencies above the resonance. This difference can be represented by a multiplicative correction factor, K_{coil}, which corrects the actual output to the ideal output. This correction factor is then a function only of frequency for a given coil. The actual EMF of the coil is:

$$EMF_a = -K_c nA\mu\omega H \quad . \tag{7}$$

The coil corrections were determined by two methods, induction and impedance. In the induction method, the coil and null meter combinations were calibrated with a standard magnetic field provided by an oscillator regulated to constant RMS output of 1.8 amperes. This known AC current was driven through a 10-turn coil of the same dimensions as the measuring coil and the frequency was varied incrementally. The calibration curve derived in this manner is shown as a dotted line in Figure 4.4.

In the impedance method, an AC voltage of constant RMS value was applied directly to the measuring coil by a tuneable oscillator and the RMS amperage was measured as the oscillator was tuned to the sequence of frequencies. The voltage output of such a coil is proportional to its impedance. This impedance curve is shown as a dashed line on Figure 4.4.

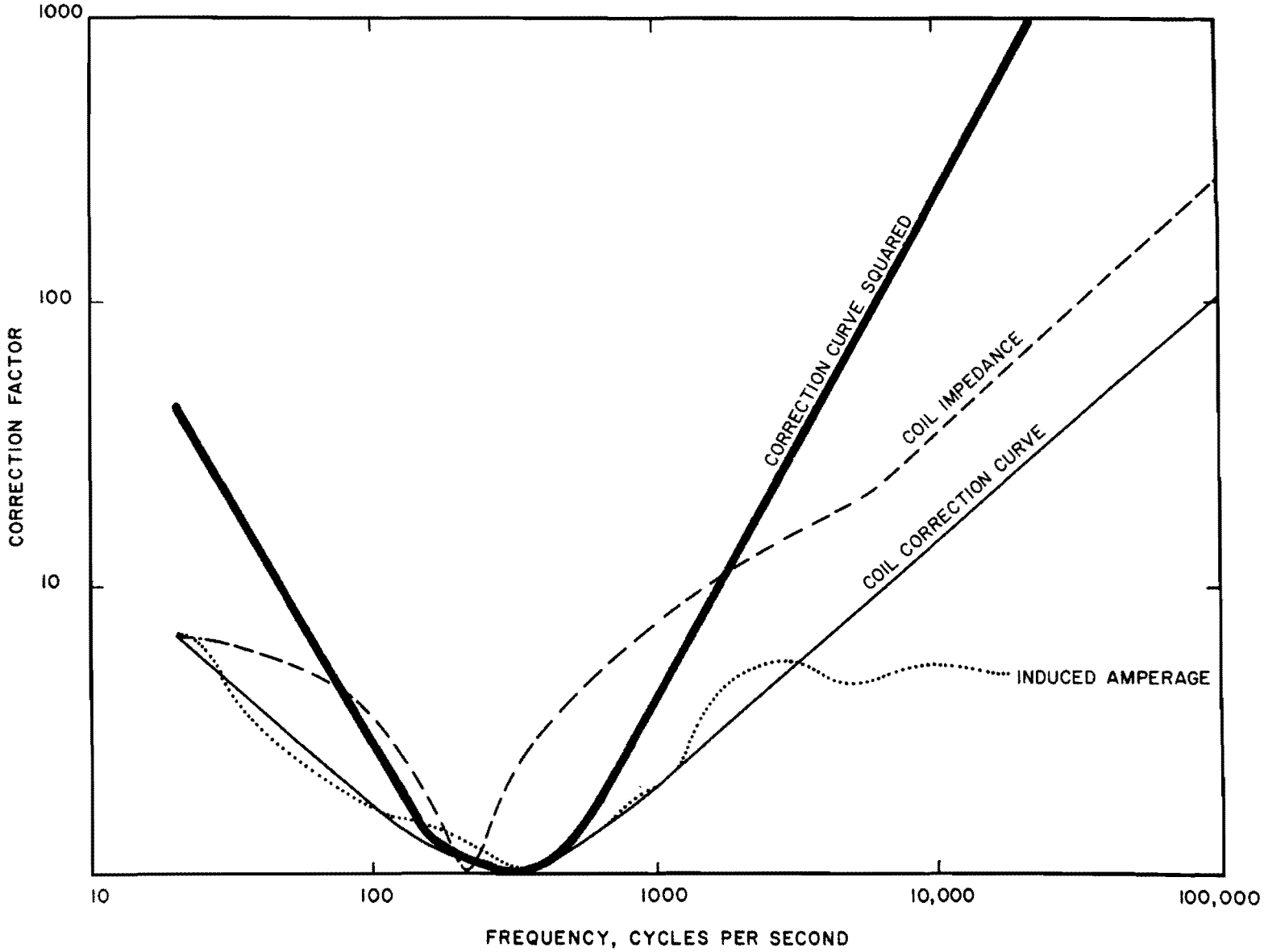

FIGURE 4.4. COIL CORRECTION CURVES AS DETERMINED BY TWO METHODS, A GENERALIZED CORRECTION CURVE, AND THE CORRECTION CURVE SQUARED FOR USE IN COMPUTER PROGRAM.

The heavy solid line, a compromise, shows the correction curve of values used in the data processing computer program. The values of the curve were squared because the corrections are applied to squared voltages. The slope of the curves indicates that the coil has parallel inductive and capacitive reactance between the wires of the adjacent windings.

Combining equations 4, 5, 6, and 7 yields the formula for computing resistivity:

$$\rho_A = \frac{\pi\mu A^2 n^2}{f\ (31.)^2}\ \frac{V_L}{EMF_R}\ \frac{V_R}{EMF_L}\ (K_F)\ \left(\frac{R_i}{R_i + R_g}\right)^2 \qquad (8)$$

where R_i = 100,000 ohms, the electrical resistance of the potentiometers. The quantity, $\frac{\pi\mu A^2 n^2}{(31.)^2}$, comprises a geometric factor for the measuring system. For the components employed in this survey, equation (8) reduces to:

$$\rho_A = \left[\frac{162.}{f}\right]\left(\frac{V_L}{EMF_R}\right)\left(\frac{V_R}{EMF_L}\right)(K_{coil})\ \left(\frac{R_i}{R_i + R_g}\right)^2 . \qquad (9)$$

The spectrum of ρ_A was computer-drawn separately, so that each station was represented by two spectra, one for each orientation. These two curves were then averaged, yielding one curve per station. The values from the averaged curves were then plotted as resistivity in a coordinate system of station numbers versus frequency with the frequency decreasing downward and station numbers representing mileage. A contour map of these values (Fig. 4.5) represents a geophysical cross-section of resistivity, which is integrated downward from the surface.

DATA INTERPRETATIONS

A rapid method of field interpretation was evolved. Two indexes were estimated: the relative average resistivity and the horizontal anisotropy at each station. At each station a "flat" reading of E and H was taken for the two electrode coil orientations. A flat reading represents the instrument's single response to the entire frequency band and is designated by the subscript "p" when the electrodes are

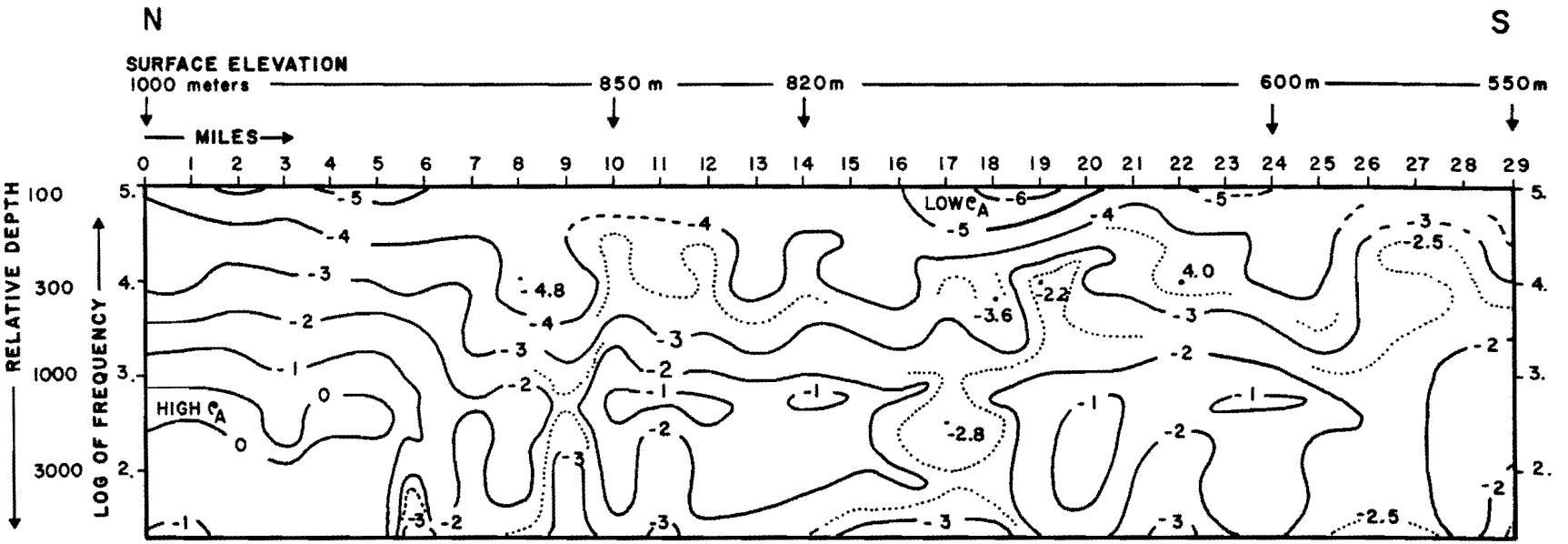

FIGURE 4.5. CONTOURED CROSS-SECTION PLOT OF ρ_A INTENSITY DETERMINED BY AMT. VERTICAL SCALE IS LOG OF FREQUENCY AND THE HORIZONTAL SCALE IS DISTANCE. THE RELATIVE DEPTH SCALE IS JUST A GUESS.

parallel to the road; "n" when they are normal or perpendicular, to the road. The relative resistivity is computed with a slide rule as:

$$\text{average } \rho = \frac{1}{2}\left[\left(\frac{E_p}{H_p}\right)^2 + \left(\frac{E_n}{H_n}\right)^2\right] \quad . \tag{10}$$

An index of the degree of horizontal anisotropy is computed as:

$$\text{ratio} = \left(\frac{E_p}{H_p}\right)^2 \quad \left(\frac{E_n}{H_n}\right)^2 \quad . \tag{11}$$

Figure 4.6 plots these two indexes versus distance. Two features are notable. Stations 0 through 5.6 show average resistivities three orders of magnitude higher than those of stations 6 through 27. Stations 6 and 7 show a strong anisotropy trending in an azimuth perpendicular to the road.

A comparison of Figures 4.5 and 4.6 allows some structural interpretations. The section can be divided into five provinces as follows:

STATION	PROVINCE
0 to 5.6	I
6 to 9	II
10 to 16	III
17 to 18	IV
19 to 29	V

Province I is underlain by material of relatively high resistivity and a high degree of horizontal isotropy, possibly Mauna Kea volcanics containing a thick fresh-water lens depressing the sea-water fresh-water interface. Province II contains vertical structures trending normally to the road, possibly a dike swarm. Province III is underlain by material showing lower resistivity, possibly containing only a thin layer of fresh water and consequently a fresh-sea-water interface close to sea level. The contrast to Province I may also represent a change in Mauna Loa volcanics. Province IV is a relatively narrow zone showing still lower resistivity, possibly a vertical structure trending 45° to the road. Province V is similar to Province III.

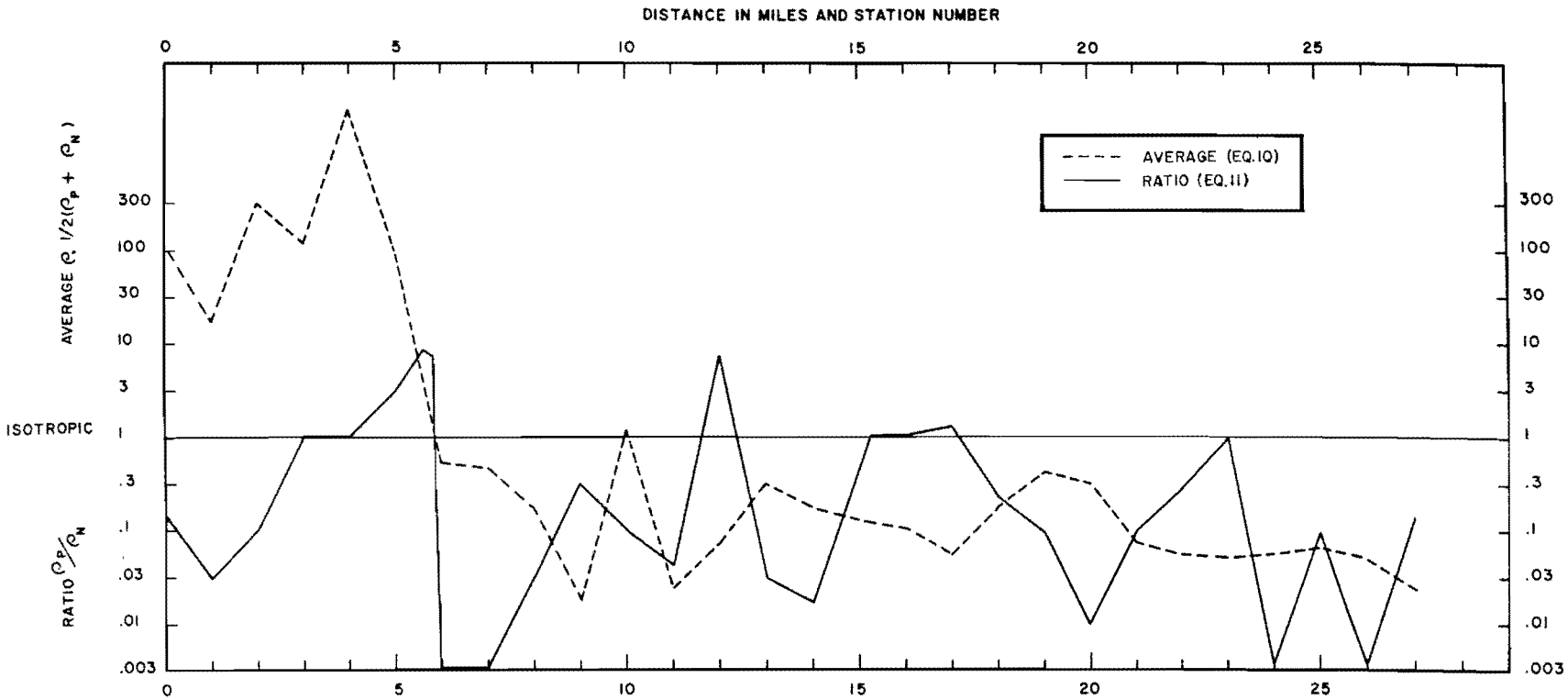

FIGURE 4.6. AVERAGE RESISTIVITY (DASHED LINE) AND RATIO OF HORIZONTAL ANISOTROPY (SOLID LINE) VERSUS STATION NUMBER (THE STATION NUMBER IS THE APPROXIMATE DISTANCE ALONG THE PROFILE, AS MEASURED IN MILES).

A comparison of the resistivity spectra to Figure 144 of Keller and Frischknecht (1966) indicates a greater depth to a conductive layer in Province I than in the other provinces. This conclusion is based on the shift of the lowermost resistivity gradient in Province I toward lower frequencies, as compared to the others (the lowermost -1.0 contour is closer to the bottom of the figure in Province I).

An indication of the maximum depth sensed can be obtained from Figure 4.5. The vertical structure sensed at station 5.6 was not indicated even at the lowest frequency (20 cps) at station 5.

FIELD DIFFICULTIES, DEVELOPMENTS, AND RECOMMENDATIONS

Four types of equipment problems were experienced: resistor inadequacies, connector failures, coil vibrations, and electrode failures.

The dynamic range of the potentiometers was frequently exceeded. Also, failure of one of the resistors showed the desirability of taking spare units.

The necessity of constant reconnection of the leads from the electrodes and coil wore out the connectors. A double-pole double-throw switch should be installed.

Wind-induced vibration of the air-cored coil considerably slowed the measurements. A solid-core coil will solve this problem.

The electrodes were made of brass 1" x 1/4" channel section and the coaxial leads were clamped on. The electrode frayed and bent almost immediately from hammering and care had to be exercised to insure good contact from the clamps. The electrodes should be made of solid (1" or larger diameter) brass rods with the leads soldered in place.

Two informative field tests were made (1) on the effect of power lines and (2) on the use of shielded cable between the electrodes. Station distances varying from immediately under the power lines near the road to several hundred yards away showed no noticeable effect on the spectra of the readings. Greater sensitivity was obtained in readings using the shielded mode but no noticeable change was seen in the range of readable values.

SUMMARY AND CONCLUSIONS

A major NNW-SSE trending vertical structure crossing the Waimea to Kailua-Kona highway at station 6 is indicated by the apparent resistivity change and the directional anisotropy of the resistivity as measured by the AMT method. A significant change of the electrical character of the deep (some hundreds of meters to a few kilometers) rocks was found on the two sides of the structure. To the north of the structure, near Kamuela, the data indicate higher resistivity than to the south, from the Saddle Road intersection to Huehue Ranch. This contrast could be due to one or both of two causes: (1) different rock material from two different volcanic groups (Mauna Kea and Mauna Loa); (2) depression of the fresh-sea-water interface to the north and lack of such depression to the south of the structure.

ACKNOWLEDGEMENTS

This study was funded jointly by the Department of Land and Natural Resources, Division of Water and Land Development and the Office of Water Resources Research. The guidance and suggestions of Dr. G. V. Keller were invaluable in the initial stages of this work.

BIBLIOGRAPHY

Cagniard, L. 1953. "Basic Theory of the Magnetotelluric Method of Geophysical Prospecting." *Geophysics*. Vol. 18, No. 3, pp. 605-635.

Keller, G. V. and F. C. Frischknecht. 1966. *Electrical Methods in Geophysical Prospecting*. Pergamon Press, pp. 197-250.

Keller, G. V. 1969. *Electro-Magnetic Surveys in the Central Volcanic Region; Preliminary Report*. Report No. 55. Geophysics Division, Dept. Sci. and Ind. Res., New Zealand.

Neves, Antonio de Sousa. 1957. *The Generalized Magnetotelluric Method*. Massachusetts Institute of Technology, Ph.D. thesis.

Swift, C. M., Jr. 1968. "The Magnetotelluric Method; Low Frequency Field Example, Arizona and New Mexico." *IN Applications of Natural Electro-Magnetic Field in Petroleum and Mining Exploration*. University of California, Berkeley.

Yungel, S. H. 1968. "Magnetotelluric Sounding Three-Layer Interpretation Curves. *Geophysics*. Vol. 26, No. 4, pp. 465-473.

D. C. RESISTIVITY

RICHIE D. HUBER AND WILLIAM M. ADAMS

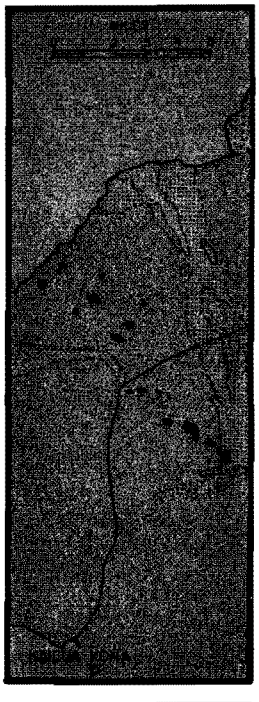

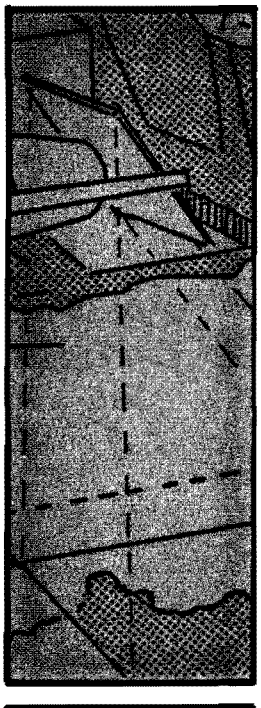

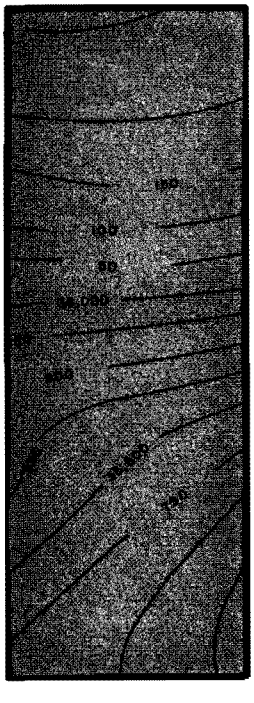

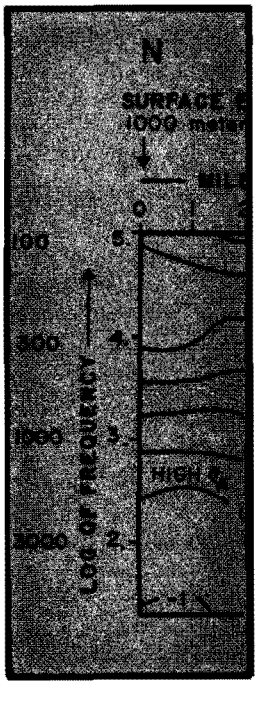

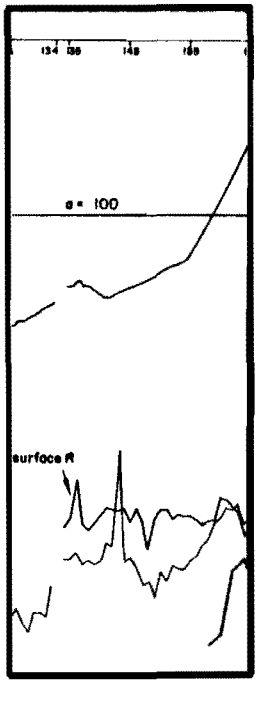

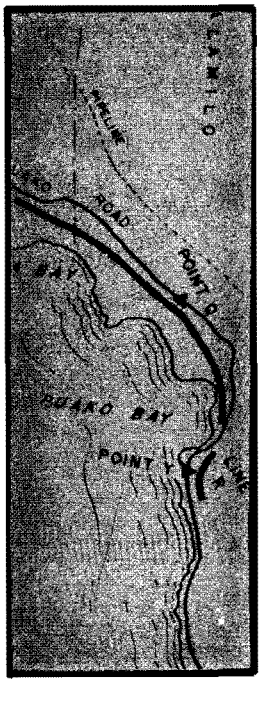

INTRODUCTION

A reconnaissance effort using the D.C. resistivity profiling technique and designed to locate locally optimum sites for further ground-water development was conducted along the coast between Kawaihae and Kailua-Kona. (See Figure 5.1). The work was done during the months of December 1968 and January, February, and June 1969. The efforts, confined to elevations no higher than 300 feet, used Wenner electrode configuration.

Two essentially continuous resistivity profiles have been established: a north section between Kawaihae and Anaehoomalu Bay and a south section between Keahole Point and Kailua-Kona. The dry surface terrain makes it impossible to establish an actual field link in the central section between the two profile segments.

THEORY

The Wenner electrode configuration consists of four equally-spaced electrodes which are arranged in a straight line. The value of the parameter a, the spacing between adjacent electrodes, will vary with each application. In this case, the a-spacing was set to equal the average elevation along the profile. Previous investigations using sounding and profiling techniques, reported by Adams (1968), indicated that the salt-fresh interface in the Kohala District generally occurred at sea level.

The depth of penetration of the current in the homogenous isotropic earth is approximately equal to the distance from the current source to the potential stake of the "a" spacing. In

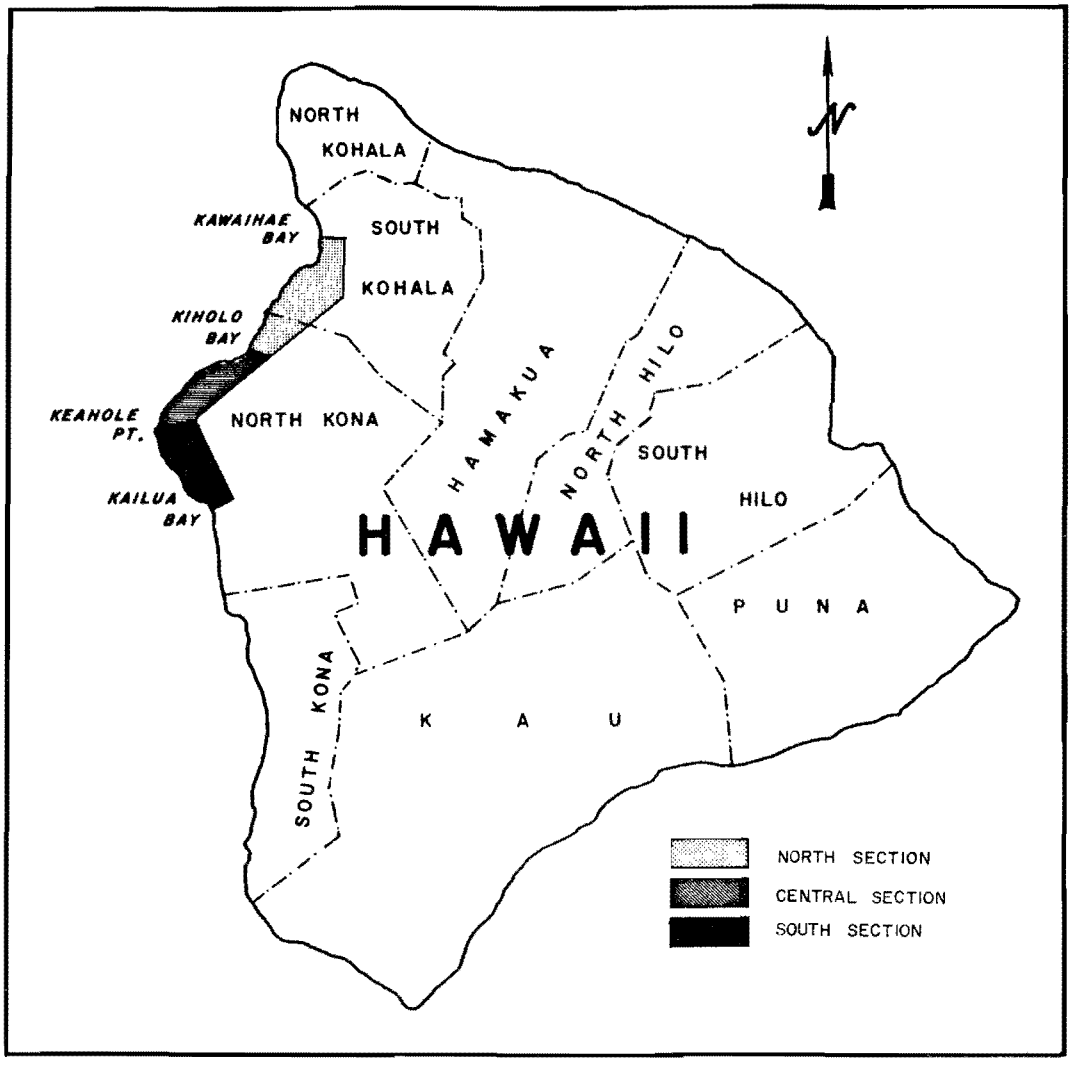

FIGURE 5.1. LOCATION MAP OF PROFILES ON ISLAND OF HAWAII.

reality, the earth is neither homogenous nor isotropic, but the depth of penetration to a first approximation may be assumed to be this distance. As a result, the resistivity profile with an a-spacing equal to the elevation will sense the electrical conductivity of the salt-fresh-water interface near sea level. In a porous and permeable rock, such as a series of normal Hawaiian lava flows, the apparent resistivity would be low because of the conductivity of the sea-water saturation of the rock to sea level. A fresh-water layer displacing the sea water downward results in a higher apparent resistivity. In general, a greater thickness of fresh water than normal would result in a positive anomaly in the resistivity. Therefore an area suitable for potential fresh-water development should be characterized by a positive resistivity anomaly. A depressed fresh-salt interface is not the only cause of a high resistivity anomaly. A similar anomaly may be caused by the resistivity contrast between dry rock and wet rock. Therefore, an anomalous profile does not positively indicate fresh water but only the more probable sites of fresh-water zones.

APPARATUS

Due to the dryness of this region, resistivities of 10,000 to 100,000 ohm-feet were expected (see Figure 1.3, p. 9). Consequently the field instruments were designed to provide high voltages (2000V) with a moderate amount of current (0.5 amps.). A schematic diagram of the power equipment is shown in Figure 5.2. The system is a development of those previously reported by Adams

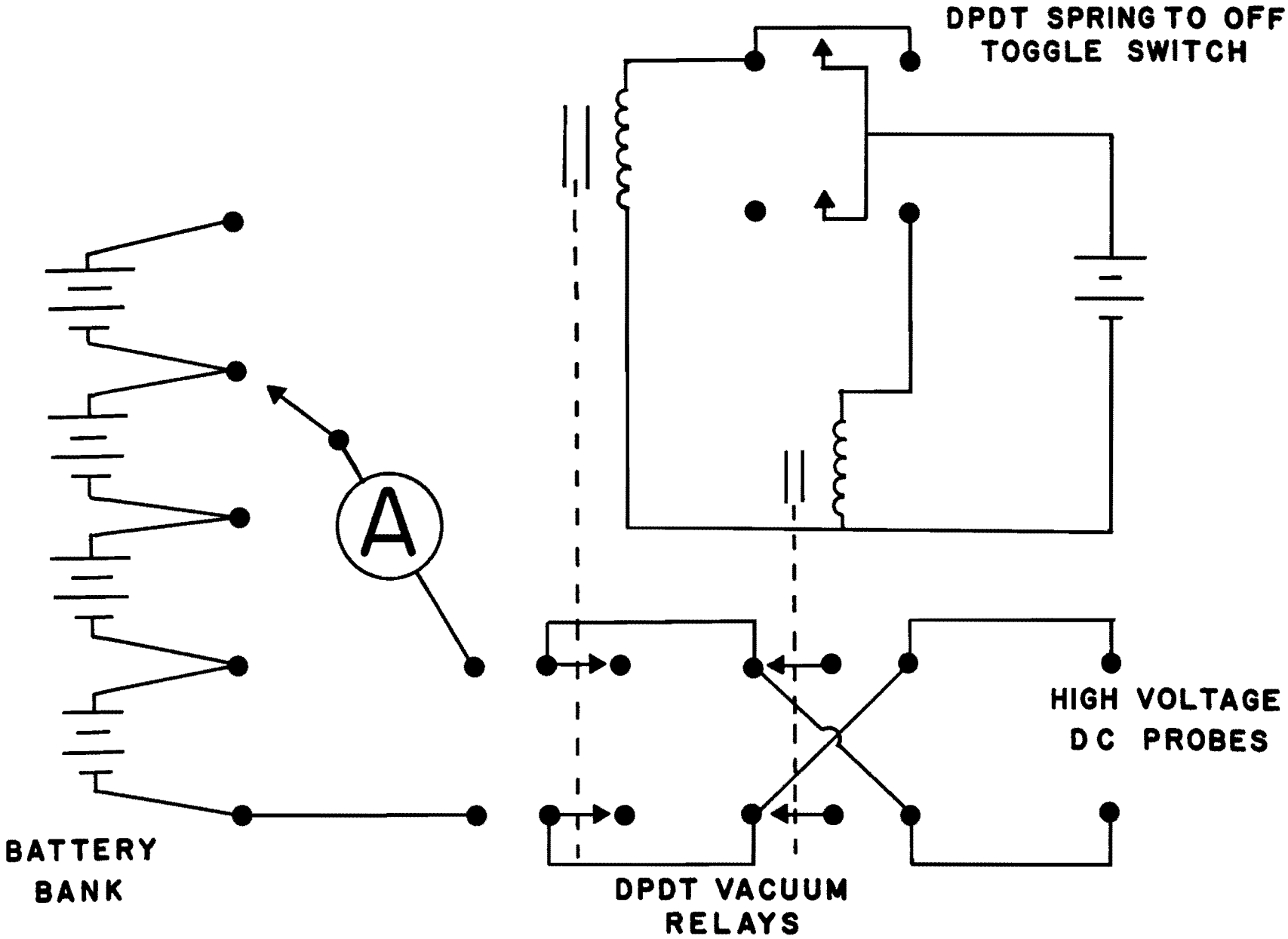

FIGURE 5.2. SCHEMATIC DIAGRAM OF RESISTIVITY GEAR (POWER SUPPLY).

(1968) and Cox, Peterson, Adams, Lao, Campbell, and Huber (1969). Two DPDT vacuum relays are used, one of which is an added safety feature. The battery banks are completely isolated from the working system when the added switch is in the "off" position. The current is monitered with a Weston Model 911 mirror-scaled milliampmeter with 10-, 30-, 100-, 300-milliamp and 1- and 3-amp ranges.

The potential drop is measured with a Heathkit millivoltmeter paper recorder when working from an automobile or a portable millivolt meter when the equipment is hand carried. Figure 5.3 shows a schematic diagram of the portable millivolt meter which was constructed at the University.

One-half inch diameter iron stakes were normally used as electrodes. However, when working on rock, wet sponges were substituted. A standard 18 AWG two-conductor (twisted pair) plastic jacketed cable was used to connect the electrodes to the power supply and millivoltmeter.

LOCATION AND DESCRIPTION OF THE SURVEY AREA

The coast between Kawaihae and Kailua-Kona is divided into three profile sections (see Figure 5.1 for the location of these areas):

North Section: Spencer Beach Park to Kiholo Bay in the north.

Central Section: Kiholo Bay to Keahole Point, which is between the other sections.

South Section: Keahole Point to Kailua-Kona to the south.

NORTH SECTION. Located between Spencer Beach Park and Kiholo Bay,

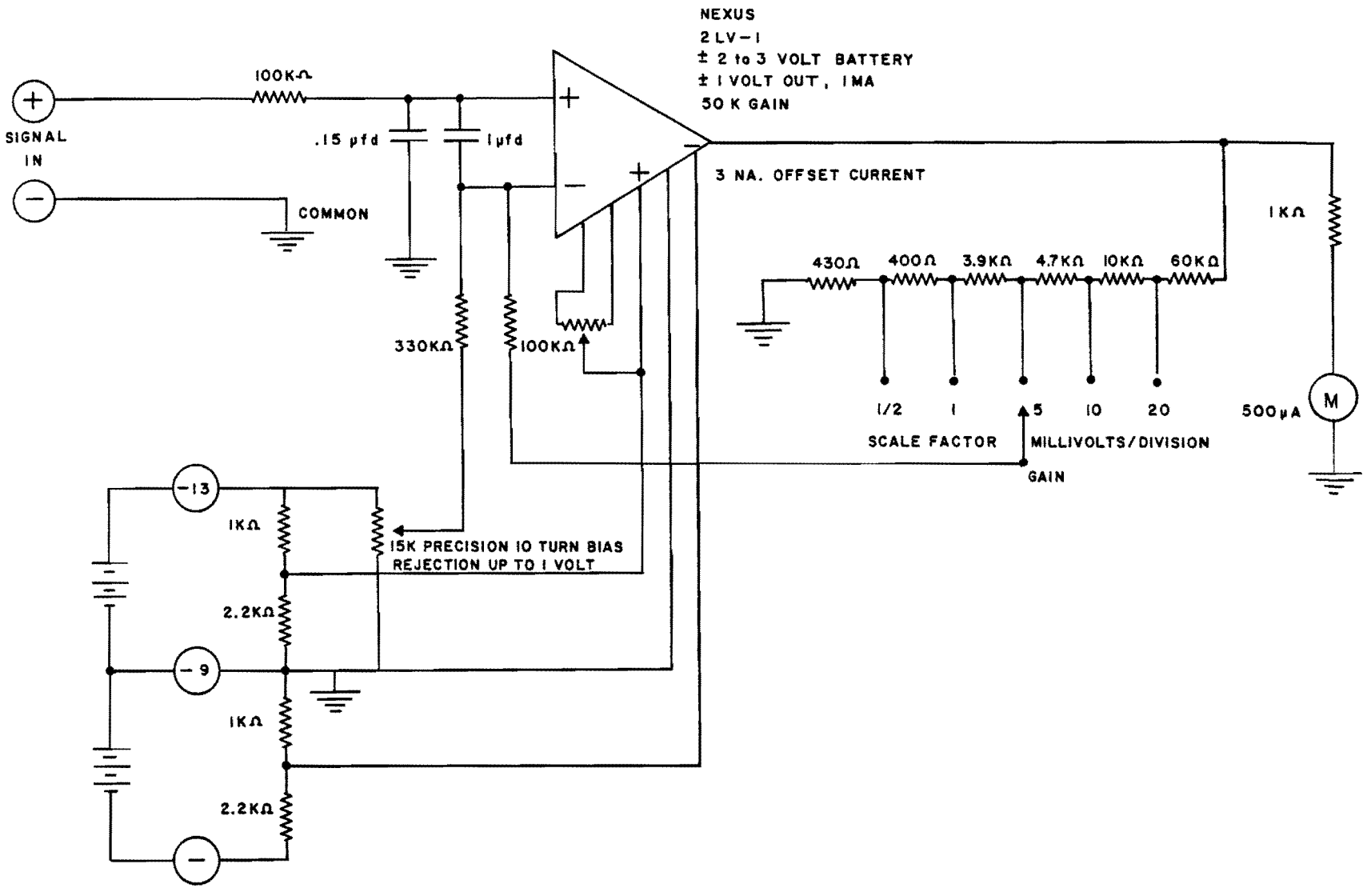

FIGURE 5.3. SCHEMATIC DIAGRAM OF MILLIVOLT METER (FROM HUSSONG AND COX, 1967).

the North Section lies on lava flows from Mauna Kea, Mauna Loa, and Hualalai (Figure 5.4). The resistivity profiling for this section was done in four segments. The first segment of the profile began at Spencer Beach Park and proceeded south along a back road to a bridge north of Mauna Kea Beach Hotel. The point of origin of the profile is at sea level. The elevation gradually rose to approximately 100-foot elevation at the bridge. The second segment began south of Mauna Kea Beach Hotel, on a back road, and continued south past Hapuna Beach Park following Puako Drive to its termination. The undulation of the terrain on which the northern half of this segment of the profile was laid ranges between 20 to 100 feet. The southern half of this segment is on terrain that is essentially level at about five feet above sea level.

The third segment begins a mile south of the second line and follows a jeep trail across pahoehoe and aa lava flows to Anaehoomalu Bay. The data from this profile have already been reported by Cox, *et al.* (1969).

The fourth segment begins at Anaehoomalu Bay and follows a foot trail south to Kiholo Bay (not shown in Fig. 5.4) along uneven terrain between 20 to 80 feet above sea level.

The climate in this area on the island of Hawaii is extremely dry with an average rainfall of only ten inches. (See Figure 1.3, p. 9.)

CENTRAL SECTION. This section extends from Kiholo Bay to Keahole Point on the lee slopes of Mt. Hualalai. This was the most remote and inaccessible area in which profiling was done. Only a few jeep trails over rugged terrain provide entry into this region.

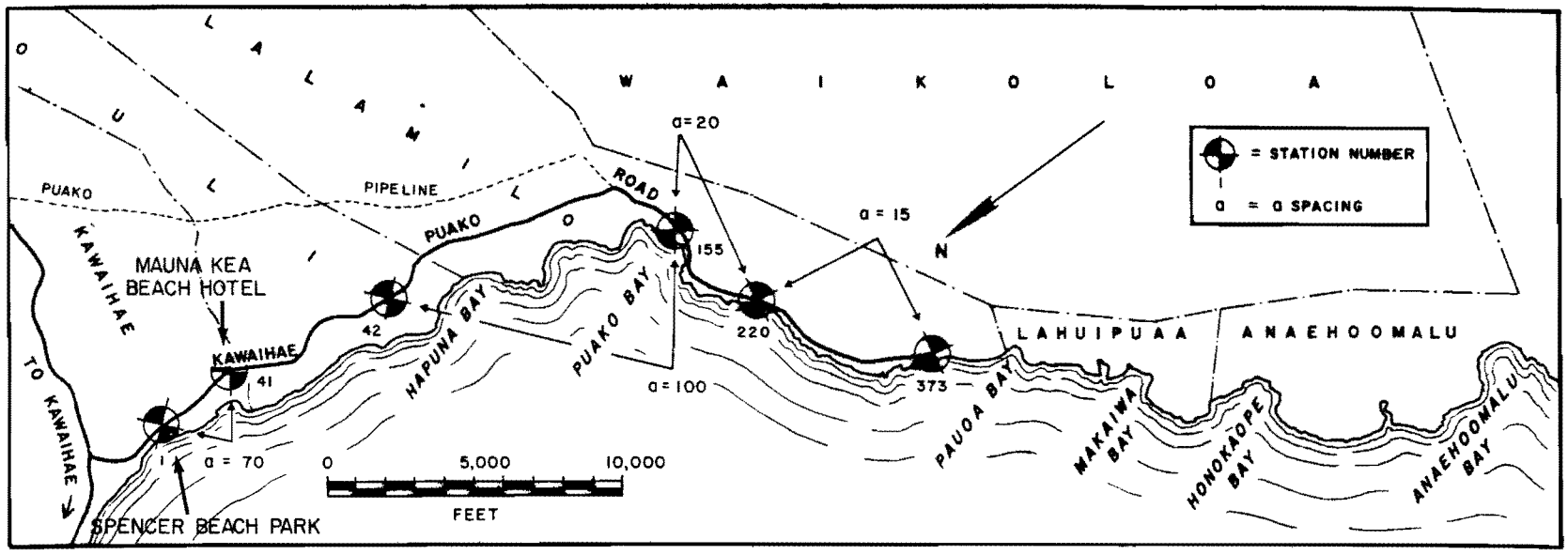

FIGURE 5.4. PROFILE LOCATION FOR NORTH SECTION.

A short profile was run on an improved jeep trail, but sharply changing topography along the line of the profile made interpretation difficult.

The climate is normally dry and warm with a mean annual rainfall of 40 inches. During the period of the survey, moderate precipitation occurred at night, but the clear, warm days dried the ground quickly.

SOUTH SECTION. This section is located on the southeast slope of Mount Hualalai (Figure 5.5). The climate of this area is similar to that described for the Central Section.

The survey line in this section begins about a mile above Kailua-Kona on the Kailua-Kona to Kawaihae Road and extends 32,000 feet along this road to its present northernmost extension, at Keahole Point. About 12,000 feet of the survey was conducted alongside the paved section of this highway and the other 20,000 feet along a section that is presently under construction.

FIELD METHOD

Sets of cables used in the Wenner configuration were constructed with breakouts at pre-measured distances for specific a-spacings. In the field, the cables were laid out and the electrodes located at the breakouts.

Generally, the equipment was transported by a four-wheel drive jeep, but when working on a narrow ancient Hawaiian trail, the field crews carried it. To improve the ground contact, the area around the base of the iron stakes, which were used as electrodes, was

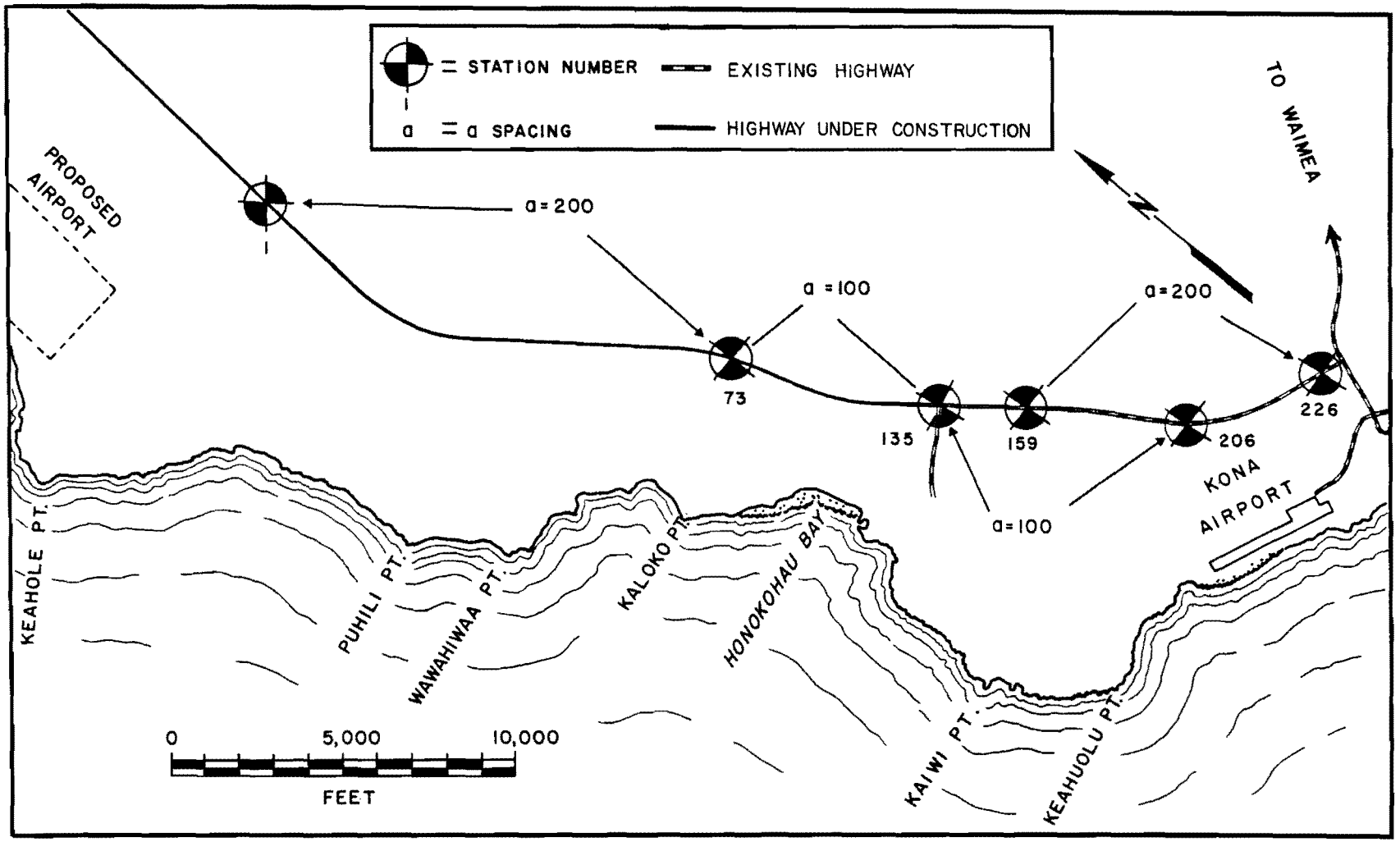

FIGURE 5.5. PROFILE LOCATION FOR SOUTH SECTION.

saturated with fresh water. When the electrodes were connected, the cable was plugged into the power supply located at the center of the spread. The potential was read using the portable millivolt meter designed and built at the University of Hawaii. The current was monitored with a milliampmeter.

Normally the spread was advanced by one a-spacing. But when the a-spacing was less than 50 feet, the spread was advanced by three a-spacings. The potential and current readings obtained were logged in fields books. Occasionally as a check, the apparent resistivity was calculated in the field. Normally, the data from a day's work were reduced each night.

DATA ANALYSIS

The resistivity profile stations for the North and South Sections are presented in Figures 5.6 and 5.7, respectively; for the Central Section, in Figure 5.8. The data for these profiles are presented in Tables 5.1, 5.2, and 5.3, respectively. Where possible, the elevations along the profile have been determined and the profile presented has been correct for elevation effects by using the method described by Adams (1968). The apparent resistivity was corrected to the resistivity of the surface layer. No elevation information exists for the profile for the Central Section.

Cross-correlation coefficients of the apparent resistivity on elevation, both before and after the elevation correction and for the different correction models, have been calculated and are listed in Table 5.4 by a-spacing.

TABLE 5.1. APPARENT RESISTIVITY AND ELEVATION DATA FOR THE PROFILE FOR THE NORTH SECTION, BETWEEN SPENCER BEACH PARK AND PUAKO BEACH DRIVE.

STATION	ρ OHM FEET	ALTITUDE FEET
1	71.3	16
2	49.7	17.5
3	99	19.6
4	64.7	22.0
5	31.7	23.0
6	83.6	23.0
7	40.4	21.0
8	55	20.5
9	51.3	21.5
10	43.4	23.0
11	56.7	25.0
12	50.2	28.0
13	42.7	28.0
14	44	26.0
15	23.6	21.0
16	23	17.5
17	20.8	16.0
18	13.3	16.5
19	42.2	19.0
20	44	21.0
21	8.4	26.0
22	84	32.0
23	109	38.0
24	114	43.5
25	143.4	50.0
26	94.7	55.0
27	132	61.0
28	115	67.0
29	106	70.5
30	108	70.5
31	77.6	69
32	163	67
33	88	67.5
34	199	70
35	139	75
36	111	81
37	181	87
38	110	93
39	162.5	99
40	136	105
41	139	110
42	1410.0	78.0
43	2100.0	83.0
44	1830.0	87.0
45	1290.0	91.0
46	1570.0	94.5
47	1140.0	98.0
48	1340.0	100.5
49	820.0	99.0
50	1700.0	95.5
51	1930.0	96.0
52	2325.0	100.0
53	1850.0	103.9
54	2450.0	107.5
55	2055.0	111.2
56	1683.0	113.2
57	2365.0	111.5
58	1906.0	105.5
59	2090.0	99.5
60	2030.0	97.2
61	2180.0	96.6
62	1930.0	92.8
63	1790.0	79.8
64	1278.0	68.5
65	1230.0	91.2
66	1055.0	76.5
67	895.0	82.0
68	820.0	87.0
69	1490.0	93.2
70	830.0	97.0
71	1370.0	94.5
72	1208.0	85.0
73	669.0	76.0
74	898.0	67.0
75	2280.0	63.0
76	1130.0	65.0
77	2280.0	67.0
78	1430.0	71.0
79	817.0	80.0
80	1083.0	90.5
81	1257.0	98.2
82	578.0	102.0
83	1309.0	103.0
84	425.0	105.0
85	1513.0	107.0
86	892.0	109.0
87	1000.0	110.0
88	1476.0	108.0
89	1005.0	104.0
90	1254.0	102.1
91	1428.0	104.0
92	807.0	104.0
93	1040.0	98.0
94	1581.0	93.3
95	1257.0	92.0
96	2595.0	91.5
97	1880.0	91.2
98	1940.0	91.0
99	1752.0	91.0
100	1136.0	90.6
101	1185.0	90.0
102	785.0	89.0
103	1137.0	84.5
104	897.0	74.5
105	1300.0	64.4
106	974.0	54.2
107	1220.0	46.5
108	800.0	43.2
109	770.0	42.8
110	762.0	39.4
111	578.0	33.0
112	1105.0	30.0
113	588.0	30.5
114	950.0	31.0
115	675.0	31.2
116	876.0	35.6
117	462.0	43.5
118	1085.0	49.8
119	810.0	54.0
120	900.0	58.7
121	1178.0	61.0
122	942.0	58.0
123	1075.0	55.0
124	760.0	58.0
125	890.0	63.0
126	732.0	77.6
127	642.0	70.6
128	1375.0	72.0
129	733.0	73.4
130	1320.0	74.8
131	923.0	76.0
132	897.0	77.6
133	962.0	78.9
134	1189.0	79.0
135	807.0	79.0
136	1254.0	79.01
137	965.0	78.04
138	667.0	74.08
139	557.0	66.59
140	58.4	57.29
141	162.0	48.8
142	14.8	45.9
143	157.0	43.6
144		41.5
145	151.8	39.5
146	75.80	39.5
147	178.0	33.0
148	150.0	27.5
149	123.0	25.5
150	140.5	28.0
151	181.0	28.0
152	132.5	23.0
153	133.0	17.0
154	102.0	13.0
155	36.5	11.2
156	7.1	10.0
157	4.60	9.2
158	.00	8.9
159	.76	8.0
160	.44	7.9
161	.17	7.9
162	.41	8.1
163	.60	8.6
164	.56	9.0
165	.62	9.0
166	.75	8.9
167	1.44	8.9
168	1.28	8.8
169	.78	8.8
170	.88	8.7
171	1.81	8.7
172	.68	8.6
173	21.8	8.5
174	29.8	8.5
175	2	8.4
176	13.0	8.3
177	13.4	8.3
178	13.6	8.2
179	19.2	8.0
180	16.4	7.9
181	17.5	7.8
182	16.2	7.7
183	33.4	7.6
184	28.8	7.5
185	18.4	7.3
186	37.2	7.2
187	39.7	7.0
188	17.8	7.0
189	.6	7.0
190	18.2	7.0
191	.6	6.9
192	11.4	6.8
193	1.6	6.7
194	6.6	6.6
195	23	6.6
196	8.6	6.5
197	0	6.4
198	30	6.3
199	0	6.1
200	11.6	6.0
201	13.2	6.0
202	0	5.9
203	3.4	6.0
204	8	6.0
205	2	6.0
206	0	6.0
207	3.8	6.1
208	8	6.2
209	5.2	6.3
210	14	6.4
211	20	6.5
212	8	6.7
213	8	6.8
214	6	6.9
215	6	7.0
216	14	7.0
217	12	7.0
218	8	7.0
219	6	7.0
220	49.5	7.0
221	30.0	7.0
222	39.0	7.0
223	139.3	7.0
224	183.0	7.0
225	148.5	7.0
226	25.5	7.0
227	30.0	7.0
228	30.0	7.0
229	82.5	7.0
230	10.5	7.0
231	10.5	7.0
232	18.0	7.0
233	25.5	7.2
234	67.5	7.4
235	55.5	7.5
236	99.0	7.7
237	48.0	7.9
238	105.0	8.0
239	127.5	7.9
240	177.0	7.8
241	124.5	7.7
242	213.0	7.6
243	110.0	7.6
244	121.5	7.6
245	39.0	7.6
246	46.5	7.5
247	43.5	7.4
248	52.5	7.3
249	76.5	7.3
250	33.0	7.2
251	123.0	7.2
252	187.6	7.1
253	109.5	7.1
254	111.0	7.0
255	111.0	7.0
256	57.0	7.0
257	54.0	6.9
258	54.0	6.9
259	156.0	6.8
260	52.5	6.8
261	67.5	6.7
262	25.5	6.6
263	48.0	6.6
264	48.0	6.5
265	120.0	6.5
266	249.0	6.4
267	12.0	6.3

TABLE 5.1. (CONT.) APPARENT RESISTIVITY AND ELEVATION DATA FOR THE PROFILE FOR THE NORTH SECTION, BETWEEN SPENCER BEACH PARK AND PUAKO BEACH DRIVE.

STATION	ρ OHM FEET	ALTITUDE FEET	STATION	ρ OHM FEET	ALTITUDE FEET	STATION	ρ OHM FEET	ALTITUDE FEET
268	151.5	6.3	304	13.5	5.0	339	10.5	7.0
269	7.5	6.2	305	19.5	5.0	340	13.5	7.0
270	25.5	6.2	306	15.0	5.0	341	21.0	7.0
271	12.0	6.2	307	16.5	5.0	342	49.0	7.1
272	19.5	6.1	308	36.0	5.0	343	36.0	7.2
273	24.0	6.1	309	13.5	5.0	344	135.0	7.3
274	103.5	6.5	310	63.0	5.0	345	151.5	7.5
275	0.0	6.0	311	0.0	5.0	346	172.5	7.5
276	33.0	6.0	312	0.0	5.0	347	15.0	7.6
277	7.5	6.0	313	3.0	5.5	348	9.0	7.8
278	9.0	5.9	314	18.0	5.5	349	21.0	7.8
279	0.0	5.7	315	39.0	5.5	350	37.5	7.8
280	4.5	5.5	316	51.0	5.5	351	84.0	7.8
281	13.5	5.2	317	25.0	5.5	352	148.5	7.8
282	24.0	5.0	318	30.0	5.5	353	48.0	7.8
283	51.0	5.0	319	15.0	5.5	354	85.5	7.8
284	15.0	5.0	320	21.0	5.5	355	57.0	7.9
285	30.0	5.0	321	7.5	5.5	356	196.5	7.9
286	37.5	5.0	322	24.0	5.6	357	6.0	7.9
287	0.0	5.0	323	49.5	5.7	358	97.5	8.0
288	45.0	5.0	324	36.0	5.8	359	87.0	8.0
289	18.2	5.0	325	31.5	5.9	360	37.5	8.1
290	36.0	5.0	326	7.5	6.0	361	25.5	8.2
291	39.0	5.0	327	7.5	6.0	362	67.5	8.3
292	12.0	5.0	328	6.0	6.2	363	28.5	8.3
293	6.0	5.0	329	6.0	6.3	364	45.0	8.5
294	12.0	5.0	330	19.5	6.5	365	102.0	8.5
295	27.0	5.0	331	22.5	6.5	366	74.5	8.5
296	28.5	5.0	332	10.5	6.5	367	251.0	8.5
297	37.5	5.0	333	27.0	6.7	368	263.0	9.0
298	42.0	5.0	334	73.5	6.8	369	60.0	9.0
299	27.0	5.0	335	57.0	6.9	370	0.0	9.0
300	10.5	5.0	336	0.0	6.9	371	58.5	9.2
301	16.5	5.0	337	1.5	7.0	372	108.0	9.2
302	12.0	5.0	338	4.5	7.0	373	109.5	9.2
303	1.5	5.0						

TABLE 5.2. APPARENT RESISTIVITY DATA FOR THE PROFILE FOR THE CENTRAL SECTION, ABOVE KONA VILLAGE.

STATION NUMBER	ρ_A OHM FEET	STATION NUMBER	ρ_A OHM FEET
1	12,250	22	8,850
2	13,800	23	7,780
3	12,500	24	6,760
4	10,600	25	3,950
5	11,600	26	2,980
6	12,600	27	2,140
7	9,600	28	5,850
8	10,950	29	4,500
9	11,600	30	1,107
10	12,400	31	1,470
11	13,300	32	1,180
12	14,700	33	2,080
13	14,000	34	1,210
14	15,350	35	713
15	17,800	36	675
16	13,950	37	664
17	13,600	38	436
18	12,800	39	525
19	11,800	40	538
20	11,300	41	451
21	10,200	42	363

TABLE 5.3. APPARENT RESISTIVITY AND ELEVATION DATA FOR THE PROFILE FOR THE SOUTH SECTION, BETWEEN KEAHOLE POINT AND KAILUA-KONA.

STATION	ρ_A OHM FEET	ALTITUDE FEET	STATION	ρ_A OHM FEET	ALTITUDE FEET	STATION	ρ_A OHM FEET	ALTITUDE FEET
1	10,500	140.5	62	6,100	95.0	122	4,370	39
2	9,200	140.5	63	5,500	95.0	123	5,500	39.5
3	9,860	140.5	64	6,430	94.0	124	4,930	40
4	9,820	140.0	65	5,750	94.0	125	4,940	40
5	8,150	139.0	66	5,550	93.0	126	4,900	41.5
6	9,400	138.0	67	4,630	92.0	127	3,960	41
7	8,600	137.0	68	6,420	91.0	128	4,500	42
8	9,350	135.5	69	5,450	90.0	129	3,840	42
9	10,300	134.0	70	50,404	89.5	130	3,400	43
10	8,400	132.0	71	6,150	89.0	131	4,350	43
11	10,090	130.0	72	4,340	88.0	132	4,360	44
12	10,380	127.5	73	3,200	87.5	133	4,100	44.5
13	10,530	125.5	73	11,730	87.5	134	5,920	45
14	11,130	124.0	74	12,300	97.0	159	7,640	148
15	9,210	122.0	75	11,400	86.5	161	7,450	144
16	9,160	121.0	76	10,830	86.0	163	7,200	136
17	8,300	120.0	77	10,800	86.0	165	6,050	128
18	8,530	119.0	78	9,850	86.0	167	4,750	119.5
19	8,400	118.0	79	7,440	85.5	169	4,730	111
20	8,180	117.0	80	8,350	85.0	171	3,710	103
21	8,500	116.0	81	10,500	84.5	173	2,760	94.5
22	8,540	115.0	82	8,840	84.0	175	2,980	86.5
23	8,340	114.0	83	10,600	84.0	177	1,920	80
24	8,820	113.0	84	9,500	83.5	179	2,630	75
25	8,450	112.0	85	9,650	83.0	181	2,260	71.5
26	8,150	110.5	86	9,050	82.5	183	1,840	68
27	8,230	109.0	87	9,760	82.0	185	2,140	64
28	7,650	107.0	88	7,590	81.0	187	1,680	60
29	7,700	105.5	89	7,900	80.5	189	2,000	56
30	128,000	104.0	90	7,370	79.5	191	2,640	52
31	7,700	101.0	91	9,080	78.5	193	2,220	51.5
32	6,680	101.0	92	9,400	77.5	195	4,550	53.5
33	17,200	99.0	93	12,020	76.5	197	3,530	56
34	7,050	96.5	94	12,500	75.5	199	4,250	58
35	7,230	94.0	95	11,500	74	201	3,900	61
36	7,530	91.0	96	6,110	73	203	4,150	64
37	5,300	89.0	97	12,000	71.5	205	4,680	67
38	4,750	86.0	98	20,250	70	207	5,120	70.5
39	4,440	83.5	99	11,310	68	208	6,790	74
40	4,520	81.0	100	10,100	67	209	6,830	77
41	4,500	78.0	101	1,100	65	210	8,000	80
42	2,810	75.5	102	9,200	63	211	8,660	83.5
43	3,750	73.0	103	11,550	61.5	212	9,450	86
44	2,430	71.0	104	9,800	59	213	7,740	87
45	2,980	70.0	105	10,150	57.5	214	8,930	85.5
46	3,330	69.5	106	10,490	55.5	215	8,700	83
47	2,910	69.5	107	7,110	54	216	7,900	81
48	3,080	70.0	108	8,760	51.5	217	7,219	83
49	1,418	71.5	109	4,810	49.5	218	6,400	85
50	3,240	74.0	110	5,830	47.5	219	6,000	86.5
51	5,700	76.0	111	7,200	45.5	220	6,420	86
52	4,520	78.5	112	6,610	44	221	4,840	83
53	5,800	81.0	113	9,980	52.5	222	5,520	79
54	6,000	83.0	114	6,420	41	223	8,100	75
55	5,800	86.0	115	9,200	40	224	7,100	71
56	6,700	88.0	116	5,020	39.5	225	3,275	66.5
57	6,400	90.0	117	7,190	39	226	2,870	62
58	5,750	91.5	118	5,720	38.5			
59	6,900	93.0	119	5,560	38			
60	4,700	94.0	120	4,610	38			
61	6,370	94.5	121	4,940	38.5			

STATION	$\rho_{SURFACE}$	ρ_A	ALTITUDE	STATION	$\rho_{SURFACE}$	ρ_A	ALTITUDE
135	------	14,300	56	171	8,930	13,000	83
136	15,100	15,100	57	172	11,020	22,200	81
137	15,150	21,300	58	173	9,950	13,850	79
138	15,010	5,916,600	59	174	11,305	14,300	77
139	15,270	15,500	61	175	12,720	13,800	75
140	15,280	17,400	62.5	176	10,410	12,100	72.5
141	15,050	14,300	64	177	13,410	15,100	71
142	15,140	17,500	65.5	178	14,890	14,100	68.5
143	19,300	16,100	67	179	16,020	14,700	66.5
144	19,600	15,700	69	180	16,460	13,100	64.5
145	12,740	17,000	70.5	181	12,480	12,250	62
146	13,650	14,910	72	182	12,740	10,005	60
147	13,230	14,850	74	183	12,000	9,300	58
148	17,370	17,750	75.5	184	12,950	8,360	56
149	14,510	13,720	77	185	13,200	7,800	54
150	11,310	17,200	79	186	13,250	7,150	52.5
151	13,530	8,016,500	80	187	13,850	7,190	52
152	11,400	15,090	82	188	12,800	7,470	51.5
153	13,180	18,720	83.5	189	15,250	6,210	51
154	12,920	16,670	85	190	14,400	6,900	50.5
155	11,350	16,920	86	191	13,000	5,160	50
156	11,600	17,620	87	192	8,900	6,140	49.5
157	10,700	15,890	87	193	13,250	5,930	49
158	12,370	18,650	86.5	194	14,400	7,420	48.5
159	11,050	17,000	85.5	195	12,330	8,270	48
160	6,030	18,650	84	196	14,800	7,880	47.5
161	13,550	19,150	83	197	14,300	28,720	47
162	17,150	21,050	81.5	198	14,700	9,400	46.5
163	20,250	22,900	81	199	14,950	9,860	46
164	17,850	19,720	82	200	13,500	7,910	46.5
165	14,680	21,500	83	201	12,100	7,580	47
166	17,400	20,250	84	202	11,100	7,960	48
167	10,300	13,450	86.5	203	12,100	7,650	48
168	9,840	13,200	86.5	204	20,500	8,670	49
169	8,430	14,150	86	205	13,100	8,060	48
170	11,750	20,400	84.5	206	11,700	8,070	48

TABLE 5.4. CROSS-CORRELATION COEFFICIENTS RELATING THE ELEVATION PROFILE WITH THE APPARENT RESISTIVITY PROFILE FOR DIFFERENT TWO-LAYER MODELS.

CASE	A-SPACING FEET	AREA	BEFORE CORRECTION	AFTER CORRECTION $\rho_2/\rho_1 = 0$	$\rho_2/\rho_1 = 1/39$	$\rho_2/\rho_1 = .54$	$\rho_2/\rho_1 = .18$
I	33	KAILUA, KONA	- .2032	--------	--------	--------	--------
II	100		.05324	- .3524	- .3627	.4790	- .2137
III	200		.4367	- .5865	- .6070	.1995	- .1510
IV	100		.6330	- .7616	- .7663	.3770	- .4971
V	200		.1591	- .1002	- .03482	- .1378	.05472
OVERALL			- .02306	- .1919	- .1392	.08548	.001557
VI		KAWAIHAE-PUAKO	.4719	- .1983	.07956	.4325	.3512
VII			- .1373	+ .08182	.06750	.01389	.02052
VIII			.6669	- .4087	- .3961	.5656	.06519
IX			.8172	- .2449	- .2449	- .2449	- .2449
OVERALL			.8734	- .04663	- .04663	- .04663	- .04663

The original correction used by Adams, based on a two-layer model with a ratio of resistivities, ρ_2/ρ_1, equal to zero, tended to overcorrect the data as indicated by the negative correlation coefficients. A series of new two-layer models with resistivity ratios ($\rho_2/\rho_1 \neq 0$) not equal to zero were calculated for modifying the correction procedure. The correlation coefficients for these modified cases are also listed in Table 5.4.

The best model for the correction procedure in this region, based on the cross-correlation coefficients, has a resistivity ratio equal to 0.18. The corrected profiles based on this model are shown in Figures 5.6 and 5.7.

The high variability of the data at short distances, especially in the Puako Area, indicates the need for a smoothing technique. A four-point smoothing method appropriate for the Wenner configuration is being developed. The data in this report has not been smoothed, however.

NORTH SECTION. This section was sub-divided and described as four segments in the section of this report entitled, "A Location and

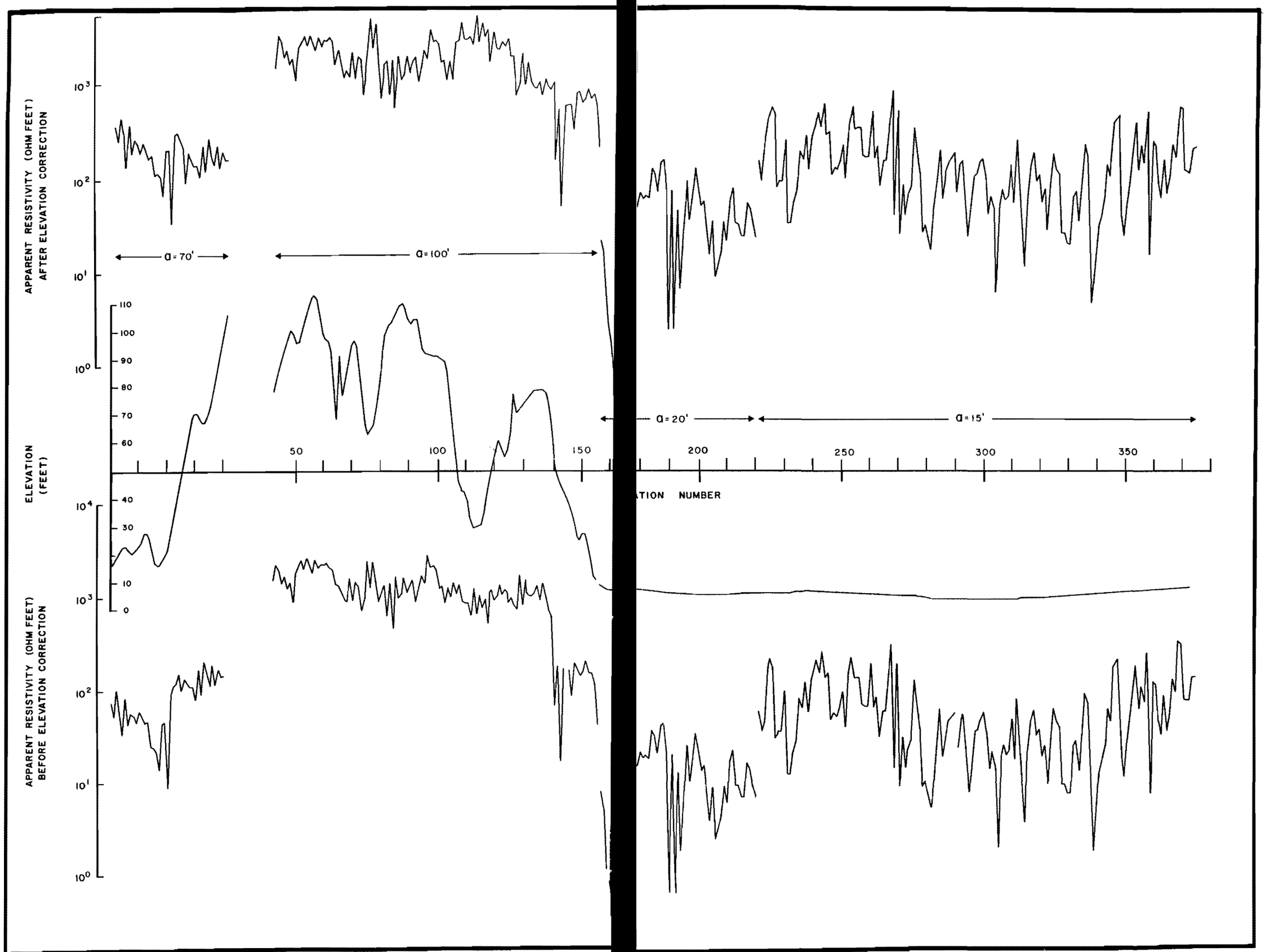

FIGURE 5.6. RESISTIVITY PROFILES, BOTH BEFORE AND AFTER TH EVATION CORRECTION, AND AN ELEVATION PROFILE FOR NORTH SECTION.

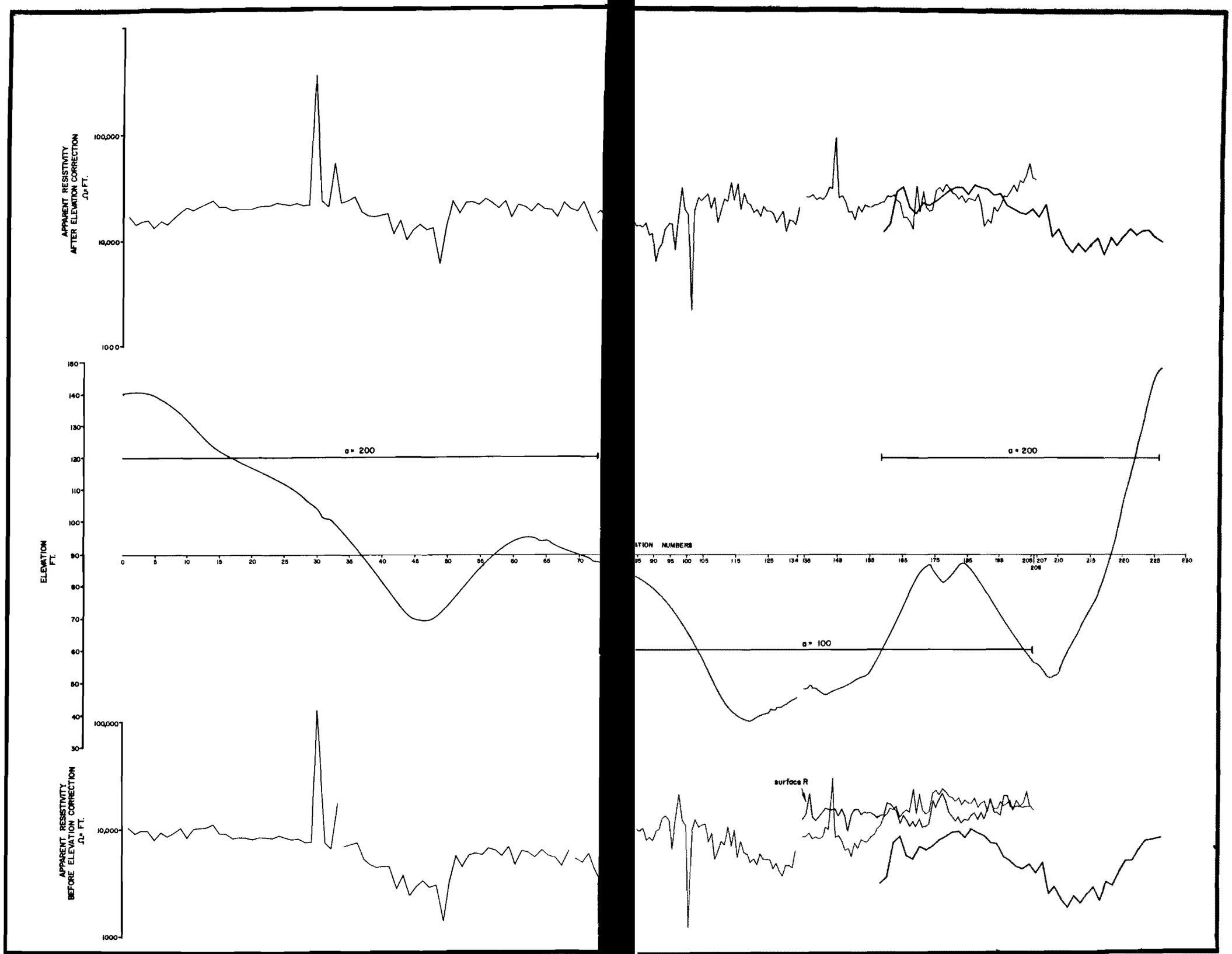

FIGURE 5.7. RESISTIVITY PROFILES, BOTH BEFORE AND AFTER THE ELEVATION CORRECTION, AND AN ELEVATION PROFILE FOR SOUTH SECTION.

Description of the Area". For the following discussion, segments one and two and segments three and four are combined and designated as Area A and Area B, respectively.

Area A. The a-spacings used in Area A are as follows: 1) a 70-foot spacing was used between Spencer Beach Park and the Mauna Kea Beach Hotel, 2) a 100-foot spacing was used from the Mauna Kea Beach Hotel to a point where Puako Drive drops to an elevation near sea level, and 3) 15- and 20-foot spacings were used along the rest of Puako Drive.(see Figure 5.4).

Two resistivity anomalies are shown on the profile plotted in Figure 5.6. The most apparent anomaly occurs at the north end of the profile between Stations 42 and 155. This anomaly corresponds to the area of highest elevation along the profile and may be due to the dryer ground condition at higher elevations. Superimposed upon this large scale high are three small features which occur between Stations 49 and 64, Stations 92 and 99, and Stations 104 and 125. Because the amplitude of these anomalies is comparable to the amplitude of the "background noise" they may not be significant. Of the three sites mentioned above, the site between Stations 104 and 125 is located in a trough. Further investigation in this area should begin near or at this site.

The third resistivity anomaly occurs between Stations 175 and 187. Very low values are observed for the area to the north of the anomalous zone and the profile also is very irregular for the area to the south. The anomaly, itself, is consistent and warrants further investigation. The rest of the profile is very irregular, probably due to the close proximity of the profile to sea level.

The very low frequency oscillation evident in the profile without the elevation correction between Stations 170 and 373 might be caused by tidal fluctuations. However, the change in the terrain in this area corresponds to the oscillations and is the probable cause of the oscillations.

Area B. Area B begins about a mile south of Puako Drive at the northern edge of an aa lava flow. A resistivity profile was conducted earlier across the flow to Anaehoomalu Bay by another team and is reported by Cox, *et al.*, (1969). A resistivity anomaly, supported by a corresponding gravity anomaly, was observed near the center of the flow. It was postulated that the anomaly was due to the massive center section of the aa flow. No other anomalies were observed along the profile.

An attempt was made to extend this profile from Anaehoomalu Bay to Kiholo Bay, but the attempt failed. The failure was attributed to the very dry and porous conditions of the volcanic terrain. A second attempt was made to reproduce the profile across the aa lava flow reported by Cox, *et al.*, (1969), but it too, was unsuccessful. The success of the earlier survey is now considered to be due to a thunderstorm that drenched the area just prior to the survey. D. C. Resistivity reconnaissance is ineffective as an exploration method when the surface layer functions as an insulator.

CENTRAL SECTION. Of the three sections, this is the most inaccessible. As a result, only one short profile, which was conducted along the access road to the Kona Village Hotel on Huehue Ranch land, exists. A 200-foot a-spacing was used for the profile. Since no elevation data exists for the profile, no correction was made.

As is apparent in Figure 5.8, the quality of the data is quite

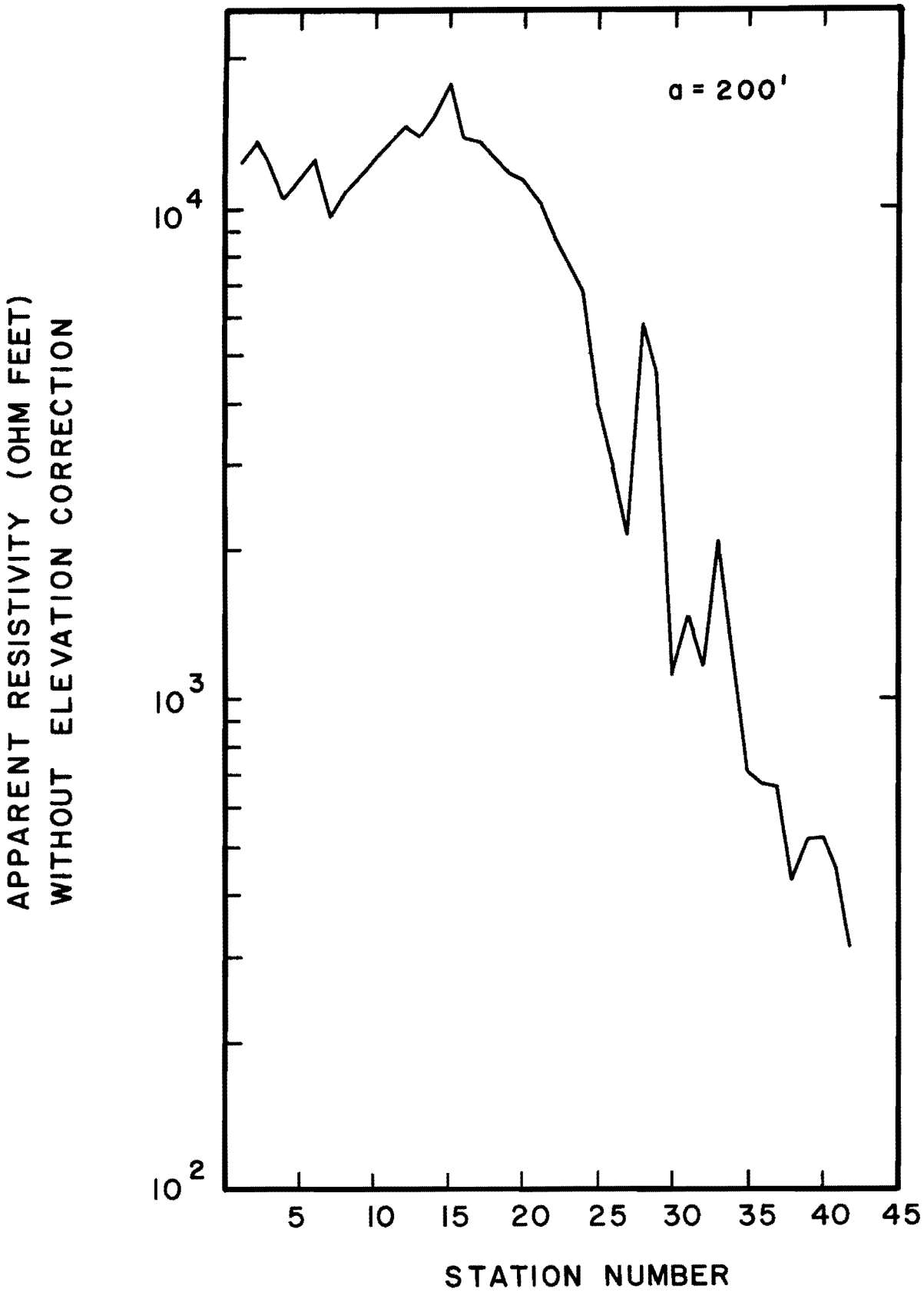

FIGURE 5.8. RESISTIVITY PROFILE FOR CENTRAL SECTION.

poor. The resistivity profile closely follows the changes in topography along the profile. The peak observed at Station 28, which is near the side of the road running beside this station, is attributed to a large hole possibly a lava blister that has caved-in. From this single profile, it is impossible to draw any significant conclusions about ground water in the area.

SOUTH SECTION. Along this section, a-spacings of 100 feet and 200 feet were used. The a-spacing was changed when the elevation seemed greater than the a-spacings or when the apparent resistivity was becoming too large. An a-spacing of 33 feet was used along part of the profile as a means of determining the surface resistivity.

Upon close inspection of the profile, two anomalies are observed. The first is a distinctive peak at Station 30. The sequence of apparent resistivity values of Stations 30, 31, 32, and 33 and the geologic information and elevation profile obtained from the State Department of Transportation indicated the presence of lava tubes in the area. The high-low-low-high sequence of the apparent resistivity values corresponds to the successive positioning of the four electrodes in the vicinity of the void. The highs correspond to the position of current electrodes near the void and the lows to the potential electrodes near the void. In fact, the low anomaly near Station 30 may be due to filled lava tubes. In any case, the peak at Station 30 is due to a small scale feature.

The other anomaly occurs at Station 165. It is most apparent on the 200-foot spread. Its broad feature appears to be that it is superimposed upon an elevation effect. The cause of the anomaly is difficult to determine. Attention is drawn to the anomaly by the fact that the amplitude of the anomaly has decreased considerably on the 100-foot profile and the surface resistivity profile.

CONCLUSIONS

Five electrical resistivity anomalies, three in the North Section and two in the South Section, have been observed. Of the four anomalies, one may positively be excluded as a potential for ground-water development. The remaining sites are local optima for additional exploration for ground water.

ACKNOWLEDGEMENTS

The work presented in this report was supported by the Department of Land and Natural Resources, Division of Water and Land Development of the State of Hawaii and Office of Water Resources Research of the U. S. Department of the Interior.

Access to the areas of interest was arranged by Mr. Payne, Sr. of Glover, Ltd., Mr. R. E. Eastman of Parker Ranch, and Mr. N. Dubbs of Boise Cascade.

The elevation data was provided by the Department of Transportation offices in Honolulu and Hilo.

The resistivity work was done with the assistance of P. Milner, H. Ishida, D. Loomis, R. Araki, R. Nishioka, J. Cochran, A. Omori, W. Kimura and D. Kimura.

For your *kokua*, gentlemen, thank you.

BIBLIOGRAPHY

Adams, William M. 1968. *An electrical resistivity profile from Mahukona to Kawaihae, Hawaii*. Technical Report 23. Water Resources Research Center, University of Hawaii. p. 32.

Cox, Doak C., Frank L. Peterson, William M. Adams, Chester Lao, John F. Campbell and Richie D. Huber. 1969. *Coastal evidences of ground water conditions in the vicinity of Anaehoomalu and Lalamilo, South Kohala, Hawaii*. Technical Report 24. Water Resources Research Center, University of Hawaii. p. 53.

Hussong, Donald M. and Doak C. Cox. 1967. *Estimation of ground water configuration near Pahala, Hawaii using electrical resistivity techniques*. Technical Report 17. Water Resources Research Center, University of Hawaii. p. 35.

CONCLUSIONS

WILLIAM M. ADAMS

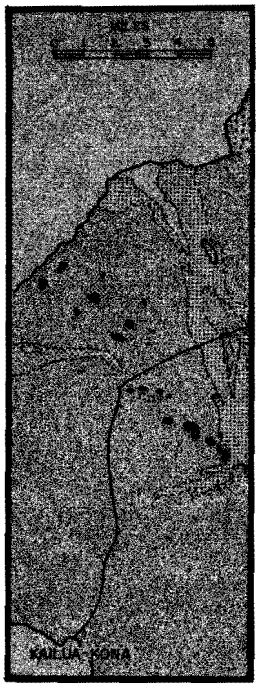

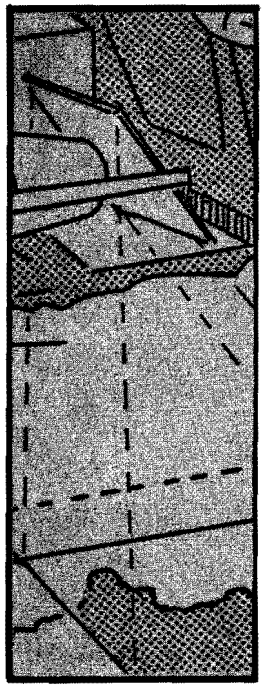

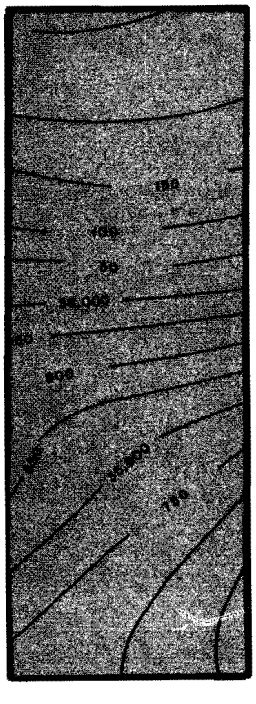

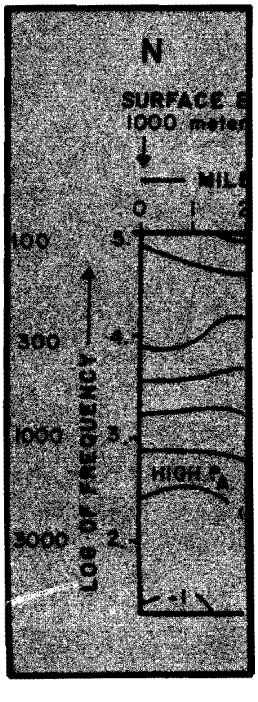

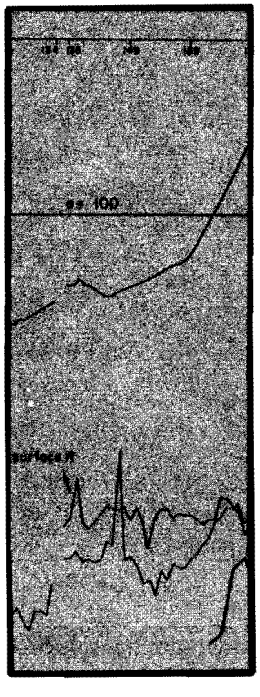

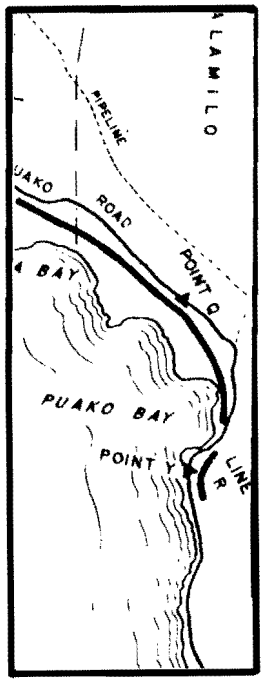

Rainfall in the area between Kawaihae and Kailua-Kona is very low. However, the rainfall in the western part of the Humuula Saddle may provide significant ground-water recharge. The geological controls on the seaward discharge of this ground water are poorly known. Review of the literature showed that the extent of the northeast rift of Hualalai, which might conceivably act to channel flow in the basal ground-water lens, is not well defined. Furthermore, the zone of intercalated flows from Mauna Kea and Mauna Loa, in the area of the Saddle and Belt Road junction, is probably further complicated by buried structures associated with the cinder cones scattered in the area.

To provide information bearing on these uncertainties, an aeromagnetic survey was made over the area and an audiomagnetotelluric (AMT) survey was run along the Belt Raod. The data from these two surveys correlated well. The AMT data indicate a deep lateral change in apparent resistivity about three miles south of the Saddle-Road-Belt-Road junction. Lateral orientation of this lateral change is provided by the position of the steep gradient region on the aeromagnetic map of the total magnetic field intensity. The resulting interpretation is Line X on Figure 6.1. The higher apparent resistivities occurring in the province to the north of Line X are attributed to the higher resistivity of the Mauna Kea lavas or to a higher water table depressing the salt-brackish interface.

The AMT data suggest that the northeast Hualalai rift zone extends from Puu Waawaa to Puu Anahulu. From the aeromagnetic total field map, the routing of the rift extension is approximated as Line H in Figure 6.1. This verified extension of the rift zone could control movement of basal water. At the junction of Lines X and H is a relatively optimum area for any further investigation.

The AMT and aeromagnetic data also agree well on the position of the two anomalies given as Lines J and K in Figure 6.1. Line K is the known northwest rift of Hualalai and Line J is without apparent surface expression. These two lines diverge from the possible recharge area of the Hualalai summit. The structural controls of basal-water movement are therefore probably not significant.

The rift zones, defined by the Lines H and X, probably have low permeability and therefore funnel the basal water into a swath between Hapuna and Anaehoomalu Bays. To further localize possible flow zones

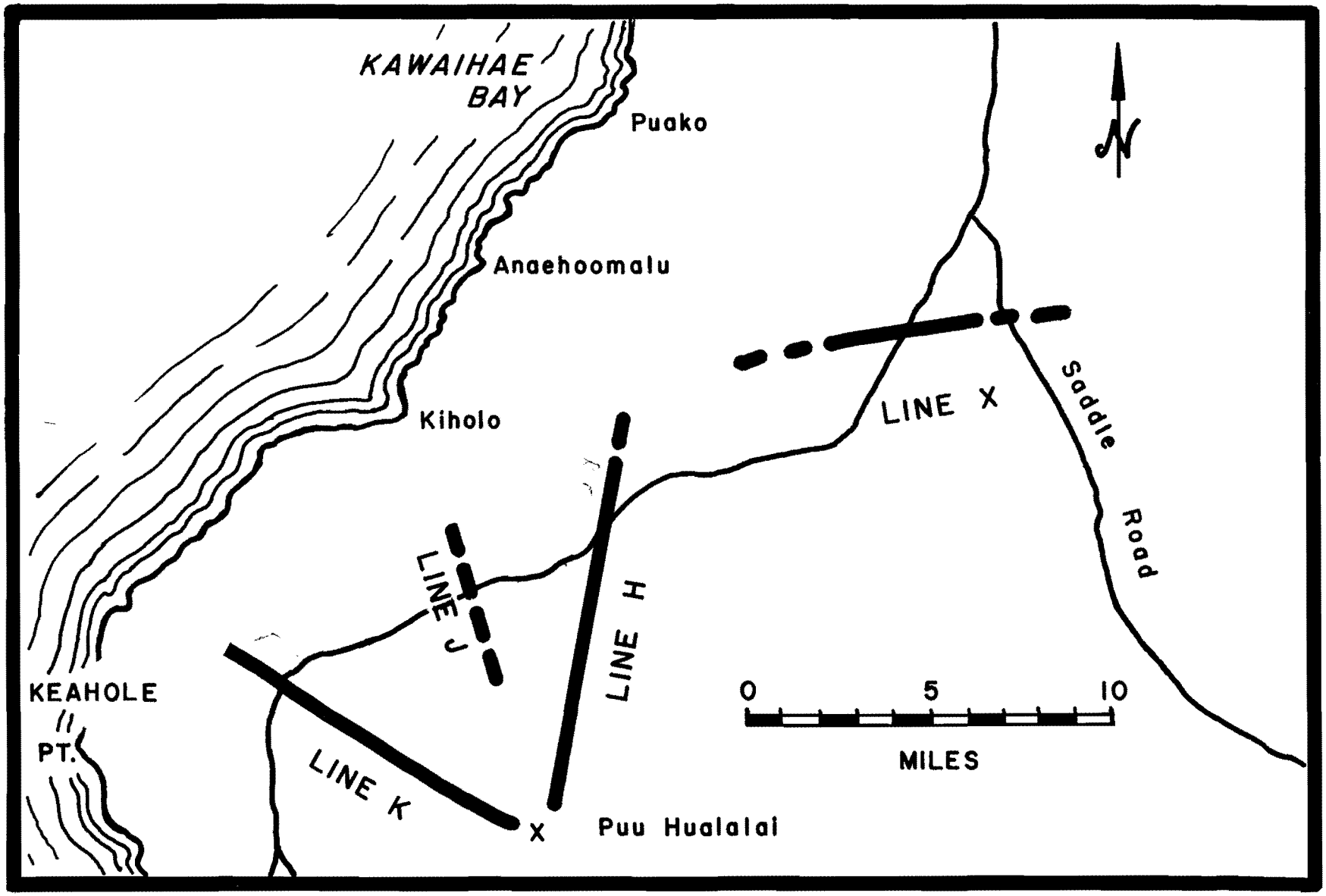

FIGURE 6.1. MAJOR STRUCTURAL FEATURES INDICATED BY AUDIOMAGNETICTELLURIC AND AEROMAGNETIC DATA.

in this swath, electrical resistivity profiles were made from Puako to Anaehoomalu Bay. Only two sections showed notably anomalous apparent resistivity. Line P in Figure 6.2 is uniformly high. The ground-water condition over the entire Line P is satisfactorily represented by that at position Q. Because electrical resistivity profiling is a relative technique, Line P is only a relatively good site. Line R in Figure 6.2 is about one order higher in electrical resistivity than the background. Position Y on Line R is an optimal site for the line. However, extensive fresh-water discharge is not indicated by either the infrared scanning or the result of an algal survey along that coastline (Brilliande and Lepley, 1969).

Further, electrical resistivity profiling and infrared scanning were conducted between Keahole Point and Kailua-Kona. A small anomaly appears at position S on Figure 6.3. A previously drilled hole, mauka of the site, has adequately tested the potential of this anomaly and found it to be unproductive.

Coastal thermal anomalies are separately indicated in the Appendix of the infrared scanning chapter. The biological indicator technique developed concommitantly to provide time-integrative information on the infrared anomalies (Brilliande and Lepley, 1969) is useful in mature ecological environments, but not on the Kona coast of Hawaii.

BIBLIOGRAPHY

Brilliande, Timothy W. and Larry K. Lepley. 1969. *Algae as an Indicator of Fresh Water Coastal Outflow in Hawaii.* Water Resources Research Center, University of Hawaii. In press.

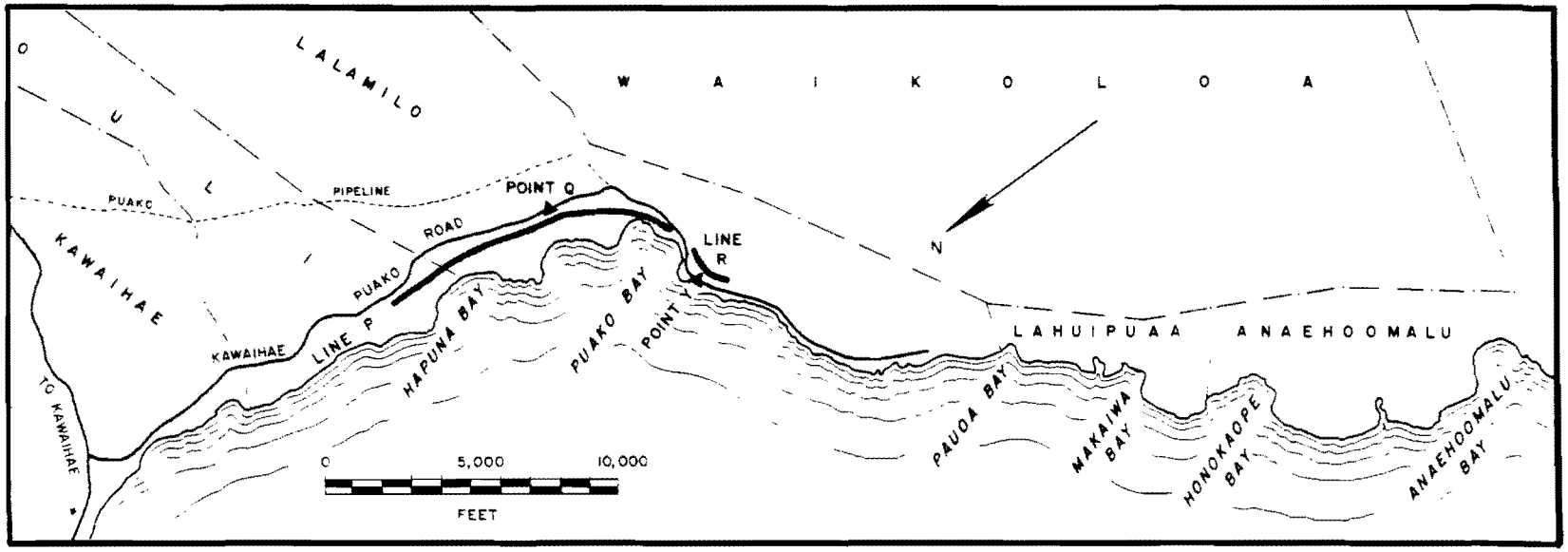

FIGURE 6.2. TWO LINES, P AND R, CORRESPONDING TO THE RELATIVELY HIGH APPARENT RESISTIVITY ANOMALIES, ARE SHOWN FOR THE HAPUNA BAY-PUAKO BAY AREAS. POINTS Q AND Y ARE CONSIDERED TO BE REPRESENTATIVE SITES FOR LINES P AND R, RESPECTIVELY.

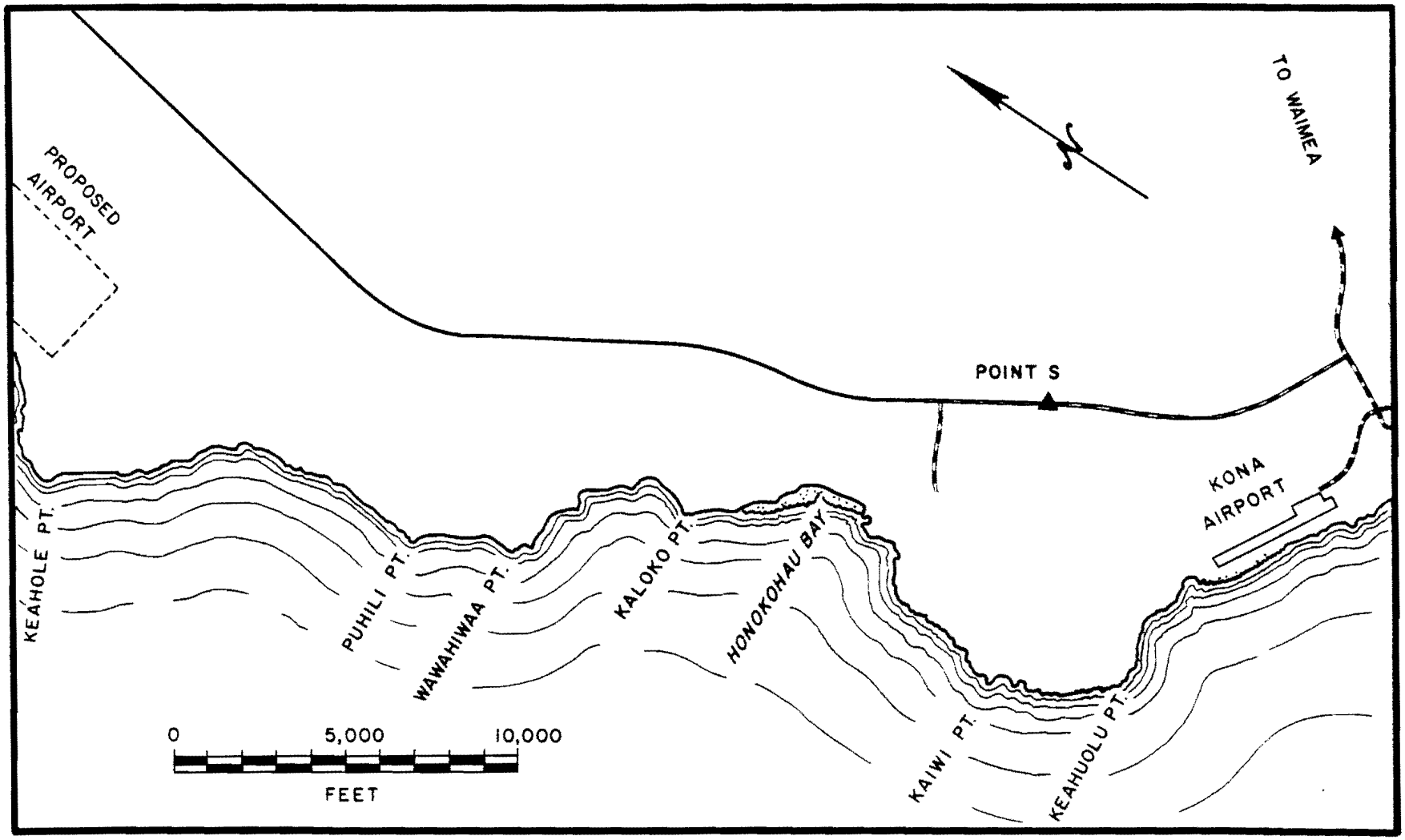

FIGURE 6.3. POINT S, CORRESPONDING TO A SMALL RELATIVELY HIGH APPARENT RESISTIVITY ANOMALY, IS SHOWN FOR THE KONA AIRPORT AREA.

If this place has a drought, then draw upon the abundant harvest elsewhere in order to relieve the distress here. If there is a drought there, draw upon the abundant harvest here in order to relieve the distress there.

From T'ien-ch'ao t'ien-mu chih-tu
The Land System of the Heavenly Kingdom; Series I, tse 4, pp. 1a-3a, 1853.